TAMPEREEN TEKNILLINEN YLIOPISTO
TAMPERE UNIVERSITY OF TECHNOLOGY

HENRIIKKA VENTO

ADHESION LIGAND-PRESENTING HYDROGELS FOR STUDYING STEM CELL BEHAVIOURS IN THREE DIMENSIONS

Master of Science thesis

Examiners: Assist. Prof. Oommen P. Oommen and Dr. Nick Walters
Examiners and topic approved by the Faculty Council of the Faculty of Natural Sciences on 31st May 2017

ABSTRACT

HENRIIKKA VENTO: Adhesion Ligand-Presenting Hydrogels for Studying Stem Cell Behaviours in Three Dimensions
Tampere University of Technology
Master of Science Thesis, 73 pages, 2 Appendix pages
December 2017
Master's Degree Programme in Bioengineering
Major: Tissue Engineering
Examiners: Assist. Prof. Oommen P. Oommen, Dr. Nick Walters

Keywords: Mechanotransduction, stem cell, microenvironment, hydrogel, biomaterial, adhesion ligand, hyaluronan, fibronectin, poly(ethylene glycol)

In their natural microenvironment, stem cells are surrounded by various mechanical and biochemical signals, and growing evidence suggests that, similarly to the biochemical cues, the biophysical properties of the microenvironment play an important role in guiding cell behaviours. However, the complex mechanisms by which different properties affect cell function, individually or in combination with other cues, is not fully understood. Hydrogels have emerged as useful biomaterials for studying cell behaviours in three dimensions (3D), as they can be precisely modified with e.g. cell adhesion ligands or enzymatically degradable sequences, in order to study a cell's interactions with its surroundings.

Research has shown that not only the density, but also the inter-ligand distance is implicated in directing stem cell fate via mechanotransductive processes. The original objective of this thesis was to contribute to the fabrication of adhesion ligand-presenting poly(ethylene glycol) (PEG)–peptide hydrogels, and to carry out preliminary studies on the effects of different adhesion ligand concentrations on cell behaviour. Due to setbacks in the hydrogel fabrication, the main focus was shifted from PEG hydrogels to hyaluronan hydrogels, to which fibronectin was added as an adhesion ligand. In addition, RNA extraction from PEG hydrogels was optimised, as the 3D environment presents additional challenges for extraction of high quality messenger RNA, which is needed in cell differentiation studies.

Human bone marrow stromal cells were encapsulated in adhesive, fibronectin-containing hyaluronan hydrogels, and their response was compared to cells encapsulated in non-adhesive hyaluronan hydrogels. Cells were cultured in the gels for seven days, and cell viability, proliferation and morphology were compared at three different time points. For the RNA extraction experiments, two commercially available RNA extraction kits were compared and two different cell lysis buffers were used.

Adhesion ligand presentation clearly improved cell survival in hyaluronan gels, as expected. Cells spread and remained more viable during the week of culture time. Cells were not able to spread and their viability was low in the gels without adhesion sites, and the permeation properties of these gels need to be investigated in more detail, as they caused issues with several assays. The highest RNA yield was achieved with the RNeasy Plus Mini Kit and its original RLT+ buffer. These results can be later used in further cell differentiation studies with PEG hydrogels.

TIIVISTELMÄ

HENRIIKKA VENTO: Adheesioligandeja sisältävien hydrogeelien käyttö kantasolujen tutkimiseen kolmiulotteisessa ympäristössä
Tampereen teknillinen yliopisto
Diplomityö, 73 sivua, 2 liitesivua
Joulukuu 2017
Biotekniikan diplomi-insinöörin tutkinto-ohjelma
Pääaine: Kudosteknologia
Tarkastaja: Apulaisprofessori Oommen P. Oommen ja tohtori Nick Walters

Avainsanat: mekanotransduktio, kantasolu, mikroympäristö, hydrogeeli, biomateriaali, adheesioligandi, hyaluronaani, fibronektiini, poly(etyleeni glykoli)

Solujen luonnollisessa elinympäristössä, kudoksessa, ympäristön vihjeet ohjaavat solujen toimintaa. Aiemmat tutkimukset ovat osoittaneet, että biokemiallisten vihjeiden ohella myös ympäristön mekaaniset ominaisuudet vaikuttavat solujen käytökseen. Kuitenkaan sitä, miten tietyt vihjeet ohjaavat muun muassa kantasolujen erilaistumista, ei tiedetä varmasti. Hydrogeelit ovat hyödyllisiä materiaaleja solujen käytöksen tutkimiseen kolmiulotteisessa (3D) ympäristössä. Hydrogeelien ominaisuuksia voidaan muokata tarkasti, ja niihin voidaan sisällyttää esimerkiksi solujen tarttumista edistäviä adheesioligandeja tai entsymaattisesti hajoavia ristisiltoja. Näin voidaan tarkemmin tutkia solujen vuorovaikutusta niiden ympäristön kanssa.

Tämän työn alkuperäinen tarkoitus oli osallistua synteettisten, adheesioligandeja sisältävien poly(etyleeni glykoli) (PEG) hydrogeelien valmistukseen ja tutkia niillä liganditiheyden vaikutusta solujen käyttäytymiseen. Ligandeja sisältävän PEG-geelin valmistuksen viivästymisen takia työn fokus kuitenkin siirrettiin hyaluronaanigeeleihin, joihin lisättiin fibronektiiniä adheesioligandiksi. Tämän lisäksi RNA-eristys optimoitiin PEG hydrogeeleille, sillä 3D ympäristö heikentää laadukkaan RNA:n saantoa. Laadukasta RNA:a tarvitaan kantasolujen erilaistumista tutkittaessa.

Kantasoluviljelyä varten valmistettiin hyaluronaanihydrogeelejä, jotka joko sisälsivät tai eivät sisältäneet fibronektiiniä. Ihmisen luuytimen kantasoluja viljeltiin geeleissä viikon ajan, ja solujen elävyyttä sekä morfologiaa tarkkailtiin kolmessa eri aikapisteessä. RNA-eristyskokeessa vertailtiin kahta kaupallista eristysmenetelmää ja kahta eri solujen hajotusliuosta.

Solujen elävyys adheesioligandeja sisältävissä hyaluronaanigeeleissä oli huomattavasti korkeampi verrattaessa geeleihin ilman ligandeja, kuten oli odotettavissa. Lisäksi näissä geeleissä solut olivat morfologialtaan levittäytyneitä ja muodostivat organisoidun aktiinitukirangan. Geeleissä, joissa ei ollut adheesioligandeja, solujen levittäytyminen ei ollut mahdollista. Näissä samaisissa geeleissä todettiin myös heikkoa läpäisevyyttä väriaineita hyödyntävissä kokeissa. Näin ollen geelin diffuusio-ominaisuuksia tulisi tutkia tulevaisuudessa. Paras RNA-eristystulos saavutettiin RNeasy Plus Mini Kit -menetelmällä alkuperäisen solujen hajotusliuoksen kanssa. Näitä tuloksia voidaan myöhemmin käyttää tutkittaessa kantasolujen erilaistumista PEG-geeleissä.

PREFACE

This Master of Science thesis was carried out in the Adult Stem Cell Group, which is one of the research groups of BioMediTech - Institute of biosciences and medical technology. First, I would like to thank the group leader Docent Susanna Miettinen for this opportunity to work in the fascinating field of stem cell research, and my supervisor Dr. Nick Walters for providing the interesting project, which nicely combined chemistry, cell biology and biomaterials.

I would like to thank Oommen P. Oommen, Vijay Singh Parihar, Vesa Hytönen and Niklas Kähkönen for providing the materials for the final experiments. I am also grateful to all the wonderful staff members at Arvo and in the Biomaterials laboratory at Tampere University of Technology, who helped me out whenever I faced issues in the lab, and who always had time for my questions. Special thanks to Mese group's Anna-Maija Honkala and Miia Juntunen for their advices and assistance.

As my studies are coming to an end with this thesis, I would like to thank my friends at the university for making these past years so special. Especially, I would like to mention here Jannika, who has been the greatest friend anyone could ask for. Out of all the unforgettable moments at TUT, writing numerous pair assignments and preparing for presentations together at the 'home office' must be some of my fondest memories. I am also beyond grateful for her peer support during this thesis project.

Last but not least, I would like to dedicate this thesis to my mom. She has always encouraged me to follow my dreams, and I could not have done this without her endless support.

Tampere, 22.11.2017

Henriikka Vento

CONTENTS

1. INTRODUCTION 1
2. LITERATURE REVIEW 3
2.1 Stem cells and their microenvironment 3
2.1.1 Mesenchymal stem cells 3
2.1.2 Extracellular microenvironment 6
2.2 Mechanotransduction 8
2.2.1 Force transmission from the extracellular matrix 9
2.2.2 Nuclear mechanotransduction 12
2.2.3 Biochemical signalling pathways 14
2.3 Hydrogels 17
2.3.1 Classification, fabrication and properties 17
2.3.2 Poly(ethylene glycol) hydrogels 19
2.3.3 Hyaluronan hydrogels 19
2.4 Effects of adhesion ligand presentation on cell behaviour 21
2.4.1 Studies carried out in 2D 21
2.4.2 Studies carried out in 3D 28
3. AIMS OF THE STUDY 33
4. MATERIALS AND METHODS 34
4.1 Workflow 34
4.2 Optimisation of PEG4NPC synthesis 34
4.2.1 PEG4NPC synthesis 34
4.2.2 Quantification of PEG functionalisation 38
4.3 Cell culture 38
4.3.1 hBMSC isolation 39
4.3.2 Evaluation of differentiation potential 39
4.4 Hydrogel preparation and cell encapsulation 40
4.4.1 Poly(ethylene glycol) hydrogels 40
4.4.2 Hyaluronan hydrogels 40
4.5 Optimisation of RNA extraction from PEG hydrogels 41
4.6 Analysis of cell number and viability in hyaluronan hydrogels 42
4.6.1 Brightfield imaging 42
4.6.2 Live/dead assay 42
4.6.3 AlamarBlue assay 42
4.6.4 CyQUANT assay 43
4.7 Immunocytochemistry 43
5. RESULTS 45
5.1 PEG4NPC – Level of functionalisation 45
5.2 RNA extraction from PEG hydrogels 46
5.3 Cell number and viability in hyaluronan hydrogels 50
5.4 Cell morphology in hyaluronan hydrogels 55

6. DISCUSSION 57
6.1 Fabrication of adhesion ligand-presenting hydrogels 57
6.1.1 PEG4NPC synthesis needs further optimisation 57
6.1.2 Fibronectin likely altered the crosslinking of HAH 59
6.2 Optimisation of RNA extraction from PEG hydrogels 59
6.3 Evaluation of cell behaviour in hyaluronan hydrogels 61
6.3.1 Fibronectin presentation enhanced cell survival 61
6.3.2 Fibronectin presentation enabled cell spreading 62
6.3.3 Assessment of the study and future perspectives 63
7. CONCLUSIONS 65

APPENDIX A: DIFFERENTIATION POTENTIAL OF HBMSCS

APPENDIX B: NMR SPECTRA FOR PEG4NPC

LIST OF FIGURES

Figure 1. *The differentiation capacity of mesenchymal stem cells. The most common differentiation lineages of MSCs are muscoskeletal and connective tissues, such as bone, cartilage, fat and connective stroma. The dotted line indicates plasticity to other cell types Reproduced with permission from reference (Uccelli et al. 2008), Nature Publishing Group. 4*

Figure 2. *The extracellular microenvironment of a cell consists of many different factors. These include physical factors, such as the elasticity and topography of the substrate, the biochemical properties of ECM molecules, contacts with neighbouring cells and secreted biochemical signals. Reproduced with permission from reference (Lane et al. 2014), Nature Publishing Group. 6*

Figure 3. *Schematic illustration of a focal adhesion complex. Integrins connect the cell to the surroundings by binding to ECM proteins outside the cell. Integrins are connected to the cytoskeleton via focal adhesions, which are large protein clusters which also act as signalling centres. (Mitra et al. 2005)..... 11*

Figure 4. *Force transmission pathway from the plasma membrane to the nucleus. Integrins are connected to actin stress fibers, which are connected from their other end to the nuclear envelope proteins, and this allows the cell to function as a uniformly interconnected system. Reproduced with permission from reference (Fedorchak et al. 2014), Elsevier..... 13*

Figure 5. *Signalling pathways activated in contractility-mediated mechanosensing and differentiation. Reproduced with permission from reference (Hao et al. 2015), Elsevier..... 16*

Figure 6. *Structure of 4-arm PEG..... 19*

Figure 7. *Structure of a hyaluronan monomer..... 20*

Figure 8. *Workflow of the thesis project. 34*

Figure 9. *Conjugation reaction for poly(ethylene glycol) and 4-NPC to yield PEG4NPC..... 35*

Figure 10. *Degree of functionalisation of PEG(10K)4OH with 4-NPC to form PEG(10K)4NPC. Functionalisation was increased by: anhydrous reaction conditions (experiment 1 vs. 2); increasing the amount of starting materials (10 times larger amounts in exp. 3 compared to exp. 2); increasing the reaction time from 24 to 72 h (exp. 3 and 4,*

respectively); and using a greater excess of 4-NPC (exp. 5 vs. exp. 3). Addition of a catalyst did not increase the level of functionalisation with smaller excess of 4-NPC and shorter reaction time (exp. 6 and 7). Experiments 8 and 9 were repetitions of experimental set up of exp. 4, but with a catalyst or with larger amount of starting materials, respectively. 45

Figure 11. *RNA extraction yield from PEG–peptide hydrogels. The total RNA yield is presented as an average of the samples for 2D samples (n = 3) and for 3D samples in RLT+ buffer (n = 3). For the buffer blank, gel blank and the 3D samples in TRI Reagent & tRNA the yield from one sample is shown (n = 1). 47*

Figure 12. *A260/230 ratio, measured with NanoDrop. 48*

Figure 13. *A260/280 ratio, measured with NanoDrop. 49*

Figure 14. *Fragment Analyzer was run for RLT+ samples (n = 1). The maximum value for RNA quality number is 10. ..... 50*

Figure 15. *hBMSC encapsulated in hyaluronan hydrogels were qualitatively evaluated using bright field imaging. HAH-FN gels (A, C & E), HAH gels (B, D & E) after 1 day (A & B), 4 days (C & D) and 7 days (E & F) of culture. The number of cells remained fairly constant at all time points and cell morphology remained rounded in both types of gels. Scale bar 500 µm. 51*

Figure 16. *hBMSC morphologies inside hyaluronan gels, after 7 days in culture. Cells were able to spread and form protrusions and cell-cell contacts in HAH-FN gels (left). Only rounded morphologies were seen in HAH gels (right). Scale bar 100 µm. 52*

Figure 17. *Viability of hBMSCs encapsulated to hyaluronan hydrogels. Viability in HAH-FN gels (A, C & E) and HAH gels (B, D & F) after 1 day (A & B), 4 days (C & D) and 7 days (E & F) of culture. Scale bar 500 µm. 53*

Figure 18. *hBMSC viability in hyaluronan gels either with fibronectin (HAH-FN) or without fibronectin (HAH), quantified with a resazurin-based mitochondrial metabolic assay. Cell number was extrapolated from the standard curve. (n = 3, error bars = SD) 54*

Figure 19. *hBMSC number and proliferation in hyaluronan gels either with fibronectin (HAH-FN) or without fibronectin (HAH), quantified with a total DNA assay. Cell number was extrapolated from the standard curve. (n = 3, error bars = SD) 55*

Figure 20. *hBMSCs encapsulated in hyaluronan hydrogels. Cells remained rounded in the HAH-FN gels on day 1 (A), and cells were able to spread in the HAH-FN gels on day 4 (B). On day 7, well spread cell clusters could be seen in HAH-FN gels (C). On day 1 in HAH hydrogels, cells remained rounded and vinculin remained diffusive around the nucleus (D). Nucleus is stained in blue, actin fibers in red and vinculin in green. Scale bar 50 µm. 56*

Figure 21. *The isosbestic point of p-nitrophenol in water. The isosbestic point of a sample is the wavelength at which the total absorbance is not affected by physical changes in the sample which might be caused by the pH of the buffer. (Biggs 1954) 58*

Figure 22. *Differentiation potential of hBMSCs from four different donors, labelled as 5/16, 6/16, 7/16 and 9/16. The cells were cultured in basic medium and either in osteogenic medium for 20 days before Alizarin Red staining, or in adipogenic medium for 14 days before Oil Red O staining. The mineral content and lipid vacuoles are stained in red. 74*

Figure 23. *^{1}H NMR spectrum for A) PEG4NPC and B) unmodified PEG4OH. The highest peak at 3.6 ppm indicates the presence on –CH_2 groups of the repeating unit of the polymer. The small peak shifted to 4.4 ppm in A) indicates the attachment of –CH2 to 4-NPC and peaks at 7.4 and 8.3 ppm indicate the presence of an aromatic ring. Solvent peak can be seen ~7.25 ppm and some impurities can be seen < 2.5 ppm. 75*

LIST OF SYMBOLS AND ABBREVIATIONS

2D	Two-dimensions/two-dimensional
3D	Three-dimensions/three-dimensional
AM	Adipogenic medium
BM	Basic medium
BMSC	Bone marrow stromal cell
CM	Chondrogenic medium
Col I	Collagen type I
cRGD	Cyclic arginine-glycine-aspartic acid peptide
DAPI	4',6-diamidino-2-phenylindole
DCM	Dichloromethane
DE	Diethyl ether
4-DMAP	4-dimethylaminopyridine
DMSO	Dimethyl sulfoxide
DPBS	Dulbecco's phosphate-buffered saline
ECM	Extracellular matrix
FA	Focal adhesion
FAK	Focal adhesion kinase
FN	Fibronectin
GAG	Glycosaminoglycan
GFOGER	Glycine-phenylalanine-hydroxyproline-glycine-glutamate-arginine peptide
HA	Hyaluronan
HAH	Hydrazide-crosslinked hyaluronan, referring to a hydrogel
HAH-FN	Hydrazone-crosslinked hyaluronan containing fibronectin, referring to a hydrogel
hBMSC	Human bone marrow stromal cell
hFGF-2	Human fibroblast growth factor-2
hMSC	Human mesenchymal stem cell
IKVAV	Isoleucine-lysine-valine-alanine-valine peptide
LINC	Linker of nucleoskeleton and cytoskeleton
MMP	Matrix metalloproteinase
mRNA	Messenger RNA
MSC	Mesenchymal stem cell
NMR	Nuclear magnetic resonance
4-NPC	4-nitrophenyl chloroformate
NPC	Nuclear pore complex
OM	Osteogenic medium
PDMS	Polydimethylsiloxane
PEG	Poly(ethylene glycol)
PEG4NPC	4-arm poly(ethylene glycol) nitrophenyl carbonate
PEG4VS	Poly(ethylene glycol) vinyl sulfone
PI3K	Phosphatidylinositol-3 kinase
PPARγ	Peroxisome proliferator-activated receptor gamma
PS-PEO-Ma	Poly(styrene-block-ethylene oxide-maleimide)
RGD	Arginine-glycine-aspartic acid peptide

RRETAWA	Arginine-arginine-glutamic acid-threonine-alanine-tryptophan-alanine peptide
Runx2	Runt-related transcription factor
SD	Standard deviation
tRNA	Transfer RNA
YIGSR	Tyrosine-isoleucine-glycine-serine-arginine peptide

1. INTRODUCTION

Stem cells have a great therapeutic potential for regenerative medicine and tissue engineering applications, due to their ability differentiate into specialised cell types and stimulate regeneration of tissues (Mason & Dunnill 2008). In their natural tissue microenvironments, stem cells are surrounded by various mechanical and biochemical signals, and growing evidence suggests that the local microenvironment of the cell is able to maintain and regulate stem cell behaviours. This presents an intriguing approach for tissue engineering, to develop materials which mimic the properties of the natural environment of the cell in order to guide stem cell fate. (Tibbitt & Anseth 2009)

The process by which cells convert mechanical cues from the surroundings into biological and biochemical responses is called *mechanotransduction*. Mechanotransduction allows the cells to alter their behaviours according to the environmental cues, and to exert forces to the surroundings and reorganise the extracellular matrix (ECM), meaning that the process is bidirectional. The mechanical signals can alter cell behaviours such as adhesion, migration, proliferation and differentiation. However, the detailed mechanisms of mechanotransduction and the associated pathways are not thoroughly known. Defects in mechanotransductive pathways are present in many diseases, including muscular dystrophies, cardiomyopathies and cancer, and therefore gaining more information about this complex phenomenon is important. (Jaalouk & Lammerding 2009)

Hydrogels have emerged as promising platforms for studying cell behaviours in three dimensions (3D). They have high water content similar to natural tissues, and properties such as stiffness, porosity, adhesiveness and degradability can be precisely modified by polymer chemistry. Their tunability allows the fabrication of modular hydrogels which mimic the properties of the local microenvironment of the cell. Using such materials, in which ECM properties can be precisely defined, more information can be gained concerning how each of these properties affects stem cell behaviour, both individually and in combination. (Slaughter et al. 2009)

The aim of this thesis project was to contribute to the fabrication of highly modular poly(ethylene glycol) (PEG)–peptide hydrogels, and to study the effects of varying concentrations of cell adhesion ligands on human bone marrow stromal cell (hBMSC) behaviour in 3D. The original hypothesis was that a higher density of adhesion ligands would support osteogenesis, and lower density of adhesion ligands would support adipogenesis, even without differentiation medium. However, as the project faced setbacks in terms of the material fabrication, the cell experiments were finally carried out with two types of hyaluronan hydrogels, one incorporating adhesion ligand-containing fibronectin

and one without adhesion ligands. Therefore, the original hypothesis about effects of ligand densities on cell behaviour could still be tested, although to a less detailed extent than originally planned. The hypothesis for cell culture studies on hyaluronan hydrogels was that adhesion ligand presentation would enhance cell viability and enable a greater degree of cell spreading.

This thesis includes a literature review, which briefly covers the following topics: stem cells and their microenvironment, mechanotransduction, hydrogels and previous studies regarding the effects of adhesion ligand density on cell behaviour. The experimental procedures of this study are described in Chapter 4, which is followed by Results and Discussion in Chapters 5 and 6, respectively. Finally, the results are concluded in the Chapter 7.

2. LITERATURE REVIEW

2.1 Stem cells and their microenvironment

Stem cells are unspecialised cells that have the ability to divide symmetrically, which means that they can self-renew by producing two identical undifferentiated stem cells, or asymmetrically, which means that they produce one stem cell and one semi-differentiated progenitor cell. Each specific type of stem cell can differentiate into either a single type or multiple types of mature cell phenotypes, a property referred to as 'potency'. Stem cells can be totipotent, pluripotent, multipotent, oligopotent or unipotent. Potency describes the number of lineages that the cells can differentiate to and this property associates with the tissue from which stem cells are isolated; cells derived from inner mass of a blastocyst, called embryonic stem cells, are pluripotent and cells derived from adult mesenchymal tissues are multipotent. (Jukes et al. 2008) It is also possible to reprogram differentiated cells back to the pluripotent state, and these cells hold great promise for personalised health care. These cells are called induced pluripotent stem cells, and they were introduced by Takahashi & Yamanaka in 2006 (Takahashi & Yamanaka 2006).

Many mature tissues contain a small population of stem cells, called adult stem cells, which are responsible for growth, maintenance, regeneration and repair of the tissues during human life. Adult stem cells are multipotent stem cells that can be further classified into different cell types according to their origin, such as mesenchymal stem cells (MSCs, from e.g. bone marrow and adipose tissue), hematopoietic stem cells (red bone marrow) and neural stem cells (brain). (Jukes et al. 2008)

In this chapter, characteristics of mesenchymal stem cells and their differentiation pathways are discussed in Section 2.1.1 and factors contributing to the stem cell microenvironment are discussed in Section 2.1.2.

2.1.1 Mesenchymal stem cells

MSCs are present in tissues of mesodermal origin, such as connective tissue, bone, cartilage and lymphatic systems. They are responsible for regeneration and maintaining tissue function and differentiate into cell types of mesodermal lineages, such as bone, fat and cartilage. In addition, MSCs have been shown to have transdifferentiation capacity to endodermic and neuroectodermic cell types, which could be explained by the development of mesenchymal tissues, as the origin of development includes the mesoderm and to a smaller extent, the cranial neural crest. The differentiation capacity of MSCs is shown in Figure 1. (Uccelli et al. 2008)

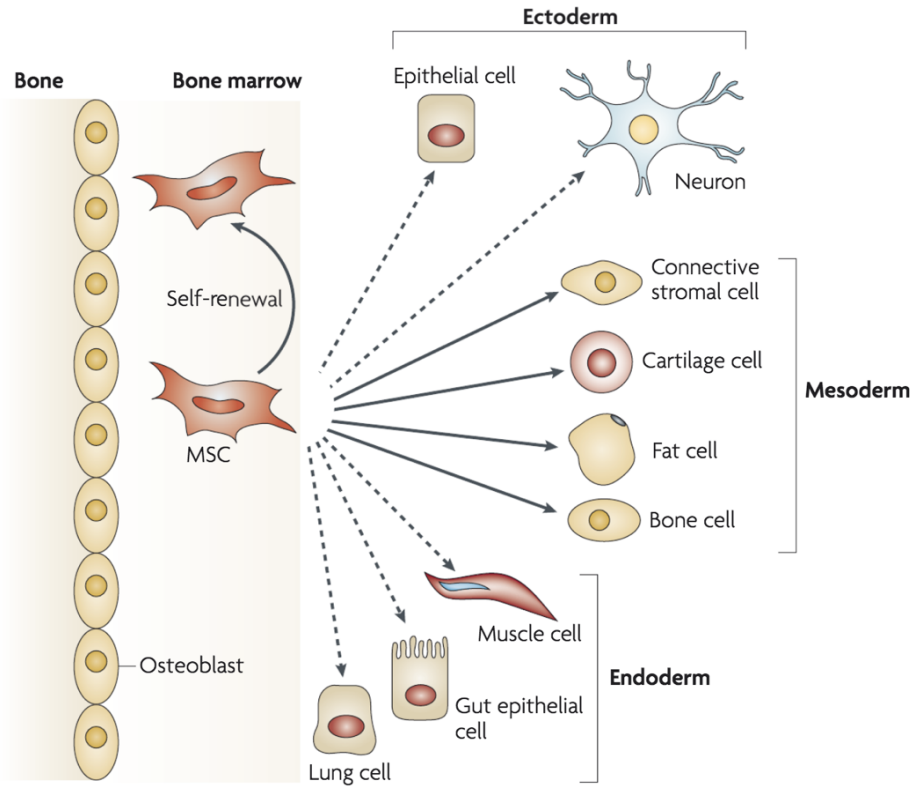

Figure 1. *The differentiation capacity of mesenchymal stem cells. The most common differentiation lineages of MSCs are muscoskeletal and connective tissues, such as bone, cartilage, fat and connective stroma. The dotted line indicates plasticity to other cell types Reproduced with permission from reference (Uccelli et al. 2008), Nature Publishing Group.*

MSCs are an attractive autologous therapy source, as they can be isolated from bone marrow or adipose tissue during standard surgeries. The advantages of isolating MSCs from adipose tissue over bone marrow are accessibility, ease of isolation via minimally invasive procedures and high yield of adult stem cells. (Bunnell et al. 2008)

To ensure the homogeneity of a cell population after isolation and expansion, and to assist in comparison between different laboratories, the Mesenchymal and Tissue Stem Cell Committee of the International Society for Cellular Therapy has proposed three criteria by which to define human MSCs. First, the cells need to be plastic-adherent under standard culture conditions. Second, they need to have specific surface antigen expression: ≥ 95% of the MSC population must express CD105, CD73 and CD90 and the population must also lack (≤ 2 %) expression of antigens that are indicative of other cell types: CD45, CD34, CD14 or CD11b, CD79α or CD19 and HLA-DR surface molecules. Third, MSCs must have trilineage differentiation potential, i.e. they must be able to differentiate to osteoblasts, adipocytes and chondroblasts *in vitro*.

The differentiation pathways of MSCs to bone (osteogenesis), fat (adipogenesis) or cartilage (chondrogenesis) have been widely studied. During osteogenesis, MSCs differentiate to osteoblasts by first proliferating, then as the differentiation proceeds, proliferation

slows down, and this is followed by matrix maturation and mineralisation. Early markers of osteogenesis include increased collagen type I (col I), fibronectin (FN) and osteopontin production and increased alkaline phosphatase activity. Late markers of osteogenesis are increased osteocalcin and osteopontin production, and increased Runt-related transcription factor (Runx2) expression. Osteogenic differentiation is commonly evaluated with Alizarin Red staining, which stains bone mineral red. To initiate the differentiation process *in vitro*, osteogenic medium (OM) containing ascorbic acid, β-glycerophosphate and dexamethasone is commonly used. (Lian & Stein 1995; Ullah et al. 2015)

Adipogenesis occurs in two stages, as determination to preadipocytes is followed by commitment stage to mature adipocytes. As cells differentiate down the adipogenic pathway, they become more spherical and start to accumulate lipid. Accumulation of lipid can be evaluated with Oil Red O staining, which stains the lipid vacuoles red. Adipogenesis can also be evaluated by studying the proteins secreted by adipocytes, such as adiponectin and leptin, and by up-regulation of peroxisome proliferator-activated receptor gamma (PPARγ) expression. Adipogenesis can be initiated *in vitro* with an adipogenic differentiation medium (AM), which contains dexamethasone, isobutylmethylxanthine, insulin and indomethacin. High cell plating density is beneficial for adipogenic differentiation. (Pittenger et al. 1999; Avram et al. 2007)

In chondrogenesis, differentiation proceeds from progenitor cells to chondroblasts and finally to chondrocytes. Chondrogenic differentiation can be evaluated by studying the accumulation of secreted ECM molecules, such as collagen type II and aggrecan. Toluidine blue staining is commonly used to stain the ECM components. Upregulation of chondrogenic transcription factors, e.g. Sox9, L-Sox5 and Sox6, can be observed during chondrogenesis. Chondrogenic differentiation medium (CM) contains dexamethasone, ascorbate-2-phosphate, insulin, selenious acid, transferrin, sodium puryvate and transformin growth factor-beta. Culturing cells as aggregates is beneficial for chondrogenesis, due to high cell density and cell-cell interactions. (Solchaga et al. 2011; Ullah et al. 2015)

As described, the *in vitro* differentiation of MSCs is commonly initiated with corresponding differentiation medium. However, the use of differentiation media can lead to a heterogeneous cell population and even to tumour formation, which is why it is important to find alternative ways of inducing stem cell differentiation, such as by harnessing mechanical cues.

In addition to the differentiation capacity of MSCs, self-renewal is an important property, as it is needed to maintain the stem cell function. One potential mechanism of maintaining this property is induction of quiescence, which means that the cell temporarily exits the cell cycle and does not proliferate. Most adult stem cell populations are maintained in this resting state. Quiescence is important, as stem cell proliferation and loss of stem cell function over time strongly correlate. (Orford & Scadden 2008)

2.1.2 Extracellular microenvironment

Stem cells reside within highly localised microenvironments which vary greatly between tissues and are referred to as 'stem cell niches', a term first proposed by Schofield in 1978 (Schofield 1978). The niche refers not only to the anatomical location but also to the functional cues provided in order to maintain stem cells as a stable functional population (Scadden 2006).

The extracellular microenvironment of the cell is composed of many components, as shown in Figure 2. Cell-cell contacts, cell-substrate and cell-growth factor interactions are the three main factors contributing to a stem cell niche. Niches have a role in stem cell self-renewal and differentiation. (Fuchs et al. 2004) Inside the niche, stem cells often remain quiescent, a state which is very difficult to maintain during two-dimensional (2D) *in vitro* cell culture. Given that adult stem cells generally have limited function outside their niche, the attempted use of biomaterials such as hydrogels in order to simulate an extracellular niche is an important area of research. (Scadden 2006)

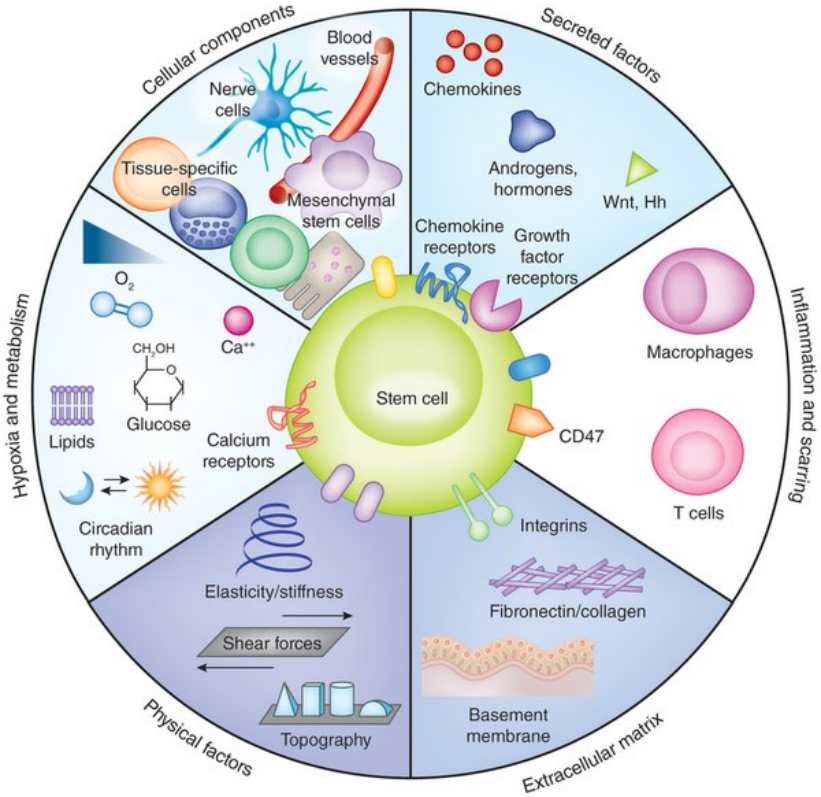

Figure 2. *The extracellular microenvironment of a cell consists of many different factors. These include physical factors, such as the elasticity and topography of the substrate, the biochemical properties of ECM molecules, contacts with neighbouring cells and secreted biochemical signals. Reproduced with permission from reference (Lane et al. 2014), Nature Publishing Group.*

The extracellular microenvironment within most tissues consists of ECM secreted by cells. ECM serves as a scaffold for cell anchorage, which is important in order to prevent

anoikis, which is the programmed cell death of anchorage-dependent cells such as MSCs when they are unable to attach to a substrate. Cells are also able to dynamically remodel the ECM, for example via matrix degradation regulated by enzymes such as matrix metalloproteinases (MMPs), and via exertion of mechanical forces to reposition matrix components. Overall, ECM proteins play in a key role in maintaining cellular homeostasis. One well-known approach towards engineering entire tissues or organs is to decellularize the ECM of natural organs for stem cell culture, in order to guide differentiation into the cell types of the corresponding organ (Nakayama et al. 2010). This demonstrates the important role of ECM composition and physical structure, and therefore the general composition of ECM is discussed next.

2.1.2.1 Composition of extracellular matrix

ECM is a hydrated 3D network of primarily organic macromolecules – and inorganic crystals, in the case of mineralised tissues such as bone and dentine – that surrounds the cells. Along with providing mechanical support, it also organises cells into specific tissues, acts as a reservoir for soluble signalling molecules and controls cellular behaviours. ECM is mainly composed of fibrous proteins, glycosaminoglycans (GAGs), glycoproteins and other small molecules. Many of these molecules have both structural and functional roles. (Badylak et al. 2008) Although similarities exist between different tissues, the ECM is characteristic for each tissue type (Tibbitt & Anseth 2009).

The mechanical strength of a tissue is mainly provided by proteins. The major structural proteins are fibrous collagen, elastin, fibronectin and laminin. (Badylak et al. 2008; Votteler et al. 2010) The most abundant protein is collagen, which can be present in over twenty different subtypes with diverse functions. Type I collagen is the most important protein in providing structural support, tensile strength and rigidity to the tissue. The elasticity and load bearing properties of many tissues are provided by hydrophobic elastin. (Scott 1995; Badylak et al. 2008)

Fibronectin and laminin are glycoproteins that have key roles in supporting cell adhesion. Fibronectin is present in large quantities within the ECM and it is the second most abundant protein. Cells adhere to it via adhesion receptors called integrins. Integrins also bind to other components of the ECM, such as collagen, heparin, fibrin and proteoglycans. (Votteler et al. 2010) Each fibronectin molecule contains multiple cell adhesion motifs, including arginine-glycine-aspartic acid (RGD) tripeptides, which are important for cell adhesion. (Badylak et al. 2008) Exposure of cryptic sites and the fibronectin assembly is mechanically regulated, as the conformation of the protein varies when cells exert force to their surroundings (Gao et al. 2003; Smith et al. 2007). Each of the structural matrix proteins seems to be critical for cell adhesion and migration during growth, differentiation, morphogenesis and wound healing. Laminin, which is mainly present in the basement membrane of epithelia, is important in the development of organised tissues because of its web-like structure. (Badylak et al. 2008; Votteler et al. 2010)

Proteoglycans contain a core protein, to which large sulphated GAGs are attached. Glycosaminoglycans are unbranched polysaccharides, and examples of those found in the ECM are hyaluronan (HA, also known as hyaluronic acid), heparin sulfate and chondroitin sulfates A and B. GAGs have high negative charge, and therefore proteoglycans have an extensive water holding capacity and provide compression-resistance to tissues. HA is widely used for producing hydrogels because of this water-holding capacity, and it is studied further in this thesis. Proteoglycans, especially heparin-rich ones, are important for binding growth factors and cytokines. (Badylak et al. 2008; Votteler et al. 2010)

2.2 Mechanotransduction

Tissue stiffness varies greatly between tissues, ranging from as low as 0.1 kPa in brain to 40 kPa in bone, as shown in Table 1 (Engler et al. 2006). Cells sense the stiffness of the surrounding environment, which has been shown to affect cell spreading, migration, signalling and differentiation.

Table 1. *The approximate stiffnesses of different tissues. (Engler et al. 2006)*

Tissue	**Stiffness (*kPa*)**
Brain	0.1–1
Muscle	8–17
Bone	25–40

The process by which cells convert mechanical cues from the surroundings into various actions is called *mechanotransduction*. It was originally thought that the proteins involved in mechanotransduction are mainly located near the outer plasma membrane of the cells and that activation of biochemical signalling pathways is a response to force application. However, the relatively immediate response that can be observed after application of tensile stress demonstrates the role of direct force transmission pathways, and that the response is not mediated by the activated biochemical pathways alone, as diffusion takes much more time (5–10 s) compared to force transmission via cytoskeleton (~ 1 ms) (Wang et al. 2009).

One of the frontrunners in the field of mechanotransduction has been Donald Ingber, who developed the tensegrity model in 1997. Rather than treating the cell as “viscous protoplasm surrounded by an elastic membrane”, Ingber viewed the cell’s cytoskeleton as an architectural structure which transduces mechanical information from the niche to the cell and vice versa. (Ingber 1997; Ingber 2008)

Mechanotransduction can be divided into *direct mechanotransduction*, which refers to the force transmission pathway from the ECM via integrins, focal adhesions (FAs) and cytoskeleton to the nucleus via the nuclear lamina, and *indirect mechanotransduction*, which refers to the activated biochemical signalling pathways (Anderson et al. 2016). Deviating slightly from this definition, ion channels and cell-cell adhesions via cadherin junctions are also force responsive, and it is suggested that cells use many mechanosensitive elements in order to probe their surroundings (Ingber 2006).

Mechanotransduction is an important field of study, as defects in mechanotransduction can contribute to various human diseases. Impaired mechanotransduction signalling can result from changes in ECM composition, mutations in transmembrane proteins or adhesion complexes, or abnormal protein composition of the cytoskeletal network or nuclear envelope. In addition, abnormalities in the biochemical signalling pathways can be a cause of a disease. Examples of diseases which have been associated with faulty mechanotransduction include arteriosclerosis, muscular dystrophies, cardiomyopathies and cancer. (Jaalouk & Lammerding 2009)

In the following sections, the process of direct mechanotransduction and the force transmission pathway are discussed, followed by a brief discussion of the activated biochemical signalling pathways.

2.2.1 Force transmission from the extracellular matrix

One of the main pathways for force transmission from the extracellular matrix is via integrins, focal adhesions and cytoskeleton. All of these structures are highly dynamic, and especially focal adhesions are very complex and highly interconnected. A common mechanism for many dynamic components in mechanotransduction is force-induced conformational change. (Ingber 2006) Another common feature is the presence of catch bonds and slip bonds. Catch bonds are bonds that strengthen in a response to an applied force, whereas slip bonds weaken in a response to an applied force. It is suggested that formation of catch bonds may be part of the cell tension-sensing mechanism. These kinds of bonds are present in e.g. integrins and myosins, and they affect the longevity of the bonds. (Kong et al. 2009; Kong et al. 2013)

2.2.1.1 Integrins

Integrins are cell surface adhesion receptors, which bind proteins in the extracellular matrix, and as one of the initiators of force transmission integrins are referred to as ‘mechanoreceptors’ (Ingber 2008). These transmembrane proteins consist of two subunits, α and β. There are eight α- and 18 β-subunits, which can assemble to form 24 different integrin heterodimeric combinations, some of which have distinct and some of which have overlapping specificities. Integrins span the plasma membrane and connect the cell to the

ECM, by binding to the filamentous cytoskeleton of the cell on the cytoplasmic side and matrix proteins outside the cell. (Geiger et al. 2001; Thompson et al. 2012)

The signalling pathway via integrins is bidirectional, as integrins can become activated when they bind to ECM proteins (outside-in signalling) or when they receive regulatory signals which originate within the intracellular domains of the cell (inside-out signalling). The activation leads to the initiation of intracellular signalling cascades or to the exertion of traction forces on the ECM, respectively. (Thompson et al. 2012)

As force-induced conformational change is common for the components of mechanotransduction, adhesion to ECM proteins induces allosteric changes in the conformation of integrins, which reveals binding sites on the cytoplasmic side for focal adhesion proteins, such as talin, vinculin, paxillin, zyxin and α-actin (Ingber 2008). These proteins link integrins to the cytoskeleton by forming protein aggregates, known as focal complexes. These are around 1 μm in size and their development is stimulated by Rho-family GTPase Rac. Generally focal complexes are found at the edges of lamellipodia. They subsequently mature into larger focal adhesions, which are 2–10 μm in size and have an elongated shape. (Geiger et al. 2001)

2.2.1.2 Focal adhesions

Focal adhesion formation is preceded by adhesion to the ECM, integrin clustering and focal complex formation. Development into focal adhesions is dependent on the activation of Rho signalling by the GTPase RhoA and the development is further stimulated by actomyosin contractility. (Chrzanowska-Wodnicka & Burridge 1996)

Focal adhesion proteins can be classified as structural proteins, such as talin, vinculin and α-actinin (actin crosslinking protein) or signalling proteins such as paxillin, zyxin, FAK and p130cas. A focal adhesion complex is illustrated in Figure 3.

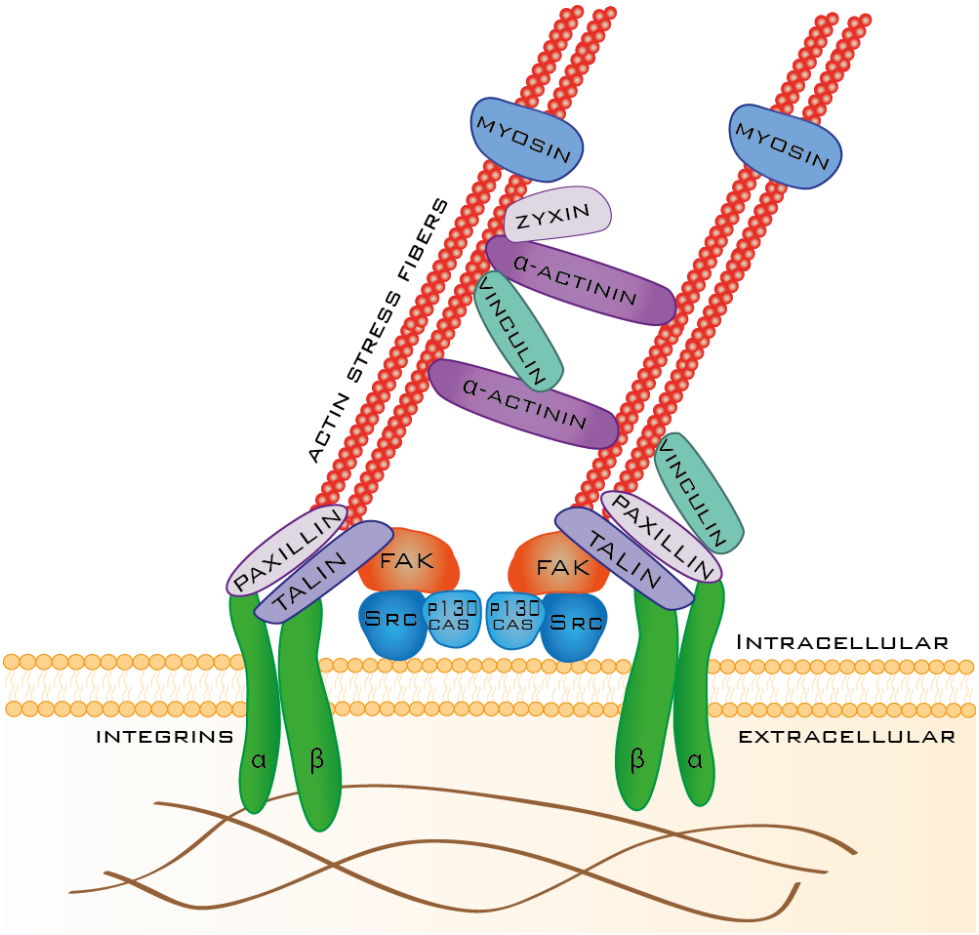

Figure 3. *Schematic illustration of a focal adhesion complex. Integrins connect the cell to the surroundings by binding to ECM proteins outside the cell. Integrins are connected to the cytoskeleton via focal adhesions, which are large protein clusters which also act as signalling centres. (Mitra et al. 2005)*

A key molecule in FA maturation is talin, which is able to connect integrins directly to the cytoskeleton. The head domain of talin binds the β-subunit of integrin and the tail domain can either bind to F-actin directly, or indirectly through vinculin (Schwartz 2010). The bond between talin and vinculin is highly force-dependent, as an unstretched talin has only one binding site available for vinculin, but many more become exposed as a result of applied tension, amplifying the effect (Del Rio et al. 2009). Vinculin reinforces the talin and F-actin linkage by binding to both of them. Loss of vinculin leads to a decrease in traction forces, as myosin-dependent traction forces are vinculin-dependent. (Case & Waterman 2015)

In addition to enabling the link between integrins and cytoskeleton, another major function of focal adhesions is to act as signalling centres. Paxillin is an important linker protein between integrins and the cytoskeleton, which recruits and activates signalling proteins such as focal adhesion kinase (FAK). FAK can activate multiple biochemical signalling pathways, and those are discussed in more detail in Section 2.2.3.

2.2.1.3 Cytoskeleton

As the tensegrity model suggests, the cytoskeleton is an important part of mechanotransduction. The cytoskeleton is responsible for distributing tensile stress to other components inside the cell, to neighbouring cells (via cell-cell interactions) and to the surrounding ECM. It acts as a linker, connecting the ECM all the way to the nuclear membrane. Filamentous cytoskeleton consists of three types of proteins: microfilaments, intermediate filaments and microtubules. All of these filaments are first polymerized out of monomers: microfilaments are polymerized from globular actin (G-actin) monomers to filamentous actin (F-actin), intermediate filaments can be composed of different proteins, according to cell type, and microtubules are hollow filaments polymerized out of α- and β-tubulin monomers. Additionally, many other proteins, such as crosslinkers like α-actinin, and molecular motors, associate with this filamentous network. (Ingber 2008)

Cell shape is closely related to the structure and conformation of the cytoskeleton. The cytoskeleton is constantly being assembled, remodelled and disassembled by the cell, in response to environmental cues. Tension, or pre-stress residing in the cytoskeleton, can be exerted as traction forces to the surroundings, which enables the cells to sense their environment by contracting. Contraction is mediated by endogenously generated tension by actomyosin stress fibers, which are composed of actin microfilaments bundled together by α-actinin and non-muscle myosin II. Pre-stressed structures are more responsive, and the amount of pre-stress determines the stiffness of the structure. (Ingber 2008) Rho family of GTPases is closely linked to the generation of contractile forces, as RhoA is in charge of the polymerization of actomyosin filaments. (Schlessinger et al. 2009) This leads subsequently to the activation of the RhoA/Rho kinase (ROCK) pathway, which is discussed in more detail in Section 2.2.3.

2.2.2 Nuclear mechanotransduction

The nucleus has been shown to respond to mechanical stresses (Lombardi et al. 2011; Booth-Gauthier et al. 2012), and nuclear deformation has been detected in a response to externally applied forces. Such deformations could have significant consequences as they may lead to changes in the nuclear protein conformation, chromatin organization and genome function. (Isermann & Lammerding 2013)

LINC (Linker of nucleoskeleton and cytoskeleton) complex anchors the nuclear membrane to the cytoskeleton and is one of the key structures in nuclear mechanotransduction. LINC complex consists of SUN proteins on the inner nuclear membrane and nesprin proteins, which contain KASH domains, on the outer nuclear membrane, as shown in Figure 4. Both of these proteins are type II membrane proteins, which contain a single transmembrane segment that allows them to form bridges across the nuclear membrane. From the cytoplasmic side, the carboxyl-terminal KASH domains enable attachment to all of

the major cytoskeletal filaments. This bridge unites the cytoskeleton with the nucleoskeleton, and it has been shown to relate closely with correct nuclear positioning. (Guilluy & Burridge 2015)

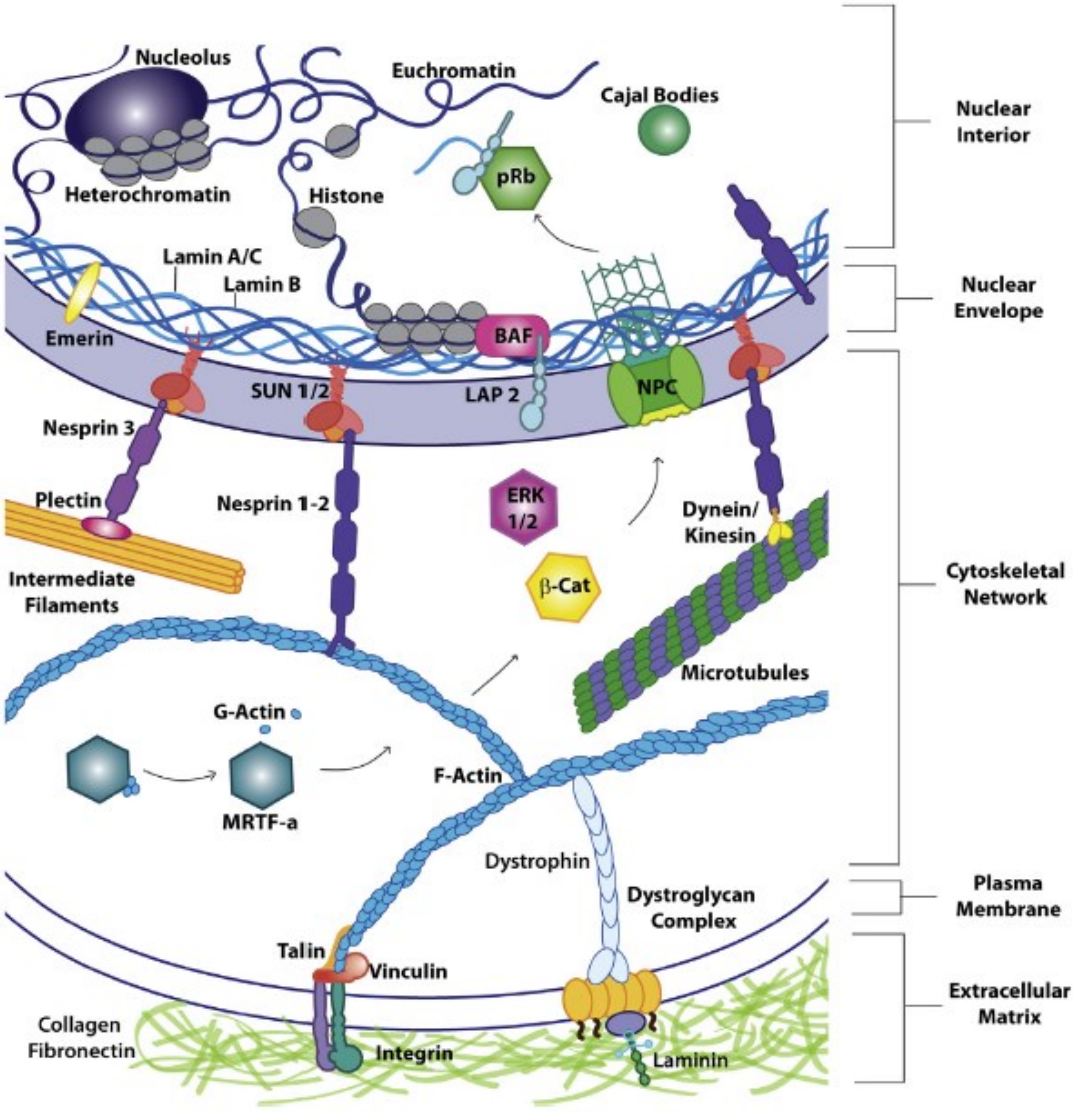

Figure 4. *Force transmission pathway from the plasma membrane to the nucleus. Integrins are connected to actin stress fibers, which are connected from their other end to the nuclear envelope proteins, and this allows the cell to function as a uniformly interconnected system. Reproduced with permission from reference (Fedorchak et al. 2014), Elsevier.*

SUN proteins have a role during mitosis, as they have been reported to participate in chromatin separation from the nuclear envelope and depletion of SUN1 and SUN2 proteins has been shown to lead to disorientation of the mitotic spindle (Turgay et al. 2014). Nesprin 1 has been identified as one of the components regulating the transmission of strain to nucleus (Driscoll et al. 2015).

Lamins are an important group of nuclear envelope proteins (intermediate filaments) that can be seen as an extension of LINC complex, as they interact with both nesprin and SUN

proteins. Lamins provide structural support for the nucleus, as they form the surface of the inner nuclear membrane and are present in the internal nuclear scaffold. Significantly, lamins can interact directly with chromatin and bind to DNA. Lamins can be divided into A-type lamins, (including lamin A and lamin C), and B-type lamin, (lamin B). A-type lamins seem to be more involved in mechanotransduction, as a lack of A-type lamins leads to altered nuclear mechanics and reduced expression of mechanosensitive genes (Lammerding et al. 2006; Wang et al. 2009). A study by Swift et al. (2013) showed that lamin A and C levels scale up in response to increasing matrix rigidity. Lamin A levels increased 30-fold in cells grown on stiffer (40 kPa) gels, compared to soft (0.3 kPa) gels. Adipogenesis was induced by low levels of lamin A on a soft matrix and osteogenesis was induced on a stiff matrix with high levels of lamin A. (Swift et al. 2013) In addition, basal-to-apical polarisation of the nuclear envelope occurs in MSCs which are either undifferentiated or going through osteogenesis, but the polarisation is abolished in cells which are going through adipogenesis. Specific epitopes of lamin A/C have been shown to get buried in the basal nuclear envelope during cell spreading on a rigid substrate or in response to compressive force. (Ihalainen et al. 2015)

Lamins bind many nuclear envelope proteins. One important binding pair is emerin. When tension is applied to the LINC complex, it triggers emerin phosphorylation, which reinforces the connection between LINC complex and lamin A-C. As lamin and emerin have been shown to interact with chromatin, it is likely that the nucleoskeletal response to mechanical stress influences chromatin structure directly. (Burridge & Guilluy 2016)

Nuclear pore complexes (NPCs) are large macromolecular complexes, composed of nucleoporins, which form aqueous channels in the nuclear envelope. NPCs allow fast and selective transport of molecules via active or passive diffusion into and out of the nucleus. As NPCs facilitate messenger RNA (mRNA) export, they are closely linked to chromatin organisation and gene expression. Besides this role as a gateway between the nucleoplasm and the cytoplasm, NPCs are also involved in the physical linkages between the cytoskeleton and nucleoskeleton. The nuclear lamina is coupled to the NPCs, which inhibits the independent movement with respect to each other. It is suggested that mechanical stresses at the nuclear envelope might affect the structure of NPCs and thus the size of the pores. (Soheilypour et al. 2016; Aureille et al. 2017)

2.2.3 Biochemical signalling pathways

Cell adhesion to the surroundings via integrins activates complex biochemical signalling cascades via focal adhesion formation and activation of various signalling pathways, depending on the specificity of integrin-ligand binding. Focal adhesion formation activates FAK, which forms a complex with non-receptor tyrosine kinase Src, and this complex further can activate many downstream signalling pathways, such as the mitogen-activated

protein kinase (MAPK), phosphatidylinositol-3 kinase (PI3K) and RhoA/ROCK pathways. Due to the complexity of these activated pathways, some of the most important ones are briefly reviewed in this section.

MAPK pathways have a role in transduction of extracellular signals into cellular responses, and the pathways are known to activate in response to various growth factors and cytokines. MAPK cascades are involved in many cellular behaviours, such as regulation of cell cycle progression, proliferation, differentiation, development, inflammatory responses and apoptosis. They can be divided to three different branches: c-Jun NH2-terminal kinase (JNK), extracellular signal related kinase (ERK), and p38 kinase. (Zhang & Liu 2002)

The ERK/MAPK signalling may be a key modulator of both osteogenesis and adipogenesis, as ERK signalling can control factors which regulate major nuclear transcription factors Runx2 and PPARγ, which are essential for osteogenesis and adipogenesis, respectively. (Anderson et al. 2016) Activation of both ERK and JNK has been shown to increase with increasing substrate stiffness, and inhibition of these kinases led to decreased osteogenesis and reduced nuclear localisation of Transcriptional coactivator with PDZ-binding motif (TAZ) (Hwang et al. 2015). TAZ and its paralog Yes-associated protein (YAP) are nuclear transducers of the Hippo pathway, which has a role in cell proliferation, tumorigenesis and stem cell renewal. TAZ has been shown to inhibit adipogenesis by inhibiting PPARγ mediated gene transcription and correspondingly activate osteogenesis by stimulating Runx2 target genes (Hong et al. 2005). YAP/TAZ has been shown to be regulated by substrate stiffness, and the activity of YAP/TAZ requires Rho activation and tension of the actin cytoskeleton (Dupont et al. 2011).

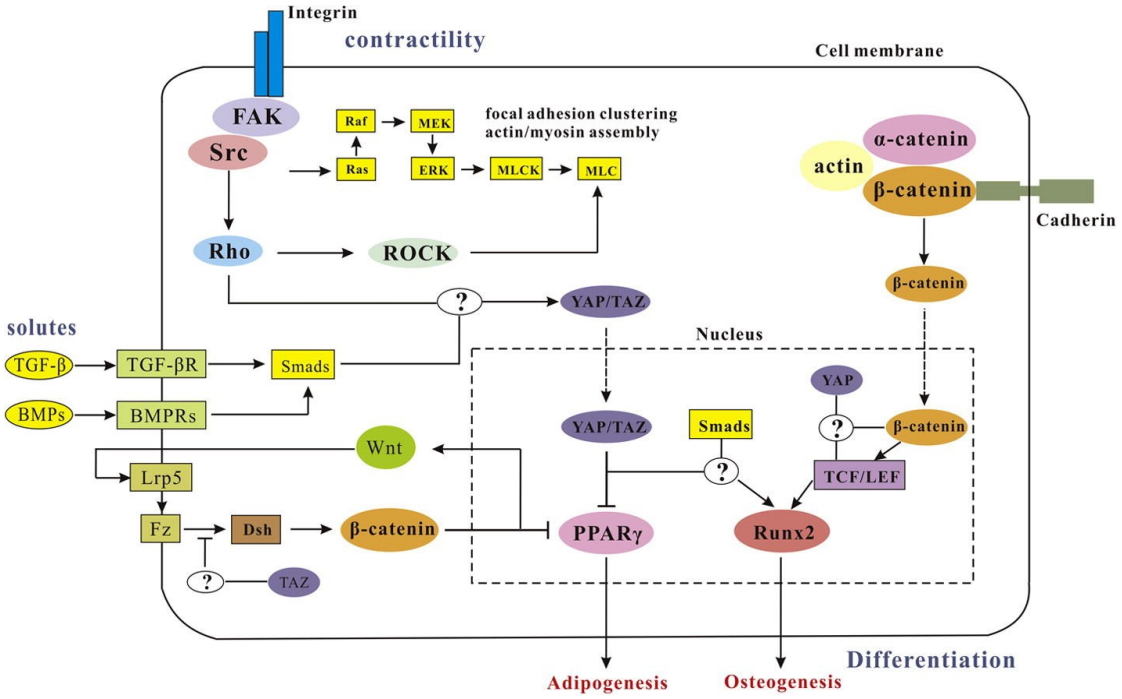

Figure 5. *Signalling pathways activated in contractility-mediated mechanosensing and differentiation. Reproduced with permission from reference (Hao et al. 2015), Elsevier.*

The Wnt pathway does not get activated in response to focal adhesion formation, but it is an important mechanosensitive pathway which transmits signals from cell-cell interfaces. Wnt pathway has a key role during development, and in adults it regulates tissue homeostasis by affecting stem cell proliferation and differentiation. (Schlessinger et al. 2009) The best-studied regulator of Wnt pathway is β-catenin, which transmits mechanotransductive signals from adherens junctions to the nuclear interior, enhancing cell proliferation and growth. It has been shown that nuclear accumulation of β-catenin requires phosphorylation by JNK, which correspondingly requires activation of Rac1, which highlights the complexity of the crosstalk between these signalling pathways (Wu et al. 2008).

RhoA/ROCK signalling controls cytoskeletal organisation of the cell and assembles it according to environmental cues. The Rho family of small GTPases include Rho, Rac and Cdc42, and they all have distinct functions in cytoskeletal organisation. Rho regulates stress fiber formation and cell contractility, Rac controls lamellipodia formation and Cdc42 regulates filopodia formation. In addition, Rho family GTPases alter microtubule dynamics and therefore cell polarity. RhoA pathway has many known effectors, the best-known being ROCK, which regulates myosin light chain phosphorylation and actin-myosin contractility. The contraction of stress fibers is regulated by myosin light chain phosphorylation and by calcium-dependent myosin light chain kinase. (Amano et al. 2010; Hao et al. 2015)

2.3 Hydrogels

Hydrogels are water-swollen 3D polymer networks. They are attractive materials for biomedical applications, as they mimic the properties of natural tissue environments better than 2D cell culture substrates. They have a high water content, similar to that of natural tissues, and the elastic modulus of hydrogels is typically within the kilopascal range, which is similar to that of natural soft tissues (Tibbitt & Anseth 2009).

2.3.1 Classification, fabrication and properties

2.3.1.1 Classification

As a versatile class of biomaterials, hydrogels can be classified in many ways. The most straightforward approach is to classify hydrogels according to their origin, either as natural, synthetic or hybrid hydrogels (Hoffman 2002). Natural hydrogels, such as collagen, HA and alginate, are often used for biomedical applications because of their biocompatibility, biodegradability and inherent biological functions. However, because of their inherent bioactivity, it is difficult to determine exactly which signals are promoting cellular behaviours. Naturally derived hydrogels also possess a threat of potential immunogenic reactions and batch-to-batch variability. Synthetic hydrogels, such as various polyesters, on the other hand, do not possess inherent bioactivity and thus engineering materials with defined properties is easier. In general synthetic hydrogels have better mechanical properties and durability compared to natural hydrogels. (Tibbitt & Anseth 2009)

Alternatively, hydrogels can be classified according to their degradability, either as biodegradable or non-biodegradable hydrogels. Other classification parameters may include the preparation method, type of crosslinks or the ionic charge of the network. (Slaughter et al. 2009)

2.3.1.2 Fabrication

The network structure of hydrogels is obtained by crosslinking. Crosslinking can be done by physical or chemical means. Physical gels are bound either by molecular entanglements or by weaker non-covalent forces, such as hydrogen bonds or ionic or hydrophobic interactions. These gels are not homogenous and the networks can have free chain ends or loops that cause temporary network defects. (Hoffman 2002) Physical hydrogels can be fabricated by photopolymerisation using irradiation or ultraviolet light, or in response to temperature. Crosslinking by radiation does not require the usage of toxic crosslinking agents or other impurities (Ahmed 2015), but it has been shown that unreacted radicals can be left in the gel, causing cells to apoptose (Raza & Lin 2013).

Hydrogels that are crosslinked by covalent bonds are called ‘chemical’ or ‘permanent’ gels. Chemically crosslinked hydrogels tend to be more homogenous, but can still contain areas with variable crosslinking density or swelling. Crosslinking is commonly done by

chemical reaction, such as click chemistry. Chemical crosslinking can often be achieved through facile reactions, but chemical residues from some reactions can be toxic to cells, which may compromise the biocompatibility of the product. (Peppas & Hoffman 2013)

Hydrogels are known for their extensive swelling properties and they consist of 'total bound water', which can be divided to primary bound water and secondary bound water. When the hydrogels start to swell the first water molecules will react with the most hydrophilic groups and therefore they are called primary bound water. After the hydrophilic groups are hydrated the secondary bound water will react with recently exposed the hydrophobic groups. As all of the polar and non-polar groups have been occupied the network absorbs additional water and will reach an equilibrium swelling level. (Hoffman 2002) The swelling ratio is inversely proportional to crosslinking density, which means that less crosslinked, and therefore softer gels generally contain more water (Singh et al. 2013).

2.3.1.3 Physical properties

Hydrogels are attractive materials for cell culture and regenerative medicine applications, as several of their physical properties can be tailored to suit specific needs. Important physical properties of hydrogels include stiffness (or elasticity), swelling, pore size (i.e. mesh size) and degradation. The stiffness of a hydrogel can be modified by increasing or decreasing the level of crosslinking of the polymer network. The pore size correlates with the swelling behaviour and mechanical properties of the hydrogel, and smaller pore size generally results in lower swelling and higher modulus. The pore size is on the nanometer scale, and it is one of the most crucial parameters of the hydrogel, as it affects the flux of nutrients through the material. Degradation of synthetic hydrogels can be modified by addition of enzymatically degradable peptide crosslinkers into the network structure. Some natural polymers such as HA are commonly enzymatically degradable even without any modifications, but others, such as gellan gum, which is not found in eukaryotic organisms, are not degradable by mammalian cells. (Caliari & Burdick 2016)

As hydrogels have stiffnesses similar to those of natural tissues, hydrogels generally have poor mechanical strength, which limits their use for load-bearing applications. Another frailty is that hydrogels consisting of fibrous proteins such as collagen can shrink during cell culture, due to the exertion of mechanical forces by cells. In addition, sterilisation of hydrogels can be challenging. For cell encapsulation, hydrogel components must be sterilised before gelation. This can be done by sterile filtering the solution containing the hydrogel components, or through germicidal UV irradiation of the solution or dry polymer components. However, special attention must be paid to the selection of the sterilisation technique, to prevent the hydrogel components from unintentional degradation or denaturation. (Caliari & Burdick 2016)

2.3.2 Poly(ethylene glycol) hydrogels

Poly(ethylene glycol) (PEG) hydrogels are synthetic hydrogels, which have gained attention among researchers due to their biocompatibility and bioinertness. PEG hydrogels do not cause immunogenic reactions, and due to their hydrophilicity they induce only minimal protein adsorption onto their surface. Therefore, they can be considered as blank slates for tissue engineering applications. (Zhu 2010)

PEG is a polyether that can have a linear or a branched structure. The branched structures can be multi-arm or star shaped, e.g. with three, four, six or eight arms. (Zhu 2010) The structure of a four-arm PEG is shown in Figure 6. PEG does not have functional groups on its backbone but the ends groups of the molecule can be easily modified with different functional groups, bioactive agents or other molecules. This is required for crosslinking or conjugation of cell adhesive groups. (Singh et al. 2013)

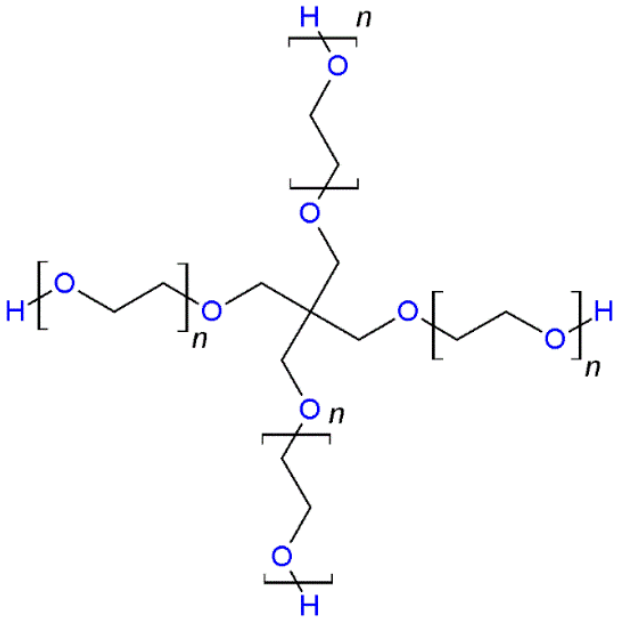

Figure 6. *Structure of 4-arm PEG.*

Due to the bio-inert nature of PEG, further modifications with biological motifs are needed in order to form hydrogels. PEG can be modified with cell adhesion ligands, growth factors or other biomolecules in order to promote cell survival or induce biological responses. PEG itself is not hydrolytically degradable, though enzymatic degradability, a property that is important for many biomedical applications, can be introduced.

2.3.3 Hyaluronan hydrogels

Hyaluronan (HA) or hyaluronic acid is a non-sulfated GAG, which is present in all of the connective tissues throughout the body as one of the components of the ECM. HA is extensively present in the vitreous of the eye and in cartilage. (Burdick & Prestwich 2011)

As a negatively charged molecule, HA has high capacity for binding water, and it is important for the hydration of tissues. It is also important for other biological processes. For example, during embryogenesis, HA makes up a large proportion of the tissues, and later on, it affects the structure and function of adult tissues and has a role in wound healing. *In vivo*, HA has a rapid turnover time, and it can be degraded enzymatically by hyaluronidases. (Burdick & Prestwich 2011)

HA is a linear polysaccharide, which consists of repeating disaccharide units of β-1,4-D glucuronic acid-β-1,3-*N*-acetyl D-glucosamine, shown in Figure 7. The molecule can be chemically modified, and the modifications usually target three functional groups: the glucuronic acid carboxylic acid, the primary and secondary hydroxyl groups and the *N*-acetyl group (Burdick & Prestwich 2011).

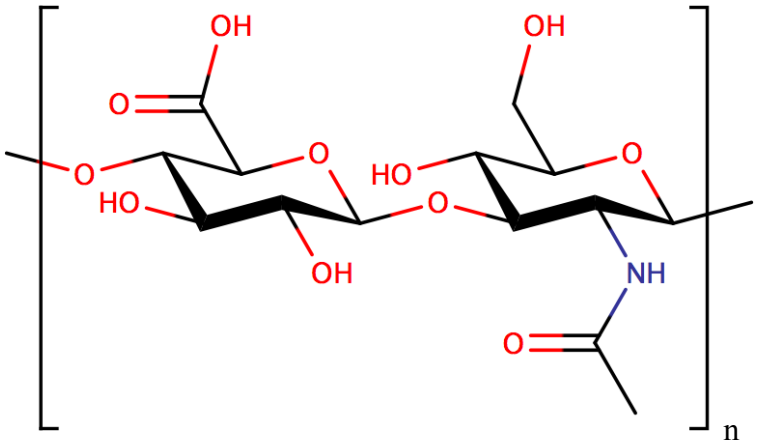

Figure 7. *Structure of a hyaluronan monomer.*

The biofunctionality, biocompatibility and multiple sites of modification make HA an attractive material for tissue engineering research. It has been noted as an important material for studying the effects of environmental cues on cell fate. Of important note, it has been shown that embryonic stem cells maintain their undifferentiated state and differentiation capacity when encapsulated in HA gels (Gerecht et al. 2007). This could be due to the high amount of HA during embryonic development.

Even though unmodified HA does not support integrin-mediated cell adhesion, cells are known to interact with HA via CD44 receptors. CD44-mediated interactions have been suggested to have a role in cell adhesion and migration (Zhu et al. 2006) and this process may be mechanosensitive to matrix stiffness (Kim & Kumar 2014). These interactions may complicate the experimental set up, and when studying effects of adhesion ligand presentation in these hydrogels, HA-CD44 interactions could potentially be blocked by antibodies.

2.4 Effects of adhesion ligand presentation on cell behaviour

Cell-matrix adhesion is crucial for preventing anoikis in anchorage-dependent cells such as MSCs. Most synthetic biomaterials do not support cell adhesion in their pure form and therefore these materials are commonly modified with cell adhesion ligands. In early studies, cell-biomaterial adhesion was improved by anchoring whole proteins to the material surface. Some proteins that enhance cellular adhesion include fibronectin, laminin, collagen, elastin, bone sialoprotein and vitronectin (Zhu & Marchant 2011).

Immobilisation of whole proteins on synthetic materials has many disadvantages, such as eliciting undesirable immune responses and introducing non-specific binding motifs. In practice, large proteins fold, denature and undergo enzymatic degradation. Short peptide sequences derived from these proteins are a more stable option for enhanced cellular adhesion. Short peptide motifs that are recognised and bound to by integrins – called adhesion ligands – can also be attached to the surface at higher densities, as they do not require as much space as whole proteins. The most commonly used ligand for immobilization is RGD, which is found in various proteins, including fibronectin, collagen, laminin, vitronectin and bone sialoprotein. *In vivo*, RGD is widely distributed amongst different tissues and it has a role in cell anchoring, behaviour and viability. RGD is available in cyclic (cRGD) and linear forms (Zhu 2010) and it can be attached on to the surface or within the bulk of the hydrogel. The cyclic form mimics the looped conformation of RGD found in fibronectin and has much higher affinity for integrin than linear RGD. Other well-known adhesion peptides include GFOGER, REDV and IKVAV. (Hersel et al. 2003)

The dimensionality of the microenvironment has a major effect on cell behaviour, as cells encapsulated within a 3D hydrogel have a very different environment compared with cells on 2D substrates. When cells are cultured as a monolayer on the bottom of a well of a cell culture plate, cell adhesion to the substrate is restricted only in a planar direction, which results in abnormal polarisation of the cells. In addition, the stiffness of the underlying substrate is usually very high, in the case of a well plate around 3 GPa (Yang et al. 2014), which is a lot higher than the stiffnesses of the natural tissues, listed in Table 1. The flow of nutrients and waste is much more hindered in a 3D matrix, compared to on a 2D substrate, and gradients of soluble factors form. (Tibbitt & Anseth 2009; Lv et al. 2015) Even though 3D environments better resemble the structure of natural tissue, carrying out single variable studies is quite challenging due to the added complexity of the 3D environment, as many of the material properties synergistically influence one another and alter cell behaviours.

2.4.1 Studies carried out in 2D

In 2D, much research has focused on evaluating the effects of adhesion ligand presentation on cell shape, integrin clustering and cytoskeletal architecture. In the case of stem

cells, the correlations between adhesion ligand presentation, cell spreading and cell differentiation have been investigated.

McBeath et al. (2004) showed that by restricting human mesenchymal stem cell (hMSC) spreading, it is possible to guide their differentiation. Micropatterned cell culture substrates were fabricated by microcontact printing different sized fibronectin islands (1,024, 2,025 and 10,000 μm^2) onto polydimethylsiloxane (PDMS) substrates, and the islands were surrounded by non-adhesive regions. MSCs were cultured on these substrates for one week in co-induction medium, which contains cues for differentiation to both adipocytes and osteoblasts. Cells cultured on the largest fibronectin islands were able to spread and they underwent osteogenesis, and on the smallest fibronectin islands where spreading was not possible, rounded cells became adipocytes. Both adipocytes and osteoblasts were observed on the intermediate sized islands. It was demonstrated that when both rounded and spread cells were infected with an adenovirus containing a constitutively active ROCK, all cells became osteoblasts, regardless of the original morphology. This kind of virally induced osteogenesis could be blocked with a myosin II inhibitor. Thus, ROCK-induced myosin-generated cytoskeletal tension was shown to regulate hMSC commitment between adipogenic and osteogenic fates. (McBeath et al. 2004)

Work with fibronectin islands was continued by Théry et al. (2006). PDMS stamps with different geometries (∇, V, T, Y and Π) were coated with fibronectin and added to silanised glass coverslips, and the surrounding areas were coated with non-adhesive PEG-maleimide solution. When culturing epithelial cells in basic medium (BM) on these fibronectin islands, cell spreading followed the shape of an equilateral triangle (excluding cells on the Π shape), and the cell membrane hung over the non-adhesive areas on V, T and Y shapes. It was noted that cytoskeletal tension was not identical within the cells, as much stronger stress fibers and larger focal adhesions were observed on the non-adhesive edges. Therefore, the results indicated that the ability of the cell to form multiple cell-ECM attachments along the edges of the membrane alters the strength of the stress fibers. (Théry et al. 2006)

Several studies have shown that it is possible to guide stem cell fate by altering the shape of the adhesive island. Kilian et al. (2010) fabricated different shapes of adhesive fibronectin islands by microcontact printing on to a PDMS substrate, and cultured individual hBMSCs in co-induction medium for a week. Fabricated shapes included rectangles with different aspect ratios (1:1, 3:2 and 4:1), and it was shown that osteogenesis increased with aspect ratio. In addition, when studying flower, pentagon and star shapes it was observed that osteogenesis increased with shapes which included steeper angles and thus increased cytoskeletal tension. On circular islands, 74% of the cells favoured adipogenic fate, and on angular, holly-shaped islands, 67% of cells differentiated to osteoblasts. When cytoskeletal contractility was inhibited, cells differentiated to adipocytes. On the other hand, when cytoskeletal contractility was increased, MSCs differentiated to osteo-

blasts. The results highlighted the importance of adhesion and contractility for osteogenesis. When studying the activation of biochemical signalling pathways, the results indicated that inhibition of ERK and JNK pathways resulted in decrease in osteogenesis. (Kilian et al. 2010)

The findings of Kilian et al. were supported by the results of Peng et al. (2011), who also cultured cells on different shapes of adhesive islands. Adhesive RGD micro-islands, with different shapes but the same adhesive area of around 900 μm^2 in each, were fabricated on PEG hydrogels. Four different shapes were compared: circle, square, triangle and star. Individual rat MSCs were cultured on these islands for six days in either OM or AM. High cytoskeletal tension was observed within the cells on multi-angular geometries, but not in the cells which were cultured on circular shapes. Correspondingly, osteogenesis was most intensively present on angular shapes, and adipogenesis on circular shapes. (Peng et al. 2011)

The work by Spatz's group has thoroughly demonstrated the effects of RGD-ligand spacing on cell adhesion, spreading and migration. Studies have been carried out on precise RGD-modified nanopatterns, prepared with diblock copolymer micelle nanolithography. Briefly explained, glass slides were first patterned with gold nanoparticles with various spacings, and the space between nanodots was covered with non-fouling PEG to prevent cell or protein adsorption. Gold nanoparticles were functionalised with cRGD ligands, and as the size of the nanoparticle was around 8 nm, each one allowed the attachment of only one integrin heterodimer (~12 nm), and thus enabled the study of lateral integrin clustering. When osteoblasts were cultured on substrates with inter-ligand nanospacings of 28, 58, 73 or 85 nm, cell spreading and co-localisation of integrin, vinculin and FAK were observed on smaller nanospacings, but not at 73 nm or 85 nm. It was determined that cells are not able to form stable focal adhesions at nanospacing of 73 nm or larger, due to limited lateral clustering of integrins. (Arnold et al. 2004) In addition, when fibroblasts were cultured on two different nanospacings, 58 and 108 nm, cells were able to attach to both substrates, but cells spread well only on 58 nm, and on 108 nm cell spreading was delayed and repeated protrusion-retraction cycles were observed. In addition, cells on 108 nm only formed unstable contacts, in which vinculin and zyxin did not co-localise with actin stress fibers. (Cavalcanti-Adam et al. 2007)

Similar to the work carried out by the Spatz group, Frith et al. (2012a) studied the effects of different nanospacings on mesenchymal stem cell behaviour. hBMSCs were cultured for 10 days in a co-induction medium on non-adhesive poly(styrene-block-ethylene oxide-maleimide) (PS-PEO-Ma) copolymer surfaces functionalised with RGD ligands at four different nanospacings: 34, 44, 50 or 62 nm. Cells cultured on 34 or 44 nm spacings had larger spread areas and well defined actin cytoskeleton, and cells on 50 or 62 nm nanospacings had more disorganised actin cytoskeleton. On 62 nm nanospacings, cells extended multiple filopodia. Larger focal adhesions were observed on smaller nanospac-

ings, and on larger nanospacings vinculin did not localise to the ends of the actin filaments. Based on gene expression analysis and Alizarin Red and Oil Red O stainings, it was concluded that 34 nm nanospacing supported osteogenesis and 62 nm spacing supported adipogenesis. (Frith et al. 2012a)

Even though many of the studies indicate that smaller nanospacing of adhesion ligands is beneficial for osteogenesis, contradictory results were obtained by Wang et al. (2013). Block copolymer micelle nanolithography was employed to fabricate varying RGD densities on PEG hydrogel surfaces, and the nanospacings under study were 37, 53, 77, 87 or 124 nm. When bone marrow stromal cells (BMSCs), isolated from a rat, were cultured in a co-induction medium for seven days on these patterns, osteogenesis was predominant over adipogenesis on larger RGD nanospacings (53–124 nm), even though opposite results had been obtained according to previous studies with nanopatterns. (Wang et al. 2013)

Contradictory results could arise from the differing elasticies of the substrates. On the stiffer block copolymer substrates used by Frith and Spatz, the cells spread very flat when the spacing between the ligands was small and there was a lot of intracellular tension. When the spacing between the ligands was large, cells could not spread and exert tension on the substrate to deform it, and thus the cells remained rounded. This correlates with the differentiation, which displayed similar behaviour to the differences seen between stiff versus soft 2D substrates. On softer hydrogels, used by Wang et al., the morphology had a similar correlation with differentiation. The reason for the increased osteogenic differentiation at higher nanospacings may be because the lower stiffness of the material allowed the cells to bind to and deform the gel, enabling them to reach ligands which are spaced further apart. The clustering of integrins may have then brought ligands within the gel closer together, making the gel more densely concentrated and stiffer than in gels with higher ligand density, which required less deformation for integrin clustering.

In addition to the studies concerning the nanospacing of adhesion ligands, the effects of ligand identity have been compared by Rowlands et al. (2008). Polyacrylamide (PA) hydrogels with varying stiffnesses (0.7, 9, 25 or 80 kPa) were coated with one of four different ECM molecules: fibronectin, laminin or collagens I or IV. hBMSCs were cultured for 14 days in basic medium on top of these gels. Osteogenesis was significantly more prominent on the stiffest gel (80 kPa) coated with col I. As collagen I makes up 80% of the protein content of bone, this demonstrates the importance of biomimetic environments for gene expression activation. On the other hand, myogenesis was observed on all gels with stiffness higher than 9 kPa, regardless of the protein coating. (Rowlands et al. 2008)

Frith et al. (2012b) studied hMSC behaviours on PS-PEO-Ma substrates which were functionalised with one of four different adhesion ligands: RGD, RRETAWA, IKVAV or YIGSR. IKVAV and YIGSR are both sequences present in laminin, and RRETAWA is

a synthetic sequence with affinity to only $\alpha_5\beta_1$ integrin. hMSCs obtained a classic fibroblastic morphology and spread well on RGD-modified surfaces. Stress-fibre formation was observed on RGD and RRETAWA-presenting surfaces, but not with IKVAV or YIGSR. When culturing cells in co-induction medium for 21 days, IKVAV was shown to support osteogenesis, and IKVAV and RRETAWA supported adipogenesis. RGD was needed to ensure the viability of hMSCs beyond initial attachment. (Frith et al. 2012b)

Studies mentioned in this section are summarised in Tables 2 and 3. All in all, the results obtained from studying cell behaviour on 2D substrates indicate that the adhesion ligand density affects the cytoskeletal architecture of the cell. Cells which are able to spread and form an organised cytoskeleton are more likely to differentiate to osteoblasts, and when cells are forced to adopt a rounded morphology, they differentiate to adipocytes. Stable focal adhesions are formed only when the ligand density is sufficient. In addition, the adhesion ligand identity can alter cell responses. Apart from the effects of adhesion ligand presentation, also the stiffness of cell culture substrate was shown to alter the study outcomes. Culturing cells on substrates with different stiffnesses can guide stem cell differentiation, and this was first demonstrated by Engler et al. (2006). (Engler et al. 2006)

Table 2. *Summary of studies carried out with adhesive microislands in 2D. Co-induction refers to a mixture of osteogenic and adipogenic medium.*

Reference	Cell type	Material	Adhesion ligand	Culture time	Culture medium	Cell response
McBeath et al. 2004	hMSCs	PDMS substrate	FN	7 days	Co-induction	Spread cells differentiated to osteoblasts and rounded to adipocytes.
Théry et al. 2006	Epithelial cells	Glass coverslip with varying geometries of PDMS stamps	FN	-	BM	Stronger stress fibers and larger FAs were formed to the non-adhesive edges of the cell membrane.
Kilian et al. 2010	hBMSCs	PDMS substrate	FN	7 days	Co-induction	Contractility of the cytoskeleton was important for osteogenesis.
Peng et al. 2011	Rat MSCs	PEG hydrogel surface	RGD	6 days	OM, AM	Higher cytoskeletal tension and increased osteogenesis were observed on angular shapes.

Table 3. *Summary of studies carried out with various ligand spacings or ligand identities. Co-induction refers to a mixture of osteogenic and adipogenic medium.*

Reference	Cell type	Material	Ligand	Ligand spacing	Culture time	Culture medium	Cell response
Arnold et al. 2004	Osteo-blasts	Glass coated with PEG	RGD	28, 58, 73, 85 nm	1 day	BM	Cells were not able to form stable FAs at nanospacing of ≥ 73 nm.
Cavalcanti-Adam et al. 2007	Fibro-blasts	Glass coated with PEG	RGD	58, 108 nm	-	BM	At 108 nm, cell spreading was delayed, with repeated protrusion-retraction cycles.
Frith et al. 2012a	hBMSCs	PS-PEO-Ma	RGD	34, 44, 50, 62 nm	10 days	Co-induction	34 nm supported osteogenesis and 62 nm adipogenesis.
Wang et al. 2013	Rat BMSCs	PEG hydrogel	RGD	37, 53, 77, 87, 124 nm	8 days	Co-induction	Osteogenesis was predominant in large nanospacings over adipogenesis.
Rowlands et al. 2008	hBMSCs	PA hydrogel	FN, laminin, col I, col IV	N/A	14 days	BM	A biomimetic ligand and high stiffness were beneficial for osteogenesis.
Frith et al. 2012b	hBMSCs	PS-PEO-Ma	RGD, IKVAV, RRETAWA, YIGSR	N/A	21 days	Co-induction	RGD was not beneficial for differentiation, but needed for maintaining cell viability.

2.4.2 Studies carried out in 3D

The importance of adhesion ligand presentation has been demonstrated in 3D environments as well. As PEG itself does not support cell adhesion, the viability of adherent cells on an unmodified material is very low. A study by Nuttelman et al. (2005) showed that after one week in culture, hMSC viability was 75% in acryl-PEG gels with an RGD concentration of 2.8 mM, and only 15% within gels with no adhesion ligands (Nuttelman et al. 2005).

Salinas & Anseth (2008b) demonstrated the importance of the way in which adhesion ligands are incorporated to the polymer network. They compared different ways of RGD ligand attachment to a PEGDA hydrogel network, and studied how it influenced cell viability and FA formation. In unmodified PEGDA gels, cell viability was only 7.3% after 14 days of culture in BM. Covalently attaching RGD to the polymer network resulted in 70% cell viability. A short, tethered RGD sequence promoted 79 % survival, while a dually attached RGD, which was bound from both ends of the peptide, supported cell viability of 61% after 14 days. Lower viability on dually attached RGD gels can be explained by steric hindrance, which occurs when the peptide is bound from both ends to the material and prevents integrins from binding the peptide, and therefore from attaching to the substrate. RGD which was attached with a spacer arm sequence to the network, enabled the highest hMSC viability, 84% after 14 days. The spacer arm sequence creates distance between the RGD ligand and the polymer backbone, which is thought to facilitate integrin binding. The most extensive focal adhesion formation was observed with the short tethered RGD and with the RGD containing a spacer arm sequence. Soluble RGD blocks integrin binding and this resulted in viability of 6%, which is similar to the viability of cells in unmodified PEG. (Salinas & Anseth 2008b)

RGD presentation has been shown to inhibit chondrogenesis in alginate and agarose hydrogels. Connelly et al. (2007) studied bovine bone marrow stromal cells encapsulated in alginate hydrogels, functionalised with either RGD ligands or non-adhesive RGE sequences. After seven days in culture in either CM or BM, the chondrogenic gene expression was higher in the cells which were cultured in chondrogenic medium, but even the differentiation medium did not stimulate the gene expression over basal levels in RGD-functionalised alginate gels. In addition, the cartilaginous matrix synthesis seemed to be inhibited in the presence of adhesion peptides, and sulphated GAG accumulation, a marker of chondrogenesis, seemed to decrease with increasing RGD density. (Connelly et al. 2007) In agarose gels, similar results were obtained by Connelly et al. (2008). Calf BMSCs were encapsulated in agarose hydrogels functionalised with 400 μM RGE or RGD. After seven days of culture in BM or CM, 24% less GAG accumulation was observed in RGD-modified gels compared to non-adhesive RGE-modified gels. The GAG levels were similar in RGE or unmodified gels. Interactions with RGD-ligand seemed to

inhibit the chondrogenic response to the differentiation medium, but it enhanced osteogenic response in basic medium. The inhibition of chondrogenesis was related to cytoskeletal organisation, as the inhibition was blocked and chondrogenesis favoured by disruption of the F-actin cytoskeleton and blocking the cell spreading. (Connelly et al. 2008)

Salinas & Anseth (2008a) fabricated biomimetic PEGDA hydrogels which contained cues specifically for induction of chondrogenic differentiation. They designed enzymatically degradable peptide sequences, which contained RGD ligands and a cleavage site for matrix MMP 13, which is found in aggrecan, a major marker of chondrogenesis. Enzymatic cleavage and degradation of these peptides results in the release of the RGD peptide. Initial attachment to fibronectin has been found to be important for chondrogenesis, but at later stages unbeneficial, as noted by Connelly et al. (2008). hMSCs were cultured for 24 days in CM. After three weeks of culture, GAG production was 10 times higher in gels with cleavable RGD sequences, compared to gels with uncleavable RGD peptides. In addition, 75% of the cells in degradable RGD gels were positive for collagen type II deposition, and only 19% were positive in the gels where RGD remained. (Salinas & Anseth 2008a)

GFOGER, a motif present in many types of collagens, has been shown to be more beneficial for inducing chondrogenesis, compared to RGD peptide. Mhanna et al. (2014) fabricated degradable and non-degradable PEG hydrogels modified with either GFOGER or RGD. After 21 days in culture in CM, proliferation of hMSCs was four times higher on GFOGER-modified degradable gels compared to degradable gels with no adhesion sequences. In addition, proliferation was two times higher on GFOGER-modified gels compared to RGD-modified gels. Degradable hydrogels enhanced cell spreading, and thicker actin filaments were observed on the cells embedded in RGD modified gels. Cells within GFOGER-modified gels contained thinner and more dispersed actin cytoskeleton, which is associated with chondrogenesis. Degradability was concluded to be essential for chondrogenesis in hydrogels modified with adhesion peptides. (Mhanna et al. 2014)

Huebsch et al. (2010) encapsulated clonally derived murine MSCs in alginate hydrogels, modified with RGD. Elastic moduli of the hydrogels was varied between 2.5 and 110 kPa, and the RGD density was varied in parallel. After seven days in culture in co-induction medium, osteogenesis was observed on the gels with intermediate stiffnesses, 11–30 kPa, and adipogenesis was observed in softer gels with moduli from 2.5 to 5 kPa. Cell morphology did not correlate with stem cell fate. However, when primary hMSCs where cultured on these gels, they exhibited more heterogeneous lineage commitment in response to the stiffness of the gels, consistent with the heterogeneity of the naïve cell population. (Huebsch et al. 2010)

Khetan et al. (2013) encapsulated MSCs in covalently crosslinked hyaluronan hydrogels, which were modified with RGD adhesion ligands and MMP-degradable crosslinks. After seven days in culture in BM, cells were more spread and could deform the surroundings

to a larger extent in the degradable gels, compared to gels in which proteolytic degradation was impeded. Cells which were encapsulated in gels without adhesion ligands remained rounded and exhibited minimal traction forces and low viability, which indicated that cell spreading and traction generation were dependent on the adhesion ligand presentation and integrin binding. Cells remained undifferentiated after seven days of culture. Cells were grown for an additional 14 days in co-induction medium, and osteogenic differentiation was observed in the degradable gels, whereas the gels which could not be degraded supported adipogenesis. Generation of cellular traction forces through matrix adhesions was concluded to be a guiding factor between osteogenic and adipogenic fates. (Khetan et al. 2013)

Studies mentioned in this section are listed in Tables 4 and 5. As a summary, the 3D environment adds complexity to the study settings. When cells are encapsulated into a hydrogel, they are forced to adopt a rounded morphology. Besides adhesion ligand presentation, degradability of the material is essential to enable cell spreading. It is suggested that adhesion ligands act as handles, by which the cells can sense the properties of their surroundings, such as stiffness of the gels. The strong correlation between cell shape and differentiation observed in 2D environments does not seem to be so extensively present in 3D environments. Some studies have shown that cell morphology and differentiation do not correlate, as rounded cells underwent osteogenesis, while others conclude that cell spreading is beneficial for osteogenesis in 3D as well. By attaching to adhesion ligands, cells are able to organise their cytoskeleton and generate traction forces, which might be the switch between adipogenesis and osteogenesis. As all the properties of the matrix affect the cell behaviours in combination, it would be important to prepare such platforms where the properties could be studied also irrespective of each other.

Table 4. *Summary of studies carried out in 3D, 1/2.*

Reference	Cell type	Material	Ligand	Ligand concentration	Culture time	Culture medium	Cell response
Nuttelman et al. 2005	hMSCs	PEGDA	RGD	0, 2.8 mM	7 days	BM	75% cell viability observed in RGD-modified gels, 15% viability in control gels.
Salinas & Anseth 2008b	hMSCs	PEGDA	RGD	-	14 days	BM	Presentation of RGD ligand altered cell responses.
Connelly et al. 2007	Bovine BMSCs	Alginate	RGD, RGE	0, 0.01, 0.1, 1mM	7 days	CM, BM	Interactions with RGD decreased the expression of chondrogenic markers.
Connelly et al. 2008	calf BMSCs	Agarose	RGD, RGE	0, 200, 400 μM	7 days	CM, BM	Interactions with the peptide increased cell spreading and inhibited chondrogenesis.

Table 5. *Summary of studies carried out in 3D, 2/2. Co-induction refers to a mixture of osteogenic and adipogenic medium.*

Reference	Cell type	Material	Ligand	Ligand concentration	Culture time	Culture medium	Cell response
Salinas & Anseth 2008a	hMSCs	Degradable PEGDA	RGD	-	24 days	CM, BM	Cleavability of RGD was beneficial for chondrogenesis.
Mhanna et al. 2014	hMSCs	Degradable and non-degradable PEG	GFOGER, RGD	0, 100 μM	21 days	CM	Ligands increased proliferation, degradability was essential for chondrogenesis.
Huebsch et al. 2010	Murine MSCs, hMSCs	Alginate	RGD	7.5, 37 and 754 μM	7 days	Co-induction	Cell fate was not correlated with morphology. Osteogenesis at 11–30 kPa and adipogenesis 2.5–5 kPa.
Khetan et al. 2013	hMSCs	Degradable HA	RGD	0, 754 μM	21 days	BM, followed by co-induction	Differentiation was dependent on degradation-mediated traction.

3. AIMS OF THE STUDY

The original aim of the study was to contribute to the fabrication of highly modular PEG-peptide hydrogels, and to study the effects of adhesion ligand density on hBMSC viability and differentiation in these gels. The results would be related only to the material properties, as no differentiation media would be used. However, as the project faced delays in the fabrication of PEG hydrogels, the focus was shifted to hyaluronan hydrogels in order to fit the cell culture studies to the time frame of this thesis. Preliminary studies concerning cell viability were carried out over a week of culture. Two types of hyaluronan hydrogels were compared: one containing fibronectin, which contains cell adhesion ligands, abbreviated as HAH-FN, and one without adhesion ligands, abbreviated as HAH.

The specific aims of the thesis were:

I To optimise functionalisation of PEG with 4-NPC and achieve as high degree of functionalisation as possible.

II To optimise RNA extraction from PEG-peptide hydrogels by comparing two commercially available RNA extraction kits and two different buffers.

III To compare cell viability, morphology and number in hyaluronan hydrogels with or without fibronectin.

4. MATERIALS AND METHODS

4.1 Workflow

The workflow of the thesis project is presented in Figure 8. First, PEG4NPC synthesis was optimised. Then, RNA extraction was optimised from PEG hydrogels which were crosslinked with a simple peptide, but did not possess any adhesion ligands.

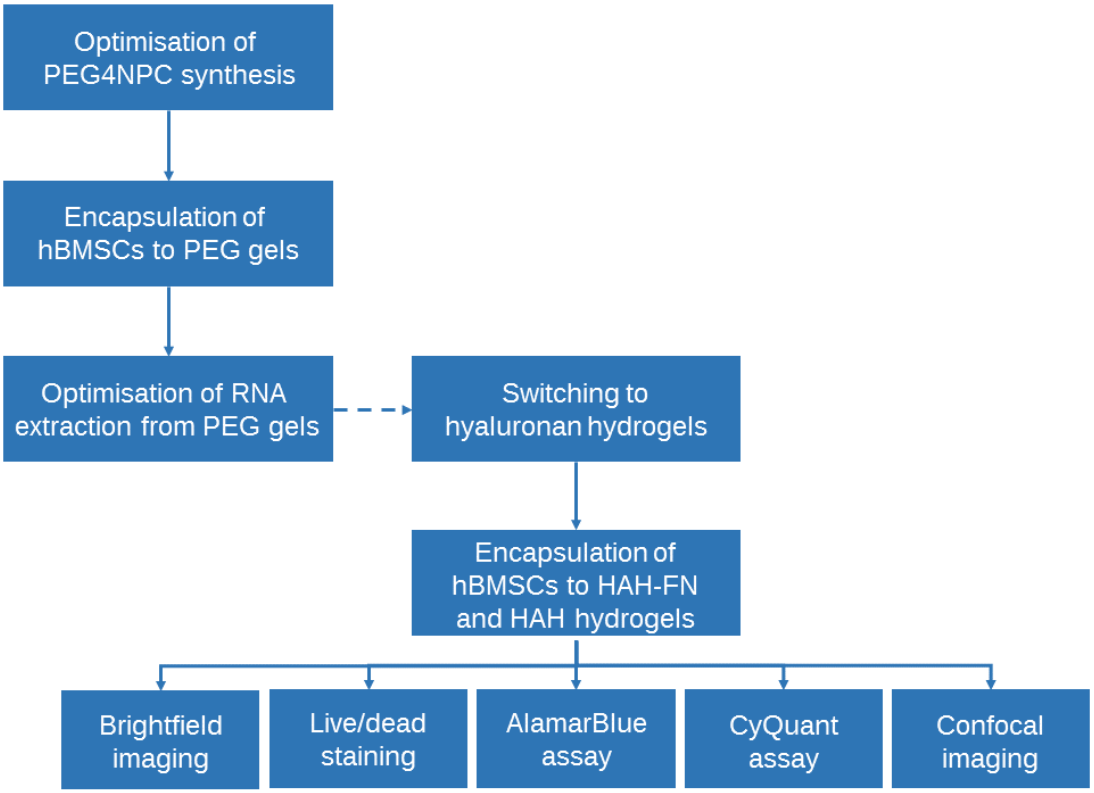

Figure 8. *Workflow of the thesis project.*

The actual cell studies were carried out with hyaluronan hydrogels, which either contained or did not contain fibronectin. Each of the cell culture assays were carried out at 1-, 4- and 7-day time points.

4.2 Optimisation of PEG4NPC synthesis

4.2.1 PEG4NPC synthesis

The aim was to functionalise four-arm PEG (M_w 10,000) with 4-nitrophenyl chloroformate (4-NPC) in order to produce four-arm PEG nitrophenyl carbonate (PEG4NPC), and to achieve as high functionalisation as possible. In subsequent steps, this functionalisation

enables the crosslinking of PEG with peptides via an amine group in a terminal lysine residue. A summary of the experiments is presented in Table 6 and the conjugation reaction is shown in Figure 9. The experimental procedure is briefly described below. The experiments varied by the reaction time, the amount of 4-NPC used and whether or not catalyst 4-dimethylaminopyridine (4-DMAP) was used.

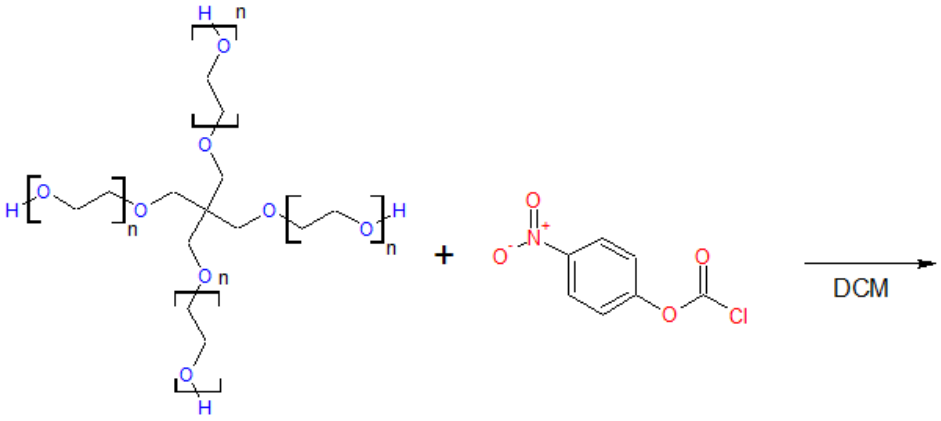

4-arm poly(ethylene glycol) 4-nitrophenyl chloroformate

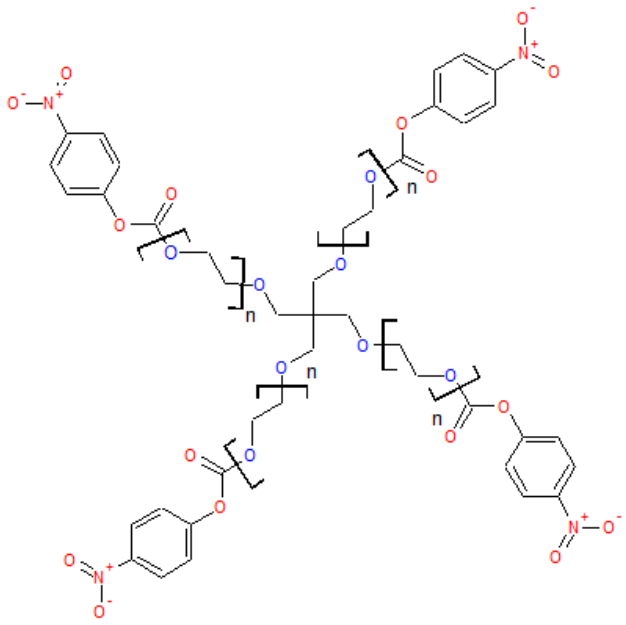

4-arm poly(ethylene glycol) nitrophenyl carbonate

Figure 9. *Conjugation reaction for poly(ethylene glycol) and 4-NPC to yield PEG4NPC.*

PEG(10K)4OH (JenKem Technology USA) and 4-NPC (Sigma-Aldrich) were dissolved in dichloromethane (DCM, Sigma-Aldrich) under anhydrous conditions, after which the solution containing PEG was added to a stirring 4-NPC solution dropwise. In experiments in which 4-DMAP (Sigma-Aldrich) was used, it was added to the 4-NPC solution. For experiments no. 2–5, the anhydrous conditions and N_2 flow were provided by N_2-filled balloons and an N_2 cylinder, which were later on replaced by an N_2 chamber. The reaction

time varied depending on the experiment, from 2.5 to 24 or 72 h, after which the solvent was evaporated.

Next, the solution was precipitated via one of two different precipitation methods. In the first (A) precipitation method, the solution was precipitated using ice-cold diethyl ether (DE, Sigma-Aldrich) and incubated at -80 °C for 20 min, after which the supernatant was removed. In the second (B) precipitation method, room temperature DE was added and the solution was centrifuged for 20 min at 4 °C, after which the supernatant was removed and the precipitation step was repeated two more times. After the precipitation step, the solvent was evaporated. From the experiment no. 4 onwards, the product was dried in a vacuum oven for 1 h at 70 °C.

The use of 4-NPC as the functional group is advantageous due to its yellow colour in alkaline solution and the ease by which the level of functionalisation can be quantified using colorimetric techniques. The level of functionalisation was quantified by UV/Vis spectroscopy and the quantification method is described in more detail in Section 4.2.2.

Table 6. *A summary of the experiments, showing the quantity of PEG(10K)4OH used, the amount of 4-NPC and DMAP used per -OH group, whether the experiment was performed under anhydrous conditions, the reaction time and precipitation method.*

No. of ex-periment	PEG(10K)OH (mg)	Amount of 4-NPC per OH group (M)	Amount of 4-DMAP per OH group (M)	Atmospheric conditions	Reaction time (h)	Precipitation method
1	20	3	-	Fume hood (not anhydrous)	24	A
2	20	3	-	N_2 flow	24	A
3	200	3	-	N_2 flow	24	A
4	200	3	-	N_2 flow	72	B
5	200	10	-	N_2 flow	24	B
6	200	1.1	0.2	N_2 chamber	24	B
7	200	2	1	N_2 chamber	2.5	B
8	200	3	1	N_2 chamber	72	B
9	1000	3	-	N_2 chamber	72	B

4.2.2 Quantification of PEG functionalisation

The level of functionalisation was determined using absorbance measurements of dissociated para-nitro phenolate. Adding the product to an alkaline solution with a pH ≥ 9 (such as 1 M NaOH) causes instant dissociation of para-nitro phenolate, which is yellow in colour, and this method was exploited in order to quantify the level of functionalisation of PEG4NPC. The level of unreacted 4-NPC impurities in the product that may have remained after the precipitation step was also determined as a control specimen, by dissolving some of the product in Dulbecco's phosphate-buffered saline (DPBS, BioWhittaker, Lonza), since he rate of dissociation of 4-NPC is relatively slow at pH 7.4. Each of the corresponding solutions was run as a blank in order to set the baseline. Absorbance of the samples was measured at 405 nm, and the degree of coupling was calculated according to Equation 1, in which:

$$Degree\ of\ coupling = \frac{\frac{A}{Extinction\ coefficient} * d * 1{,}000{,}000}{[\frac{\frac{1}{DF}}{Mw(PEG(10K)4NPC} * 1{,}000{,}000] * 4} * 100\ \%, \qquad (1)$$

where A is the absorbance of the sample, d is the path length and DF is dilution factor. According to the literature, the extinction coefficient for 4-NPC at 405 nm is 18,000 M^{-1} cm^{-1} (Zhang & VanEtten 1991).

4.3 Cell culture

In order to confirm the differentiation potential of cells from four different donors (labelled as 5/16, 6/16, 7/16 and 9/16) the cells were first expanded to passage 3 in basic medium, which consisted of MEMα Medium (Gibco, Thermo Fisher Scientific) supplemented with 5% human serum (HS, Biowest) and 1% penicillin-streptomycin (P/S, 10,000 U penicillin/mL, 10,000 U streptomycin/mL, Lonza, BioWhittaker). During cell maintenance but not during experiments, 5 ng/mL of human fibroblast growth factor-2 (hFGF-2, Miltenyi Biotec) was added to basic medium at each medium change to maintain hBMSC multipotency.

In order to induce osteogenic differentiation, cells were cultured in osteogenic medium, which consisted of basic medium supplemented with 200 µM L-ascorbic acid 2-phosphate (Sigma-Aldrich), 10 mM β-glyserophosphate (Sigma-Aldrich) and 5 nM dexamethasone (Sigma-Aldrich). In order to induce adipogenic differentiation, cells were cultured in adipogenic medium, which consisted of basic medium supplemented with 1 µM dexamethasone (Sigma-Aldrich), 33 µM biotin (Sigma-Aldrich), 17 µM panthotenate (Fluka, Thermo Fisher Scientific) and 100 nM human recombinant insulin (Gibco, Thermo Fisher Scientific). Medium was changed twice per week, and in the first medium change, 0.5 µL/mL of 3-isobutyl-1-methylxanthine (Sigma-Aldrich) was added to adipogenic medium.

For the RNA extraction experiments, cells were cultured to passage 7 or 8 in basic medium containing 5 ng/mL of hFGF-2. After encapsulation, the 3D hydrogel samples and 2D control samples were maintained in basic medium overnight, before RNA extraction.

For encapsulation in hyaluronan hydrogels, hBMSCs were first cultured to passage 5 in basic medium containing 5 ng/mL of hFGF-2. After encapsulation, the samples were maintained in basic medium at 37 °C, 5% CO_2 and 95% relative humidity. The medium was changed three times per week.

4.3.1 hBMSC isolation

Human bone marrow stromal cells from a healthy male donor (labelled 9/16) born in 1924 (aged 92 at the time of isolation) and with no history of diabetes or osteoporosis were isolated. The bone marrow sample was diluted in DPBS and filtered through a cell strainer, after which it was centrifuged at 1,200 rpm for 5 min. The supernatant fat layer was removed and the rest of the sample was carefully pipetted onto Ficoll (GE Healthcare). The solution was centrifuged at 800 ×G for 20 min at room temperature, after which the cells were collected from the interphase between the formed layers. αMEM was added to the collected interphase. The suspension was centrifuged 1,500 rpm for 15 min at room temperature and the supernatant was removed. The wash step was repeated, after which cell pellets were suspended in basic medium.

Cells from three other donors (5/16, 6/16 and 7/16) had previously been prepared according to the same protocol.

4.3.2 Evaluation of differentiation potential

The osteogenic and adipogenic differentiation potential of cells from four donors (5/16, 6/16, 7/16 and 9/16) were confirmed by treatment with either osteogenic or adipogenic induction media. Three parallel samples from each cell line were tested for each condition. For osteogenic differentiation studies, the cells were seeded onto 24-well plates (Costar, USA) at two different plating densities, 500 or 3,000 cells per well. Cells were cultured for 20 days, after which Alizarin Red S (Sigma-Aldrich) staining was carried out to qualify osteogenesis. For adipogenic differentiation studies, the cells were seeded in 24-well plates at a density of 70,000 cells per well. Oil Red O (Sigma-Aldrich) staining was carried out on day 14 to qualify adipogenesis. The results from these assays are shown in Figure 22 in Appendix A.

The surface marker expression of the cells was confirmed with fluorescence-activated cell sorting (FACS) (results not shown).

4.4 Hydrogel preparation and cell encapsulation

4.4.1 Poly(ethylene glycol) hydrogels

4.4.1.1 PEG-KDWERC synthesis

Custom synthesised Ac-KDWERC-NH_2 peptide (Peptide Protein Research Ltd.) was used to crosslink PEG(10K)4NPC and poly(ethylene glycol) vinyl sulfone (PEG(5K)4VS) (JenKem Technology USA). First, the peptide was deprotected by removing the trifluoroacetic acid, which protects the exposed amine groups on the peptide, using an organic base, triethylamine. The peptide was dissolved in dimethyl sulfoxide anhydrous (DMSO, Sigma-Aldrich) in order to minimise hydrolysis that would occur under an aqueous solution. Trimethylamine was then added (1.5 M equiv. per NH_2 group of KDWERC) and the mixture was rocked at 200 rpm for 1 h. Then, PEG4NPC was dissolved in DMSO, added to the deprotected peptide and rocked at 200 rpm for 30 min. In order to cleave any disulfide bonds which may have formed during the conjugation reaction, 1,4-dithiothreitol was dissolved in DMSO (3 M equivalent per SH group) and added to the conjugate. This mixture was rocked at 200 rpm for a further 30 min. DMSO was removed via lyophilisation overnight. The sample was purified by using Bio-Spin P-6 gel columns (Bio-Rad) according to the manufacturer's protocol, from which the buffer had been exchanged to 50 mM HEPES at pH 8.2, and then lyophilised again overnight.

4.4.1.2 Cell encapsulation

For RNA extraction experiments, 50 µL hydrogels containing 250,000 cells were prepared. The gels were prepared by mixing together three fractions, containing 10 µL of PEG4VS solution, 10 µL PEG-KDWERC solution and 30 µL of cell suspension.

PEG-KDWERC conjugate, PEG4VS and the cell pellet were all dissolved separately in 50 mM HEPES at a pH of 8.2, with concentrations of 18 mg/mL, 7 mg/mL and 8,333,330 c/mL, respectively. The cell suspension was added to the PEG4VS solution, and briefly vortexed. The PEG-KDWERC solution was added to this mixture and briefly vortexed. The solution was added to moulds and left to gelate at room temperature for 30 min and another 30 min at 37 °C.

4.4.2 Hyaluronan hydrogels

HA-aldehyde and HA-hydrazide components were provided by the Bioengineering and Nanomedicine Lab at Tampere University of Technology. The fibronectin was provided by the Protein Dynamics group from the University of Tampere.

Fibronectin solution was prepared by dissolving fibronectin in sterile DPBS at pH 7.42, with a final concentration of 2.8 μg/μL. HA-aldehyde was dissolved at 16 mg/mL in sterile DPBS at pH 7.42, and HA-hydrazide was dissolved at 16 mg/mL in either sterile DPBS at pH 7.42 or in the fibronectin-DPBS solution.

A cell pellet was suspended in HA-aldehyde solution with concentration of 200,000 cells/mL. This cell suspension was mixed with HA-hydrazide or HA-hydrazide-fibronectin solution at a 1:1 volume ratio in sterile moulds fabricated from syringes with the ends cut off, in order to make 50 μL hydrogels containing 50,000 cells. The gel samples were incubated for 1 h at 37 °C, after which the samples placed in cell culture plates.

The overall concentration of HA in all hydrogels was 16 mg/mL (0.8 mg per 50 μL hydrogel). The fibronectin concentration was 0 or 0.7 mg/mL (0 μg per 50 μL HAH hydrogel and 35 μg per HAH-FN hydrogel).

4.5 Optimisation of RNA extraction from PEG hydrogels

In order to optimise the extraction of RNA from PEG hydrogels, two commercial kits, QIAGEN RNeasy Plus Mini Kit and QIAGEN AllPrep DNA/RNA/Protein Mini Kit, were compared along with two different lysis buffers, RLT+ which is supplied with the QIAGEN RNeasy Plus Mini Kit, and TRI Reagent & transfer RNA (tRNA). The use of TRI Reagent and tRNA was based on the work by Gasparian et al. (2015), as they showed that addition of tRNA from *Saccharomyces cerevisiae* minimises non-specific binding of mRNA to the gel components (Gasparian et al. 2015).

The cell-hydrogel samples were transferred to ceramic bead-containing tubes (Mo Bio, QIAGEN), and the corresponding buffer, RLT+ or TRI Reagent (Molecular Research Center) & tRNA (Sigma-Alrich) was added. Hydrogels were homogenised using a PowerLyzer homogenizer (Mo Bio) with two cycles at 3,500 rpm for 45 s each, with 30 s interval between the cycles. The homogenised samples were incubated at room temperature for 5 min before carrying on with the extraction.

For the samples in RLT+ buffer, the extraction proceeded according to the manufacturer's protocol. An additional step was carried out for the samples in TRI Reagent & tRNA before proceeding to the manufacturer's protocol. Chloroform was added to the homogenised samples in order to separate RNA, DNA and protein into different phases. The samples were incubated at room temperature for 3 min, after which they were centrifuged at 12,000 ×G for 15 min at 4 °C. The upper aqueous phase, containing the RNA, was carefully transferred to the column, and processed according to the manufacturer's protocol.

The protocols used were “Purification of Total RNA from Animal Tissues” for RNeasy Plus Mini Kit and “Simultaneous purification of Genomic DNA, Total RNA, and Total Protein from Animal and Human Tissues” for AllPrep DNA/RNA/Protein Mini Kit.

The quality and quantity of all samples was measured with a NanoDrop 2000 Spectrophotometer (Thermo Fisher Scientific). The quality and quantity of samples extracted using RLT+ buffer were also analysed with a Fragment Analyzer (Advanced Analytical Technologies). The manufacturer’s protocols were used in both cases.

4.6 Analysis of cell number and viability in hyaluronan hydrogels

4.6.1 Brightfield imaging

Brightfield images of cells were obtained with Zeiss Axio.A1 microscope at 1-, 4- and 7-day time points. The brightness and contrast of the images were adjusted using ImageJ software.

4.6.2 Live/dead assay

Cell viability was analysed using qualitative live/dead fluorescence staining (Invitrogen, Thermo Fisher Scientific) at 1-, 4- and 7-day time points.

First, cells were washed once with DPBS, after which they were incubated for 45 min at room temperature in working solution containing 0.5 µM calcein acetoxymethyl ester (Invitrogen, Thermo Fisher Scientific) and 0.25 µM ethidium homodimer-1 (Invitrogen, Thermo Fisher Scientific) in DPBS. The samples were imaged with Olympus IX51 fluorescence microscope. The images were edited with ImageJ software.

4.6.3 AlamarBlue assay

Cell viability was analysed using alamarBlue assay (Invitrogen, Thermo Fisher Scientific). The assay is based on the reducing environment within the cytosol of living cells. The blue coloured active ingredient of alamarBlue, resazurin, is able to permeate through the cell membrane. Within the cytosol, resazurin is reduced to resorufin, which is red in colour and high in fluorescence. Thus, viable cells convert resazurin to resorufin and this signal can be measured. (Bonnier et al. 2015)

First, samples were washed once with DPBS. AlamarBlue reagent was diluted 10X in DPBS, and 600 µL this working solution was added to each well and the samples were incubated for 4 h in the dark at 37 ºC. After incubation, a sample was taken from each

well and transferred to a black 96-well plate. The fluorescence of the samples was measured with Wallac Envision Multiplate reader (PerkinElmer) at an excitation wavelength of 570 nm and emission wavelength of 585 nm. This assay is subsequently referred to throughout this thesis as “a resazurin-based mitochondrial metabolic assay”.

In order to quantify the number of viable cells at each time point, a standard curve was prepared by encapsulating cells at four different cell densities (200,000, 100,000, 50,000 and 25,000) in 50 µL HAH-FN gels.

4.6.4 CyQUANT assay

After 1, 4 or 7 days of culture, gels were transferred to microcentrifuge tubes, and 0.1% Triton-X-100 (Sigma-Aldrich) was added to each of the samples. Samples were stored at -80 ºC up to three weeks.

Thawed samples were transferred to ceramic bead-containing tubes and homogenized with PowerLyzer at 1,000 rpm for 15 s. The samples were then transferred back to the microcentrifuge tubes and spun down for 5 s.

Cell number was quantified with CyQUANT Cell Proliferation Assay Kit (Life Technologies, Thermo Fisher Scientific). A working solution was prepared by adding cell lysis buffer and CyQuant GR dye to deionised water. From each sample, 20 µL was pipetted into a 96-well plate, and 180 µL of working solution was added to each well. The plate was measured using a microplate reader (Victor 1420 Multilabel Counter, PerkinElmer) at an excitation wavelength of 480 nm and an emission wavelength of 520 nm. This assay is subsequently referred to throughout this thesis as “a total DNA assay”.

4.7 Immunocytochemistry

First, samples were fixed. Samples were washed with DPBS, after which they were incubated for 15 min in 0.2% Triton-X-PFA fixing solution at room temperature. Samples were immersed in DPBS and stored at 4 ºC prior to imaging.

Fixed samples were incubated in blocking solution consisting of 1% BSA in DPBS for 1 h at 4 ºC. The primary monoclonal antibody, rabbit anti-vinculin (Invitrogen, Thermo Fisher Scientific) was diluted 1:100 in blocking solution and applied to the samples, prior to incubation overnight at 4 ºC.

After incubation, samples were washed four times with DPBS, with incubation for 3 min each time. Phalloidin-tetramethylrhodamine B isothiocyanate (Phalloidin-TRICT) and Alexa Fluor 488 donkey anti-rabbit IgG were diluted together in 1% BSA in DPBS blocking solution at ratios of 1:500 and 1:800, respectively. Samples were incubated in this

solution at 4 ºC for 55 min. Then, the samples were washed twice with DPBS, and incubated again for 3 min each time. To the third wash solution, 4',6-diamidino-2-phenylindole (DAPI) was added at a ratio of 1:2000, applied to the samples and incubated for 5 min at room temperature. The samples were washed once with DPBS and rinsed twice briefly with deionised water.

The samples were imaged with Zeiss LSM 700 laser scanning confocal microscope. The images were edited using Huygens Essential software.

5. RESULTS

5.1 PEG4NPC – Level of functionalisation

PEG functionalisation with 4-NPC was optimised in order to achieve as high degree of functionalisation as possible. The functionalisation was needed for the later stages of the hydrogel fabrication, to conjugate peptides to the network and gain control over material properties. The experimental setups are listed in Table 6. The degree of functionalisation was quantified by measuring the absorbance of dissociated para-nitro phenylate groups at 405 nm, and the results are presented in Figure 10.

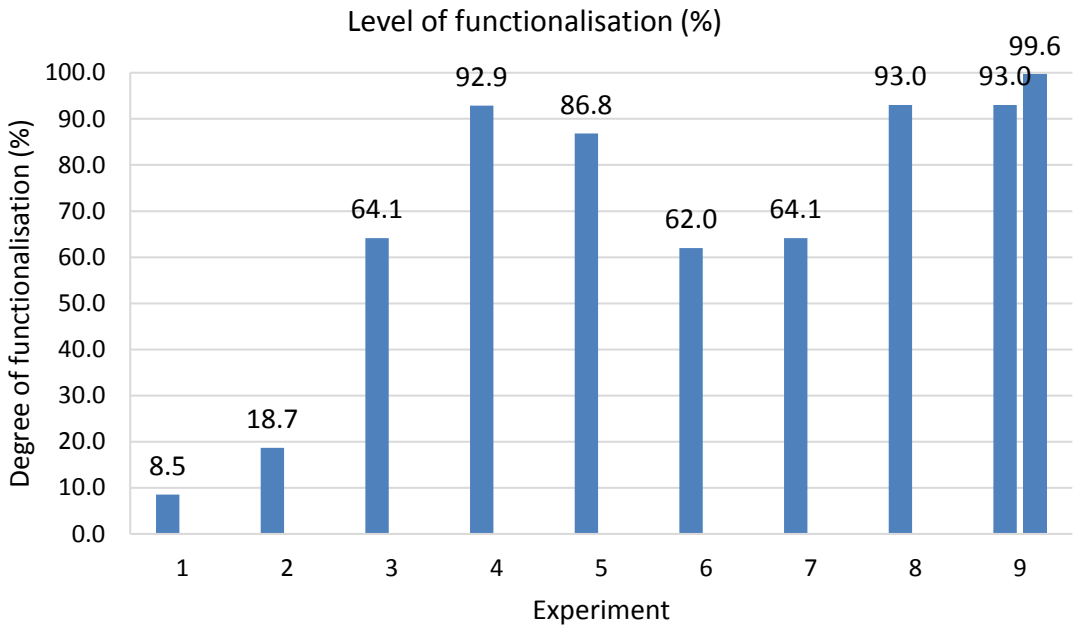

Figure 10. *Degree of functionalisation of PEG(10K)4OH with 4-NPC to form PEG(10K)4NPC. Functionalisation was increased by: anhydrous reaction conditions (experiment 1 vs. 2); increasing the amount of starting materials (10 times larger amounts in exp. 3 compared to exp. 2); increasing the reaction time from 24 to 72 h (exp. 3 and 4, respectively); and using a greater excess of 4-NPC (exp. 5 vs. exp. 3). Addition of a catalyst did not increase the level of functionalisation with smaller excess of 4-NPC and shorter reaction time (exp. 6 and 7). Experiments 8 and 9 were repetitions of experimental set up of exp. 4, but with a catalyst or with larger amount of starting materials, respectively.*

The results indicate that the main factors increasing the level of functionalisation were a longer reaction time, a high excess of 4-NPC and an anhydrous atmosphere. A high degree of coupling, around 90.0%, was achieved in four experimental set ups during the optimisation process. Briefly described, the degree of coupling of 86.8% was achieved with 10 M excess of 4-NPC and 24 h reaction time, 92.9% with 3 M excess of 4-NPC

with 72 h reaction time, and both 93.0% and 99.6% were achieved with the same experimental set up, with 3 M excess of 4-NPC with 72 h reaction time but larger amount of starting materials. Addition of a catalyst to the experimental set up with 3 M excess of 4-NPC and 72 h reaction time did not increase the level of functionalisation. Catalyst and smaller excess of 4-NPC did not improve the level of functionalisation after 24 h (62.0%), and with larger excess of 4-NPC and shorter reaction time (2.5 h) similar degree of coupling was achieved (64.1%).

Nuclear magnetic resonance (NMR) spectroscopy was later run on the PEG4NPC sample with 99.6% degree of coupling (as indicated by the colorimetric assay), to confirm the level of functionalisation. The NMR spectra are shown in Figure 23 in Appendix B. The highest peak at 3.6 ppm indicated the presence of $-CH_2$ groups from the repeating units of the polymer, and a smaller peak shifted to 4.4 ppm arose from the $-CH_2$ groups which had conjugated to the electronegative ester groups. Peaks at 7.4 and 8.3 ppm indicated the presence of an aromatic ring. This confirms that the functionalisation was successful, but estimation of the exact level of functionalisation is challenging. The degree of coupled 4-NPC groups seemed to be close to 100%, and the amount of free 4-NPC in the sample was around 12.5%.

5.2 RNA extraction from PEG hydrogels

The extraction of RNA from PEG hydrogels was optimised by comparing two commercial kits: QIAGEN RNeasy Plus Mini Kit and QIAGEN AllPrep DNA/RNA/Protein Kit; and by comparing two lysis buffers; RTL+ buffer which comes with the RNeasy Plus Mini Kit, and TRI Reagent & tRNA buffer.

The results for RNA extraction yield are presented in Figure 11. The number of samples for buffer and gel blanks was one, and for 2D and 3D cell samples three, besides the TRI Reagent & tRNA samples, where there was one sample, due to loss of samples during gelation. The results are presented as an average of the samples with their respective standard deviations (SDs), or as a single value.

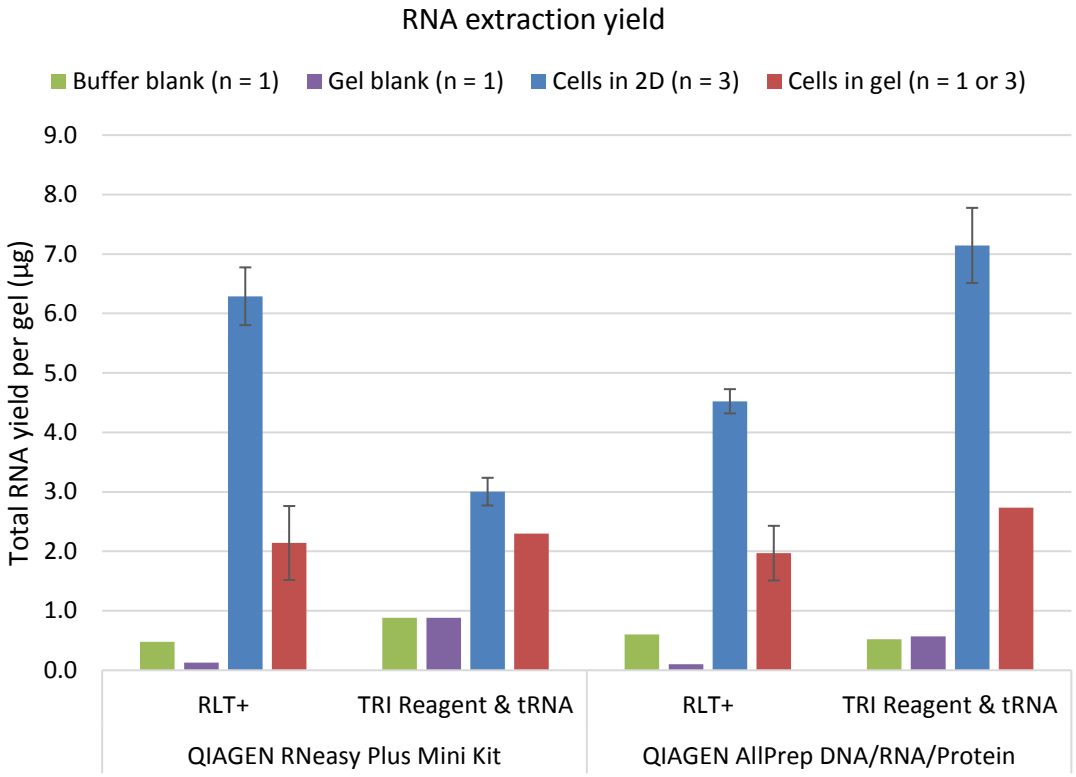

Figure 11. *RNA extraction yield from PEG–peptide hydrogels. The total RNA yield is presented as an average of the samples for 2D samples (n = 3) and for 3D samples in RLT+ buffer (n = 3). For the buffer blank, gel blank and the 3D samples in TRI Reagent & tRNA the yield from one sample is shown (n = 1).*

For analysing nucleic acid samples with NanoDrop, there are two absorbance ratios which can be considered as measures for purity, A260/230 and A260/280. The results obtained with each of the ratios are presented in Figure 12 and Figure 13, respectively.

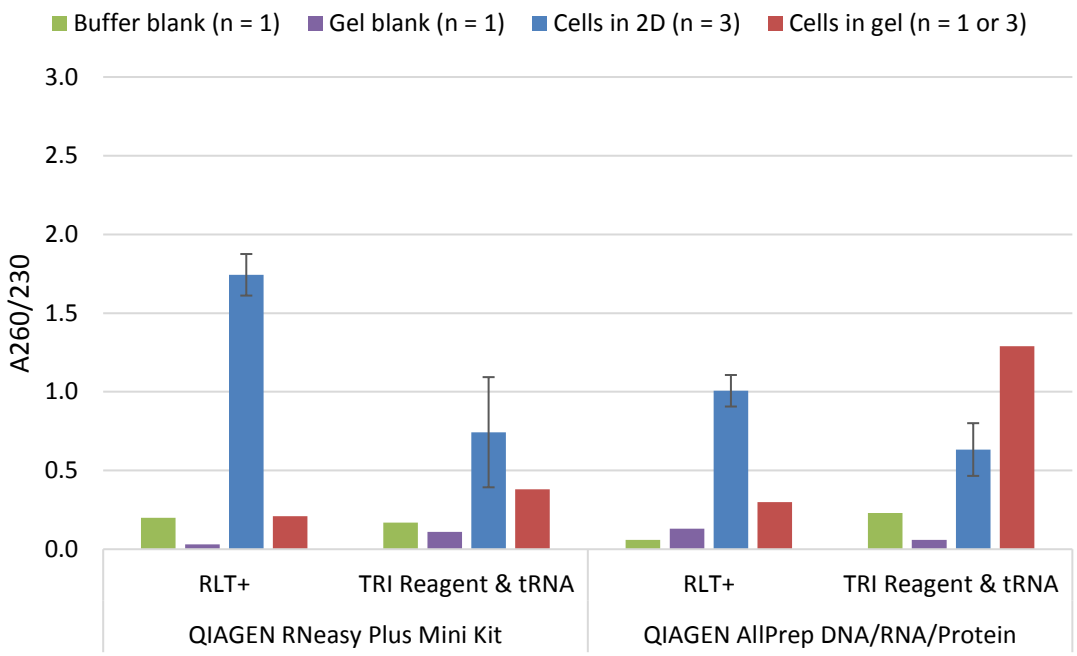

Figure 12. *A260/230 ratio, measured with NanoDrop.*

The A260/230 ratio of RNA extracted from hydrogels was low compared to the 2D controls. The 2D control samples extracted with RLT+ buffer and RNeasy kit, had an A260/230 ratio close to two, which is considered to indicate high RNA purity. It was hypothesised that impurities resulting from the hydrogel components or the extraction process may have interfered with the A230 values, and therefore the A260/280 ratio was assessed and samples were further studied using a Fragment Analyzer.

The A260/280 ratios were closest to two for 2D and 3D samples extracted with RLT+. The A260/280 ratio was almost as high for the samples extracted with TRI Reagent & tRNA.

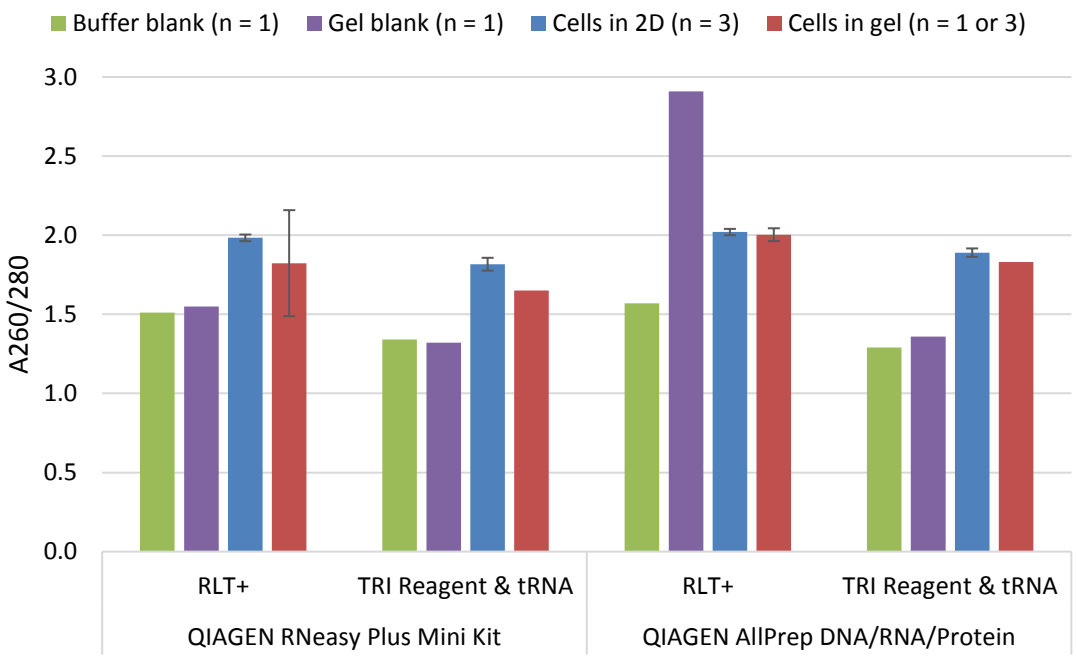

Figure 13. *A260/280 ratio, measured with NanoDrop.*

To ensure that the homogeniser had not fragmented the RNA too harshly, samples extracted with RLT+ buffer were analysed with Fragment Analyzer. The results are shown in Figure 14. RNA quality was sufficiently high for real time quantitative polymerase chain reaction (RNA quality number for 2D samples was ~10/10, whereas for 3D samples it was ~6.4/10, on average).

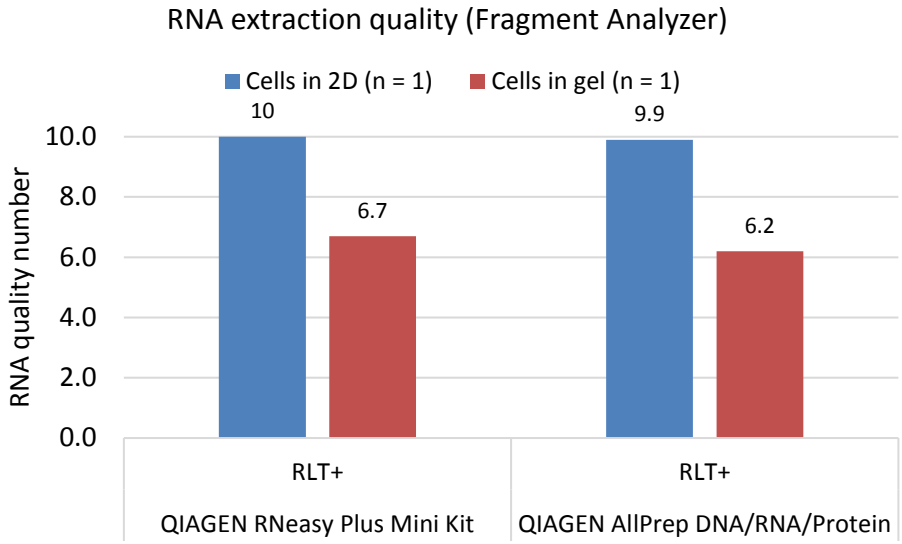

Figure 14. *Fragment Analyzer was run for RLT+ samples (n = 1). The maximum value for RNA quality number is 10.*

5.3 Cell number and viability in hyaluronan hydrogels

In order to study cell number and viability, several viability assays were used to gain information about different variables, such as cell metabolism and the DNA content of the samples, and in order to determine which assays are suitable for studying cells encapsulated in hyaluronan hydrogels. For qualitative analysis, brightfield imaging and live/dead staining were used, and for quantitative analysis, a resazurin-based mitochondrial metabolic assay and a total DNA assay were used. All the assays were performed at 1-, 4- and 7-day time points.

Brightfield images of cells encapsulated in HAH-FN and HAH gels are shown in Figure 15. The cell numbers seemed to remain constant in the gels (based on visual estimation), and the overall cell morphology was rounded during the seven days of culture. However, cells were able to spread and form multiple protrusions in the HAH-FN gels on day seven, as shown in Figure 16. Only rounded morphologies were seen in the HAH gels during the entire week of culture.

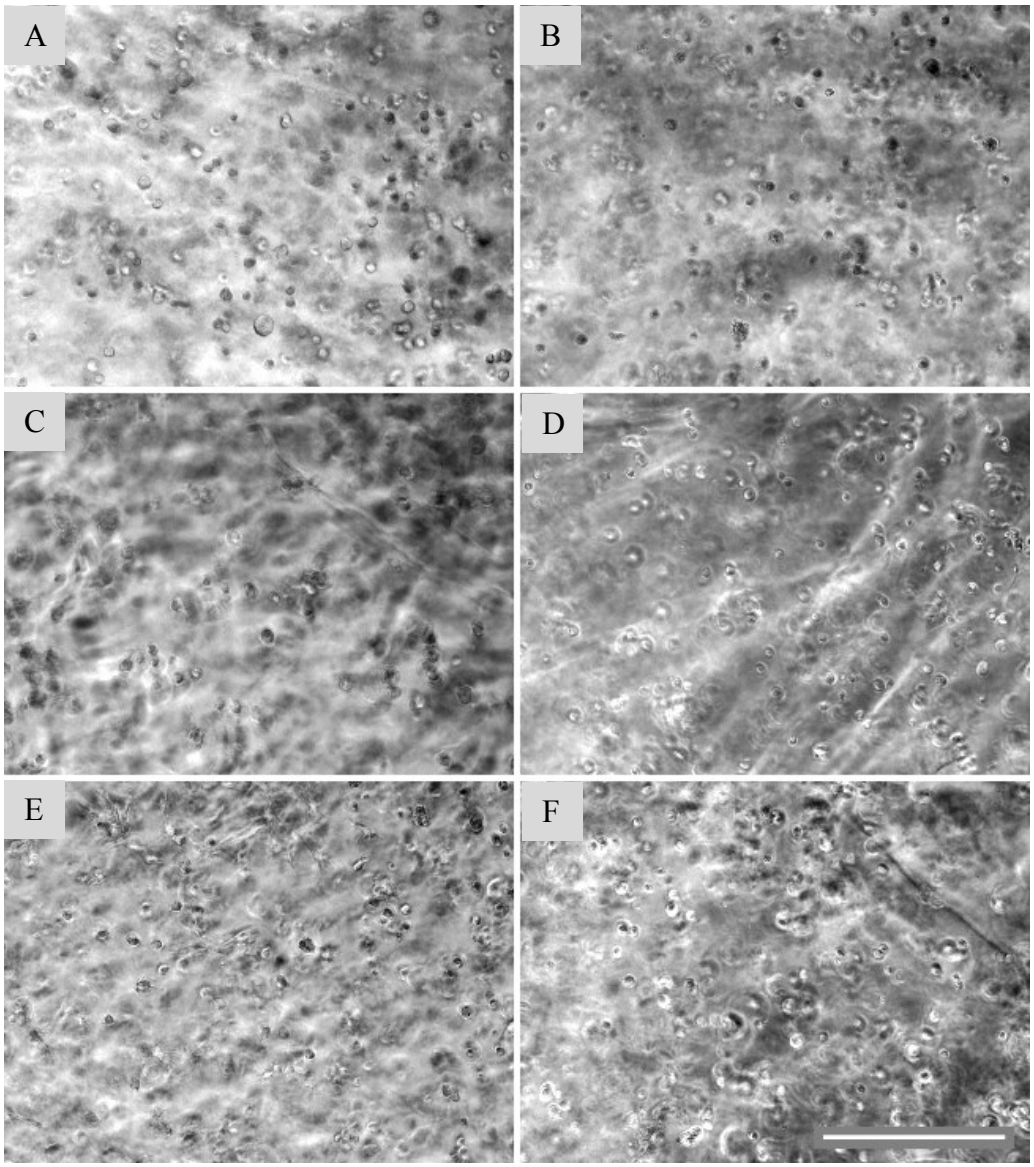

Figure 15. *hBMSC encapsulated in hyaluronan hydrogels were qualitatively evaluated using bright field imaging. HAH-FN gels (A, C & E), HAH gels (B, D & E) after 1 day (A & B), 4 days (C & D) and 7 days (E & F) of culture. The number of cells remained fairly constant at all time points and cell morphology remained rounded in both types of gels. Scale bar 500 µm.*

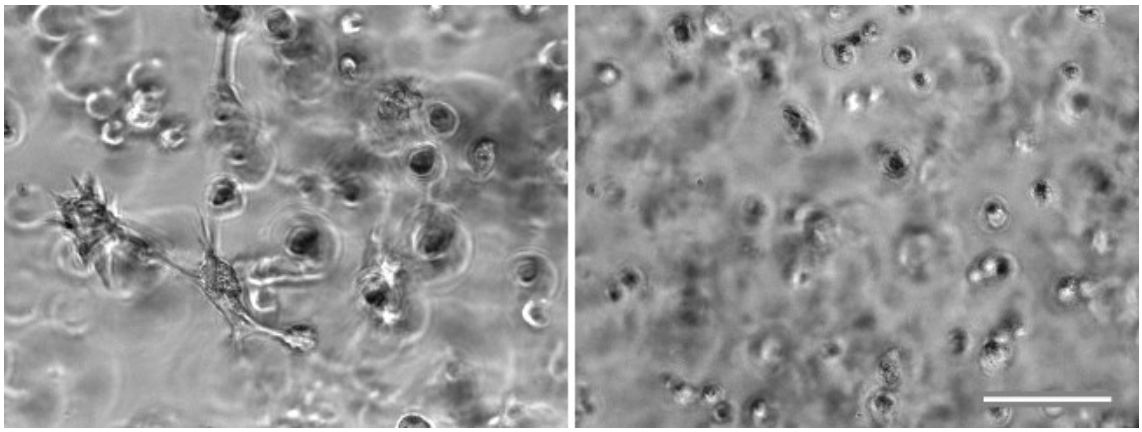

Figure 16. *hBMSC morphologies inside hyaluronan gels, after 7 days in culture. Cells were able to spread and form protrusions and cell-cell contacts in HAH-FN gels (left). Only rounded morphologies were seen in HAH gels (right). Scale bar 100 µm.*

Results obtained from live/dead staining are shown in Figure 17. Viability of hBMSCs in HAH-FN gels was high at each time point, and there were not many dead cells. In addition, cell numbers seemed to remain constant in these gels. However, almost no cells could be observed in the HAH gels.

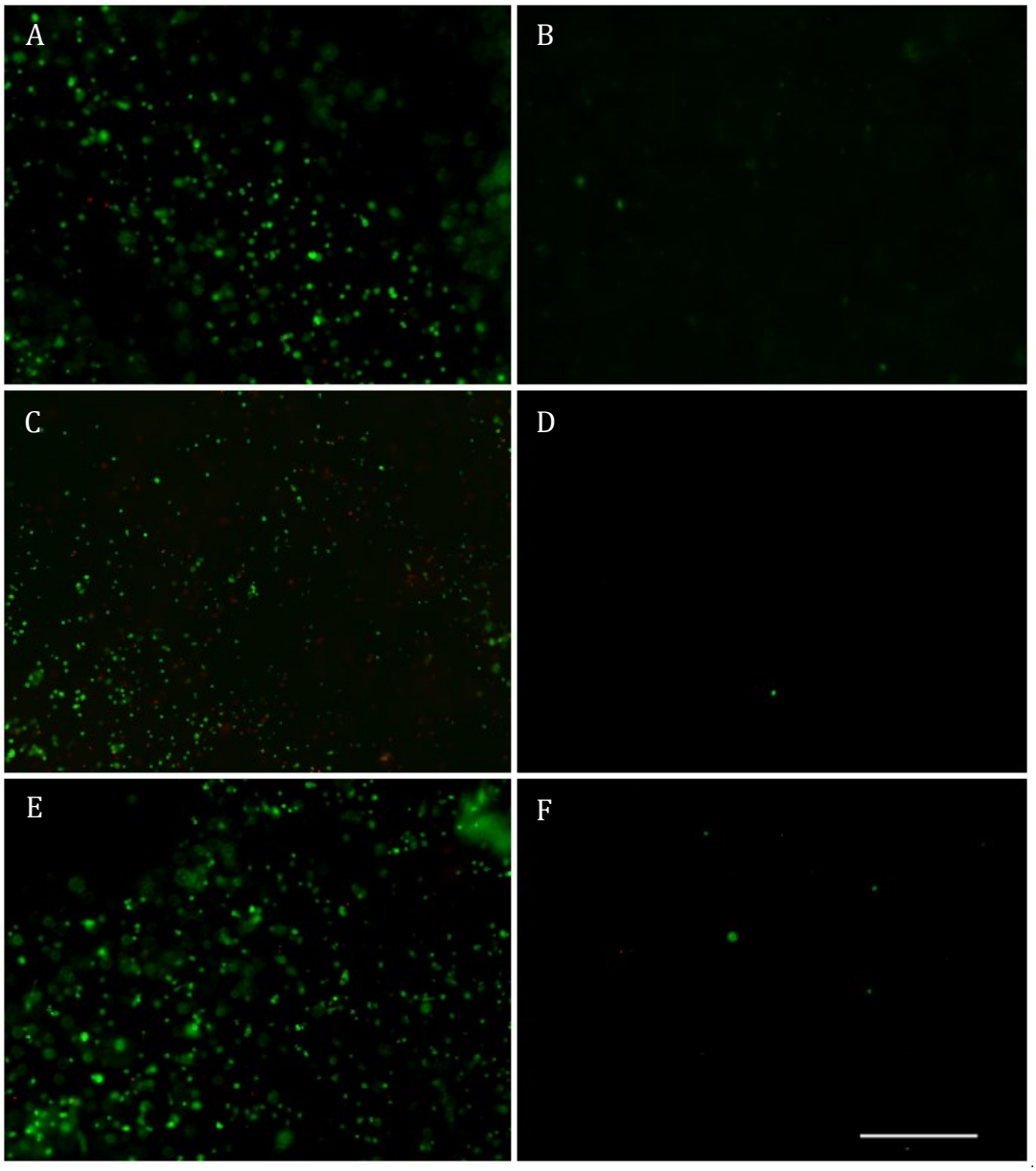

Figure 17. *Viability of hBMSCs encapsulated to hyaluronan hydrogels. Viability in HAH-FN gels (A, C & E) and HAH gels (B, D & F) after 1 day (A & B), 4 days (C & D) and 7 days (E & F) of culture. Scale bar 500 µm.*

A resazurin-based mitochondrial metabolic assay was used to indicate the cell number and viability. The results shown in Figure 18 are presented as mean of three samples with their respective standard deviations, with cell number extrapolated from standard the curve. As 50,000 cells were encapsulated per 50 µL hydrogel, the cell density in HAH-FN gels was extremely high already on day one. In addition, the cell number increased in the HAH-FN gels during the week of culture. On the contrary, there was only a very low signal from the cells which were encapsulated in HAH and the cell number did not drastically change during the week of culture.

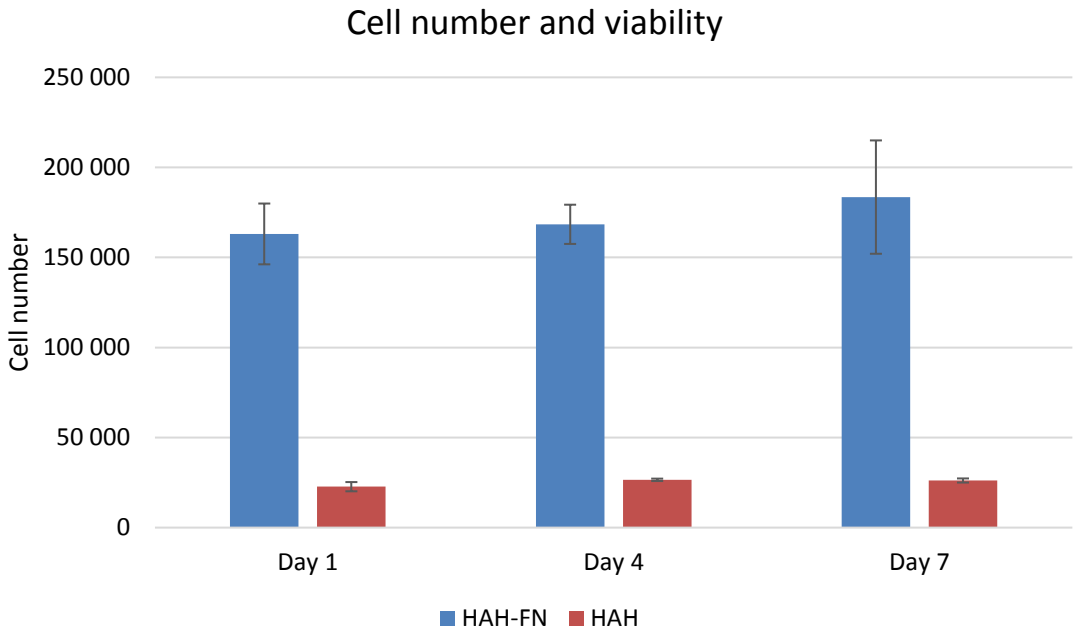

Figure 18. *hBMSC viability in hyaluronan gels either with fibronectin (HAH-FN) or without fibronectin (HAH), quantified with a resazurin-based mitochondrial metabolic assay. Cell number was extrapolated from the standard curve. (n = 3, error bars = SD)*

The total DNA content of the samples was analysed. The results are presented as a mean of three samples, with their respective standard deviations, with cell number extrapolated from standard the curve, and shown in Figure 19.

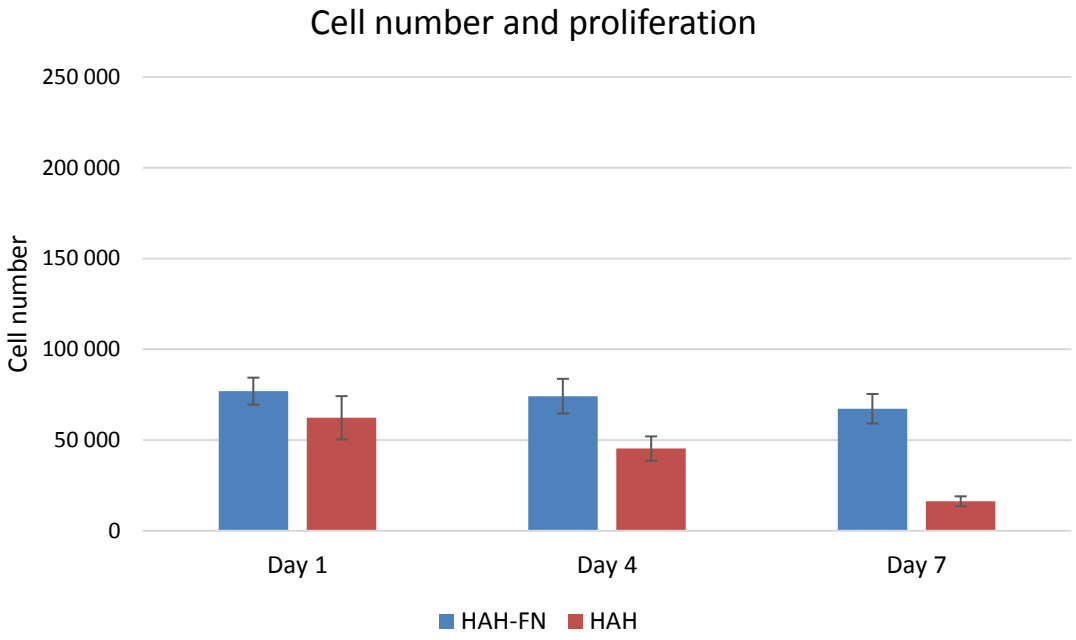

Figure 19. *hBMSC number and proliferation in hyaluronan gels either with fibronectin (HAH-FN) or without fibronectin (HAH), quantified with a total DNA assay. Cell number was extrapolated from the standard curve. (n = 3, error bars = SD)*

The results from total DNA assay indicate that the cell viability decreased drastically in HAH hydrogels during the seven days in culture. There was also a small but most likely statistically insignificant decrease in viability in HAH-FN gels.

5.4 Cell morphology in hyaluronan hydrogels

Cell morphology was evaluated at each time point by immunocytochemistry. The cells were stained for vinculin (green), actin fibers (red) and nucleus (blue). The confocal images are shown in Figure 20.

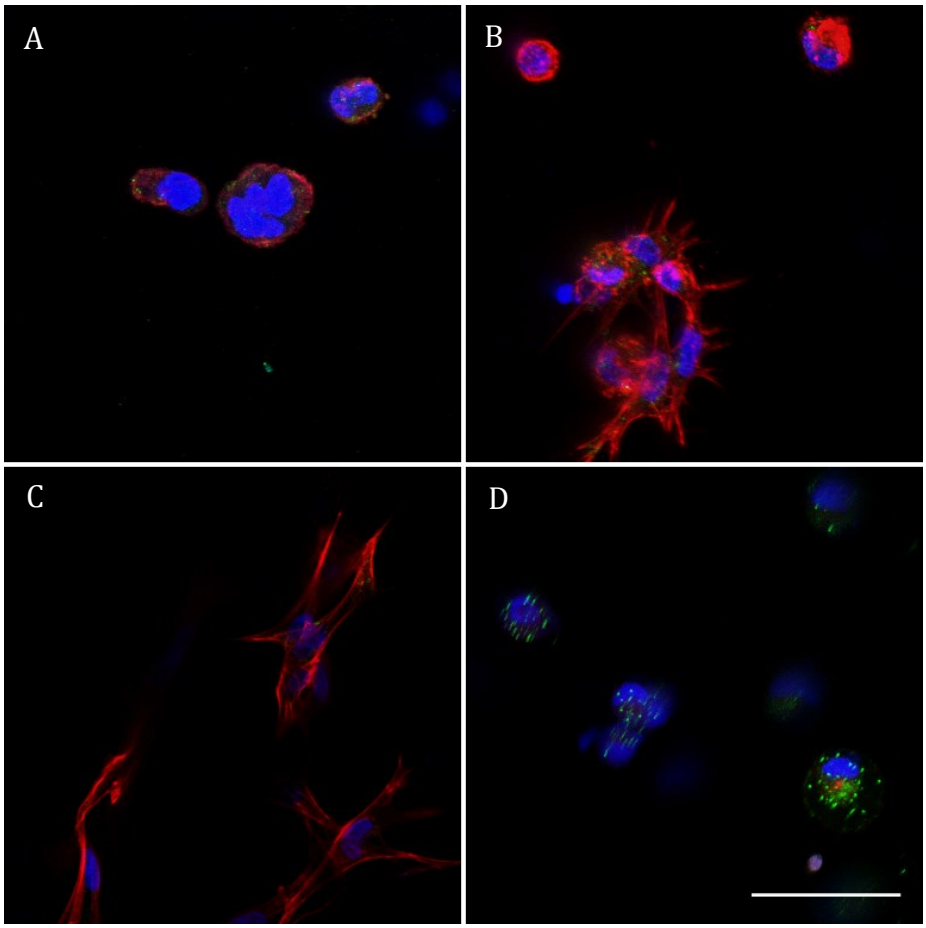

Figure 20. *hBMSCs encapsulated in hyaluronan hydrogels. Cells remained rounded in the HAH-FN gels on day 1 (A), and cells were able to spread in the HAH-FN gels on day 4 (B). On day 7, well spread cell clusters could be seen in HAH-FN gels (C). On day 1 in HAH hydrogels, cells remained rounded and vinculin remained diffusive around the nucleus (D). Nucleus is stained in blue, actin fibers in red and vinculin in green. Scale bar 50 µm.*

After one day in culture, hBMSCs remained rounded in both types of hydrogels. Fibronectin content enabled cell spreading and protrusion formation in HAH-FN gels on day four. However, as shown in the upper part of Figure 19B, most of the cells still remained rounded and could not form an organised cytoskeleton. After a week in culture, most of the cells in HAH-FN hydrogels remained rounded, but the cells which were able to spread could form big spindle shaped cell clusters. The cells had organised cytoskeletons with defined actin fibers. However, vinculin was not shown to be localised to the end of the actin fibers. For the HAH gels, only the day one result is shown as the samples did not stain well, and no actin fibers could be seen. However, vinculin was extensively stained in HAH gels, even though it could not be detected in HAH-FN gels.

6. DISCUSSION

6.1 Fabrication of adhesion ligand-presenting hydrogels

Adhesion ligand-presenting hydrogels provide useful platforms for studying mechanotransduction in 3D. Adhesive interactions with the microenvironment and integrin clustering are prerequisite for the activation of many signalling pathways, and therefore by varying the adhesion ligand presentation it is possible to alter cell behaviours and gain fundamental insights into mechanotransduction. However, carrying out single variable studies in 3D is demanding, because other material properties, such as stiffness and degradability, can affect the mechanosensing of cells as well. To gain control over a single or multiple material properties, synthetic hydrogels are commonly preferred, because naturally derived hydrogels have inherent bioactivity, which can also alter cell responses.

The fabrication of modular poly(ethylene glycol) hydrogels turned out to be challenging. Although the original results for PEG4NPC synthesis seemed promising, the self-synthesised PEG4NPC did not perform as expected in the further hydrogel fabrication. In addition, the fabrication of PEG hydrogels faced setbacks due to delays in receiving PEG components and custom-synthesised peptides, which are time-consuming to produce. In order to fit the cell culture studies into the time frame of this thesis, focus was shifted to hyaluronan hydrogels. In order to include adhesion sites within these gels, fibronectin molecules were physically embedded to the hydrogel structure. The incorporation of the large fibronectin molecule (440 kDa) was expected to have altered the crosslinking kinetics and mechanical properties of the hydrogels, meaning that differences between the non-adhesive HAH and the adhesive HAH-FN hydrogels are caused not only by variations in ligand density, but also by changes in mechanics. It also affected the ability of the dyes used in various assays to penetrate the gels, likely giving false negative results for the more densely crosslinked HAH gels.

6.1.1 PEG4NPC synthesis needs further optimisation

The original results from PEG4NPC synthesis indicated that the achieved level of functionalisation was high (99.6%), and it was achieved in anhydrous conditions with a 3 M excess of 4-NPC, with a 72 h reaction time and a large amount of starting materials. Thus, the main factors improving the level of functionalisation were a longer reaction time, a high excess of 4-NPC over PEG, and anhydrous reaction conditions. By using a larger amount of starting materials, the inaccuracies which arise from working with small amounts of material were diminished. Anhydrous conditions were essential for the success of the coupling, and changing the N_2 flow to work in N_2 chamber increased the repeatability of experiments and diminished the number of error sources.

As the hydrogel fabrication using the self-synthesised PEG4NPC proceeded, it was noted that the level of peptide conjugation which could be achieved was not as high as expected, based on the level of functionalisation with 4-NPC. The observation was made when results were compared with a collaborating research group that was able to achieve a higher level of peptide conjugation to the commercially produced PEG4NPC that they were using, which had 88% functionalisation with 4-NPC.

In order to confirm the level of functionalisation achieved for the self-synthesised PEG4NPC, absorbance of the sample was measured at the isosbestic point, at 350 nm, in three different buffers with pH 7.4, 8.2 or 9.0, and with 2 M excess of cysteine per expected 4-NPC group. Normally, a physical change, such as the ionisation of a sample, affects its absorbance. The isosbestic point of a compound, illustrated in Figure 21 at the point at which the absorbance curves of samples with different pHs cross over, is the wavelength or frequency at which such properties do not affect the total absorbance, and therefore it excludes any effect which might arise from the pH of the buffer. However, the results (not shown) were inconsistent. Therefore, the level of functionalisation was finally measured with NMR spectroscopy.

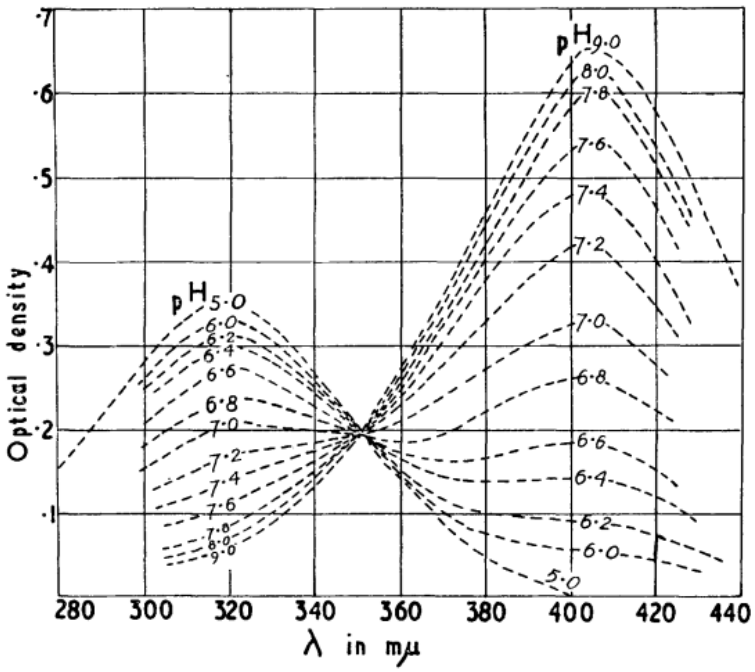

Figure 21. *The isosbestic point of p-nitrophenol in water. The isosbestic point of a sample is the wavelength at which the total absorbance is not affected by physical changes in the sample which might be caused by the pH of the buffer. (Biggs 1954)*

The NMR results showed that the 4-NPC had conjugated to the 4-arm PEG, yielding PEG4NPC. The level of functionalisation seemed to be high, close to 100%, which is contradictory to the observations of the performance of the self-synthesised PEG4NPC

with the peptide conjugation. Thus, the achieved level of functionalisation could not be determined with full certainty in the time frame of this thesis.

6.1.2 Fibronectin likely altered the crosslinking of HAH

In order to prepare adhesion ligand presenting-hyaluronan hydrogels, fibronectin was physically embedded within the hydrogel structure. Addition of fibronectin resulted in visibly softer HAH-FN gels compared to non-adhesive HAH hydrogels. As fibronectin is a large macromolecule (~440 kDa), it likely interfered with the crosslinking of the hydrogels, resulting in a looser polymer network with a lower stiffness.

The fibronectin content of 50 µL HAH-FN gels was 35 µg. This was decided by a simple experiment (data not shown), whereby two different fibronectin contents were compared. Based on the solubility of fibronectin in the buffer, two types of gels were prepared; either with 35 µg or 70 µg of fibronectin. As the hydrogel with higher fibronectin content was very soft, it was determined to be unsuitable for the cell experiments, and hyaluronan gels with 35 µg fibronectin content were used in the further cell studies.

6.2 Optimisation of RNA extraction from PEG hydrogels

The 3D matrix provides additional challenges for studying cell differentiation in hydrogels, as the gene expression analysis method, real time quantitative polymerase chain reaction, requires high quality RNA to be extracted from the samples. For this purpose, RNA extraction from PEG hydrogels was optimised by comparing two commercial RNA extraction kits and two different lysis buffers. The number of parallel samples was three, except for the blanks and for the hydrogels in the TRI Reagent & tRNA buffer. Due to the small amount of samples, the reliability of the results is limited by this study setting, as repetition of the experiment did not fit to the time frame of this thesis study.

The RNA extraction yield was high with the TRI Reagent & tRNA buffer with both of the kits. However, the high readings from the buffer blank and gel blank showed that there were still some contaminants from the added tRNA in the samples. Therefore, it was concluded that RLT+ buffer was more reliable for RNA extraction. A higher yield of RNA from the 2D sample was obtained with the RNeasy Plus Mini Kit compared to the AllPrep DNA/RNA/Protein Mini Kit, and the yield for 3D samples was in both cases quite similar. The yield obtained would be a sufficient quantity for a gene expression study on a wide panel of genes relating to mechanotransduction and differentiation down multiple lineages.

The quality of the extracted RNA was studied in detail. According to the technical bulletin for NanoDrop Spectrophotometers, the A260/280 ratio is considered to be the primary measure of nucleic acid purity, and a value of ~2.0 is considered to indicate high RNA

purity. The A260/230 ratio is used as a secondary measure, and the ratio for pure RNA is generally in the range of 2.0–2.2.

The A260/280 ratio was ~1.5–2.0 for all the cell samples, which indicates that there were likely to be some contaminants present. The A260/230 ratio was even lower for all the samples. One explanation for this conflicting result is that the TRI Reagent, which is a phenolic solution, absorbs at 230 nm. However, this does not explain the lower values for the RLT+ buffer. Another explanation may be the presence of traces of hydrogel component contaminants that absorb at any of the wavelengths measured (230, 260 or 280 nm).

The RLT+ samples were analysed with Fragment Analyzer, which utilises a parallel capillary electrophoresis technique and expresses "RNA quality number" out of a maximum score of 10. The maximum value was obtained with both of the kits for the 2D samples. The RNA quality numbers for the RNA extracted from 3D samples were 6.7 and 6.2, for the RNeasy Plus Mini Kit and for the AllPrep DNA/RNA/Protein Kit, respectively. The lower RNA quality number is due to the fragmentation of the RNA, which almost certainly results from the harsh homogenisation procedure which was carried out for the gels at the beginning of extraction. In general, Fragment Analyzer is considered to be more reliable for studying RNA quality. Thus, the quality of extracted RNA seems to be relatively high. A value of ≥ 6 is sufficiently high for gene expression studies via real-time quantitative polymerase chain reaction. In future, however, it is likely possible to reduce the speed and duration of the homogenisation step to one 15 s cycle at 1,000 rpm, in order to minimise fragmentation and yield higher quality RNA for applications such as gene expression arrays, which demand higher quality RNA. Efficient homogenisation of the hydrogel matrix and cells without causing damage to the RNA has been stated to be a challenge in other studies as well (Köster et al. 2016).

The user protocols of the two commercial RNA extraction kits are quite similar for the RNA extraction steps, which explains why the obtained yields do not differ much. Increased precision and more careful pipetting could decrease the amount of contaminants in TRI Reagent & tRNA samples. As different types of hydrogels have very different matrix properties, it should be evaluated whether the RNeasy Plus Mini Kit and RLT+ buffer is the most beneficial combination for other hydrogels and whether the results are translatable to other materials. It is important to note that in this extraction experiment, hydrogels with very high cell densities were used (250,000 cells per 50 µL hydrogel) and therefore the yield of RNA extracted from gels with lower cell densities will be lower.

6.3 Evaluation of cell behaviour in hyaluronan hydrogels

6.3.1 Fibronectin presentation enhanced cell survival

The viability and proliferation of encapsulated hBMSCs were evaluated over a week of culture. The assays equally show that fibronectin improved cell survival inside the hydrogels, and after one week the viability was over four times higher in the HAH-FN gels, compared to the HAH gels, according to the total DNA assay. This result is in line with the hypothesis that adhesion ligand presentation enhances cell viability, and it is known that cell adhesion is fundamental for cell survival for adherent cells such as MSCs.

The cell viability was lower in HAH gels already on day one, and the viability further decreased during the culture time. A small but most likely statistically insignificant decrease in viability could be seen in HAH-FN gels as well, according to the total DNA assay. However, this may be due to insufficient gas, nutrient or waste product exchange through the gels, due to poor permeability, rather than being an effect of ligand density.

Problems with stainings emerged early on, and the consistent results from different stainings indicate that the structure of HAH gels was likely so tight that the dyes could not penetrate the hydrogel. In addition, hyaluronan has a negative charge, which might also have prevented the dyes from entering the hydrogel. The permeation of gas, nutrients and waste products is fundamental for cell survival within hydrogels, and this might have been compromised in the HAH gels, therefore resulting in low viability of the cells.

It is important to select suitable assays for each study setting, and this need is especially highlighted when culturing cells in 3D. During this preliminary study, the selected three viability assays gave very different results, and some of the limitations of these assays were highlighted. The total DNA assay appeared to be the most reliable assay for these hyaluronan hydrogels, likely because the hydrogels were homogenised before the quantification of results. Cell numbers obtained with the total DNA assay were slightly higher than expected, which may relate to inaccuracies of the standard curve. However, as the cell samples were fabricated at the same time point, the cell numbers between samples were comparable and the decrease in viability could be seen at each of the time points.

The issues with the results obtained from the other two viability assays, the resazurin-based mitochondrial metabolic assay and live/dead staining, related mainly to the material properties. According to the resazurin-based mitochondrial metabolic assay, the HAH-FN samples contained over 150,000 cells already on day one, and the cell number increased during the culture. Changes in the hydrogel structure were the likely cause of these conflicting results between the mitochondrial metabolic assay and the total DNA assays. The cell numbers were extrapolated from a standard curve with four different cell densities. As the standard curve specimens were only incubated in the medium for 20 min before addition of the mitochondrial metabolic assay reagent, the gels of the standard

curve were likely not as permeable for the dye as the samples were. As the hydrogels swell, become wetted (and eventually get degraded during the culture time), they become more permeable for the dye, which becomes more accessible for the cells. However, after seven days, the HAH gels did not seem to become more permeable for the live/dead stains, which could relate to possible dye-hydrogel interactions.

Due to the simultaneous use of multiple viability assays, it was possible to gain a lot of information about the cell-hydrogel samples that is indicative of their varying structures. The problems with the dye permeation were consistent, and it can be therefore concluded that the assays which are based on stainings are not suitable as such for the non-adhesive HAH hydrogels. Therefore, the use of the resazurin-based mitochondrial metabolic assay is not recommended for studying cell viability in these gels.

6.3.2 Fibronectin presentation enabled cell spreading

Cell morphology was evaluated at each time point by immunocytochemistry and bright-field imaging. Imaging of the samples could be carried out easily due to the transparency of the hydrogels. Spread cells were observed only in the HAH-FN hydrogels, and spread cell clusters were detected already on day four. However, most of the cells in HAH-FN gels remained rounded during the week of culture, and most likely only the cells which were able to reach fibronectin were able to spread. Cells encapsulated within the gels without fibronectin remained rounded, which supports this finding. The results are as expected, as it is well-known that fibronectin presentation provides adhesion sites for the cells, which enables spreading (Kasten et al. 2014). In addition to the adhesion ligand presentation, the altered crosslinking caused by addition of fibronectin resulted in softer gels, and this may have enabled the cells to easier deform the surroundings to allow cell spreading, and possibly even migration throughout the matrix.

In the HAH-FN gels, spread cells had defined stress fibers visible with immunocytochemical stains, but rounded cells did not, as only the cells which were able to attach to the surroundings were able to organise their cytoskeleton. The lack of vinculin in the adhesion sites is unexpected, as it is a focal adhesion protein and it was expected to be present in cells which have attached to their surroundings via integrins. This finding could relate to problems with the staining protocol, or the density of vinculin may have been too low to detect. The same protocol had been previously used successfully with collagen hydrogels, but it needs to be further optimised for hyaluronan hydrogels.

In the HAH gels, actin fibers were not visible in the cells at all, which relates to the problems with the dye penetration. However, nuclei and vinculin were could be easily seen, and vinculin seemed to remain diffusive around the nucleus. Similar observations of diffuse vinculin within cells in non-adhesive hyaluronan gels have been previously reported (Khetan et al. 2013; Kim & Kumar 2014). As both types of the gels used in this study were stained with the same protocol, it is unexpected that the vinculin could be seen in

the HAH gels, but it was lacking in the cell adhesion sites in HAH-FN gels. According to this contradictory result, it might be that fibronectin somehow interferes with the vinculin staining. In this study, the material blanks were prepared from HAH gels, and therefore the effects of fibronectin content could not be further evaluated.

6.3.3 Assessment of the study and future perspectives

The results of the preliminary cell culture study indicate that the material design work should continue for the hyaluronan hydrogels. Preparation of hydrogels with smaller polymer content, e.g. 1.4% (w/v) instead of the 1.6% used in this study, could potentially be used to decrease the level of crosslinking and to increase the mesh size. However, as the level of crosslinking is related to the stiffness of the hydrogel, lower crosslinking might compromise the mechanical properties of the hyaluronan hydrogels.

Thorough material testing should be carried out before continuing to further cell studies. Effective solute transport is one of the most critical design parameters for hydrogels (Slaughter et al. 2009), and the diffusion properties need to be tested for both types of the hydrogels, as it remains unclear whether the fibronectin presentation affected the crosslinking throughout the entire gel, or if some parts were more densely crosslinked than others. Diffusion properties of hydrogels can be determined by studying the progression of labelled molecular probes with varying molecular weights through the samples over time. (Hoffman 2002; Zustiak et al. 2010)

The HAH-FN hydrogels seemed to be softer than the non-adhesive HAH hydrogels, and this observation was confirmed with compression testing (results not shown). In addition, the stiffness of the hydrogels seemed to decrease during the week of culture, and HAH-FN gels become more permissive for the reagent of the resazurin-based mitochondrial metabolic assay. Therefore, it would be important to study the swelling and degradation properties of these gels. Determination of the degradation time of these hydrogels would be beneficial for future cell culture studies as well.

Besides the need for material testing, the results of this study highlight the need for optimisation of assays for each specific 3D environment, as the material properties can affect the outcomes of the assays. For the stainings, live/dead and immunocytochemistry, the dilutions of the dyes and incubation times should be adjusted in order to achieve proper staining of the samples, without overstaining the material. For example, in an immunochemistry protocol optimised mainly for hyaluronan hydrogels, the suggested incubation times are two hours for phalloidin and 20 min for DAPI (Khetan & Burdick 2009). In this study, the corresponding incubation times were 55 minutes and 5 minutes, respectively.

One way to improve the experimental set up of the preliminary study would be to stain the fibronectin within the HAH-FN gels with fibronectin antibody. This would be beneficial for evaluation of cell adhesion, as now the interpretation of the results includes some

assumptions about the fibronectin presentation. A possible error source in this study is the small number of parallel samples. Therefore, the results should be further confirmed with higher number of samples and preferably with cells from different donors as well.

In the future, comparing the effects of different fibronectin densities on cell behaviours would be of great value to the field of mechanotransduction. Fibronectin is an interesting mechanosensitive molecule, but it presents other biologically relevant sequences in addition to adhesion ligands, which could alter cell responses. Excluding the other potential effects of fibronectin presentation in addition to altered adhesion ligand presentation is challenging. In addition, with regards to the mechanical properties of these hyaluronan hydrogels, the current fibronectin content seemed to be near the upper limit. Thus, one intriguing approach would be to fabricate hyaluronan hydrogels with engineered fibronectin fragments which only include the adhesion sites, similarly to the work by Kisiel et al. (2013). The smaller size of the molecule means that it would be less disruptive to crosslinking and therefore it could be incorporated to the hydrogels at higher levels. (Kisiel et al. 2013) In order to proceed to cell differentiation studies with the hydrogels used in this study, the gels should remain undegraded at least for two to three weeks, as the *in vitro* differentiation of MSCs is commonly assessed after two weeks for osteogenesis and three weeks for adipogenesis. With some modifications, the HA hydrogels used in this study have great potential to be used in the future to unravel the mechanisms of mechanotransduction.

7. CONCLUSIONS

The aim of this thesis was to study the effects of adhesion ligand presentation on cell behaviour in three dimensions. In order to prepare the 3D matrix, contributions were made to the hydrogel synthesis by optimising PEG conjugation with 4-NPC. However, the achieved degree of coupling remains unclear, as the results from absorbance measurements, NMR and the performance in practice gave conflicting outcomes, and the reason why the self-synthesised PEG4NPC did not perform well in further use could not be determined in the time frame of this thesis.

As the material fabrication faced delays with the delivery of custom-synthesised peptides, PEG hydrogels were crosslinked using a simpler peptide which did not possess any adhesion ligands. RNA extraction was optimised from these gels, and the successful high yield and satisfactory quality achieved means that the developed method can be applied in practice when proceeding to cell differentiation studies with the finished PEG hydrogels, functionalised with RGD adhesion ligands. As expected, the extraction yield was lower compared to that obtained from 2D samples, but it is sufficient for gene expression studies, and the best yield and quality were achieved with QIAGEN RNeasy Plus Mini Kit with the supplied RLT+ buffer.

Preliminary studies concerning the effects of adhesion ligand presentation were carried out with hyaluronan hydrogels, either without or with fibronectin as an adhesive ligand. Changes in cell viability and morphology were evaluated over a week in culture. Fibronectin clearly improved cell survival within the hydrogels and enabled cell spreading, which correlates with the hypothesis, and demonstrates that mechanosensing and adhesion ligand presentation can alter cell behaviours. However, as the consistent results from different stainings indicate, the crosslinking density of the non-adhesive HAH hydrogels was too high to enable sufficient dye permeation. The dense crosslinking most likely also hindered the flow of waste products, gas and nutrients through the gels, which could have been an even bigger contributor to the decreased cell viability than the lack of adhesion ligands.

This work highlights the importance of assay optimisation for different types of hydrogels and the need for throughout material testing before proceeding to cell culture studies. The material chemistry and physical properties provide additional complexity to the 3D cell culture platforms. In this work, some of the limitations of different cell viability assays were underlined, and these can be considered when planning future cell culture studies with hydrogels.

REFERENCES

Ahmed, E.M. (2015). Hydrogel: Preparation, characterization, and applications: A review, Journal of Advanced Research, Vol. 6(2), pp. 105-121.

Amano, M., Nakayama, M. & Kaibuchi, K. (2010). Rho-kinase/ROCK: A key regulator of the cytoskeleton and cell polarity, Cytoskeleton (Hoboken, N.J.), Vol. 67(9), pp. 545-554.

Anderson, H.J., Sahoo, J.K., Ulijn, R.V. & Dalby, M.J. (2016). Mesenchymal Stem Cell Fate: Applying Biomaterials for Control of Stem Cell Behavior, Frontiers in Bioengineering and Biotechnology, Vol. 4pp. 38.

Arnold, M., Cavalcanti-Adam, E.A., Glass, R., Blümmel, J., Eck, W., Kantlehner, M., Kessler, H. & Spatz, J.P. (2004). Activation of Integrin Function by Nanopatterned Adhesive Interfaces, ChemPhysChem, Vol. 5(3), pp. 383-388.

Aureille, J., Belaadi, N. & Guilluy, C. (2017). Mechanotransduction via the nuclear envelope: a distant reflection of the cell surface, Current opinion in cell biology, Vol. 44pp. 59-67.

Avram, M.M., Avram, A.S. & James, W.D. (2007). Subcutaneous fat in normal and diseased states. 3. Adipogenesis: From stem cell to fat cell, Journal of the American Academy of Dermatology, Vol. 56(3), pp. 472-492.

Badylak, S., Gilbert, T. & Myers-Irvin, J. (2008). 5. The Extracellular Matrix as a Biologic Scaffold for Tissue Engineering, in: Van Blitterswijk, C. (ed.), Tissue Engineering, Elsevier, pp. 122-140.

Biggs, A.I. (1954). A spectrophotometric determination of the dissociation constants of p-nitrophenol and papaverine, Transactions of the Faraday Society, Vol. 50pp. 800-802.

Bonnier, F., Keating, M.E., Wróbel, T.P., Majzner, K., Baranska, M., Garcia-Munoz, A., Blanco, A. & Byrne, H.J. (2015). Cell viability assessment using the Alamar blue assay: A comparison of 2D and 3D cell culture models, Toxicology in Vitro, Vol. 29(1), pp. 124-131.

Booth-Gauthier, E.A., Alcoser, T.A., Yang, G. & Dahl, K.N. (2012). Force-induced changes in subnuclear movement and rheology, Biophysical journal, Vol. 103(12), pp. 2423-2431.

Bunnell, B.A., Flaat, M., Gagliardi, C., Patel, B. & Ripoll, C. (2008). Adipose-derived Stem Cells: Isolation, Expansion and Differentiation, Methods (San Diego, Calif.), Vol. 45(2), pp. 115-120.

Burdick, J.A. & Prestwich, G.D. (2011). Hyaluronic Acid Hydrogels for Biomedical Applications, Advanced materials (Deerfield Beach, Fla.), Vol. 23(12), pp. H41-H56.

Burridge, K. & Guilluy, C. (2016). Focal adhesions, stress fibers and mechanical tension, Experimental cell research, Vol. 343(1), pp. 14-20.

Caliari, S.R. & Burdick, J.A. (2016). A practical guide to hydrogels for cell culture, Nature Methods, Vol. 13(5), pp. 405-414.

Case, L.B. & Waterman, C.M. (2015). Integration of actin dynamics and cell adhesion by a three-dimensional, mechanosensitive molecular clutch, Nature cell biology, Vol. 17(8), pp. 955-963.

Cavalcanti-Adam, E.A., Volberg, T., Micoulet, A., Kessler, H., Geiger, B. & Spatz, J.P. (2007). Cell Spreading and Focal Adhesion Dynamics Are Regulated by Spacing of Integrin Ligands, Biophysical Journal, Vol. 92(8), pp. 2964-2974.

Chrzanowska-Wodnicka, M. & Burridge, K. (1996). Rho-stimulated contractility drives the formation of stress fibers and focal adhesions, Journal of Cell Biology, Vol. 133(6), pp. 1403-1415.

Connelly, J.T., Garcia, A.J. & Levenston, M.E. (2007). Inhibition of in vitro chondrogenesis in RGD-modified three-dimensional alginate gels, Biomaterials, Vol. 28(6), pp. 1071-1083.

Connelly, J.T., García, A.J. & Levenston, M.E. (2008). Interactions between integrin ligand density and cytoskeletal integrity regulate BMSC chondrogenesis, Journal of cellular physiology, Vol. 217(1), pp. 145-154.

Del Rio, A., Perez-Jimenez, R., Liu, R., Roca-Cusachs, P., Fernandez, J.M. & Sheetz, M.P. (2009). Stretching single talin rod molecules activates vinculin binding, Science, Vol. 323(5914), pp. 638-641.

Driscoll, T.P., Cosgrove, B.D., Heo, S.-., Shurden, Z.E. & Mauck, R.L. (2015). Cytoskeletal to Nuclear Strain Transfer Regulates YAP Signaling in Mesenchymal Stem Cells, Biophysical journal, Vol. 108(12), pp. 2783-2793.

Dupont, S., Morsut, L., Aragona, M., Enzo, E., Giulitti, S., Cordenonsi, M., Zanconato, F., Le Digabel, J., Forcato, M., Bicciato, S., Elvassore, N. & Piccolo, S. (2011). Role of YAP/TAZ in mechanotransduction, Nature, Vol. 474(7350), pp. 179-184.

Engler, A.J., Sen, S., Sweeney, H.L. & Discher, D.E. (2006). Matrix Elasticity Directs Stem Cell Lineage Specification, Cell, Vol. 126(4), pp. 677-689.

Fedorchak, G.R., Kaminski, A. & Lammerding, J. (2014). Cellular mechanosensing: Getting to the nucleus of it all, Progress in biophysics and molecular biology, Vol. 115(2-3), pp. 76-92.

Frith, J.E., Mills, R.J. & Cooper-White, J.J. (2012a). Lateral spacing of adhesion peptides influences human mesenchymal stem cell behaviour, Journal of cell science, Vol. 125(2), pp. 317-327.

Frith, J.E., Mills, R.J., Hudson, J.E. & Cooper-White, J.J. (2012b). Tailored integrin-extracellular matrix interactions to direct human mesenchymal stem cell differentiation, Stem cells and development, Vol. 21(13), pp. 2442-2456.

Fuchs, E., Tumbar, T. & Guasch, G. (2004). Socializing with the Neighbors: Stem Cells and Their Niche, Cell, Vol. 116(6), pp. 769-778.

Gao, M., Craig, D., Lequin, O., Campbell, I.D., Vogel, V. & Schulten, K. (2003). Structure and functional significance of mechanically unfolded fibronectin type III1 intermediates, Proceedings of the National Academy of Sciences of the United States of America, Vol. 100(25), pp. 14784-14789.

Gasparian, A., Daneshian, L., Ji, H., Jabbari, E. & Shtutman, M. (2015). Purification of high-quality RNA from synthetic polyethylene glycol-based hydrogels, Analytical Biochemistry, Vol. 484(Supplement C), pp. 1-3.

Geiger, B., Bershadsky, A., Pankov, R. & Yamada, K.M. (2001). Transmembrane extracellular matrix-cytoskeleton crosstalk, Nature Reviews Molecular Cell Biology, Vol. 2(11), pp. 793-805.

Gerecht, S., Burdick, J.A., Ferreira, L.S., Townsend, S.A., Langer, R. & Vunjak-Novakovic, G. (2007). Hyaluronic acid hydrogel for controlled self-renewal and differentiation of human embryonic stem cells, Proceedings of the National Academy of Sciences of the United States of America, Vol. 104(27), pp. 11298-11303.

Guilluy, C. & Burridge, K. (2015). Nuclear mechanotransduction: Forcing the nucleus to respond, Nucleus, Vol. 6(1), pp. 19-22.

Hao, J., Zhang, Y., Jing, D., Shen, Y., Tang, G., Huang, S. & Zhao, Z. (2015). Mechanobiology of mesenchymal stem cells: Perspective into mechanical induction of MSC fate, Acta Biomaterialia, Vol. 20pp. 1-9.

Hersel, U., Dahmen, C. & Kessler, H. (2003). RGD modified polymers: biomaterials for stimulated cell adhesion and beyond, Biomaterials, Vol. 24(24), pp. 4385-4415.

Hoffman, A.S. (2002). Hydrogels for biomedical applications, Advanced Drug Delivery Reviews, Vol. 54(1), pp. 3-12.

Hong, J.-., Hwang, E.S., McManus, M.T., Amsterdam, A., Tian, Y., Kalmukova, R., Mueller, E., Benjamin, T., Spiegelman, B.M., Sharp, P.A., Hopkins, N. & Yaffe, M.B. (2005). TAZ, a transcriptional modulator of mesenchymal stem cell differentiation, Science, Vol. 309(5737), pp. 1074-1078.

Huebsch, N., Arany, P.R., Mao, A.S., Shvartsman, D., Ali, O.A., Bencherif, S.A., Rivera-Feliciano, J. & Mooney, D.J. (2010). Harnessing traction-mediated manipulation of the cell/matrix interface to control stem-cell fate, Nature Materials, Vol. 9(6), pp. 518-526.

Hwang, J.-., Byun, M.R., Kim, A.R., Kim, K.M., Cho, H.J., Lee, Y.H., Kim, J., Jeong, M.G., Hwang, E.S. & Hong, J.-. (2015). Extracellular matrix stiffness regulates osteogenic differentiation through MAPK activation, PLoS ONE, Vol. 10(8), .

Ihalainen, T.O., Aires, L., Herzog, F.A., Schwartlander, R., Moeller, J. & Vogel, V. (2015). Differential basal-to-apical accessibility of lamin A/C epitopes in the nuclear lamina regulated by changes in cytoskeletal tension, Nature Materials, Vol. 14(12), pp. 1252-1261.

Ingber, D.E. (2006). Cellular mechanotransduction: Putting all the pieces together again, FASEB Journal, Vol. 20(7), pp. 811-827.

Ingber, D.E. (2008). Tensegrity-based mechanosensing from macro to micro, Progress in biophysics and molecular biology, Vol. 97(2-3), pp. 163-179.

Ingber, D.E. (1997). Tensegrity: The architectural basis of cellular mechanotransduction, Annual Review of Physiology, Vol. 59pp. 575-599.

Isermann, P. & Lammerding, J. (2013). Nuclear mechanics and mechanotransduction in health and disease, Current Biology, Vol. 23(24), .

Jaalouk, D.E. & Lammerding, J. (2009). Mechanotransduction gone awry, Nature Reviews Molecular Cell Biology, Vol. 10(1), pp. 63-73.

Jukes, J., Both, S., Post, J., van Blitterswijk, C., Karperien, M. & de Boer, J. (2008). Chapter 1. Stem cells, in: Van Blitterswijk, C. (ed.), Tissue Engineering, Elsevier, pp. 1-26.

Kasten, A., Naser, T., Brüllhoff, K., Fiedler, J., Müller, P., Möller, M., Rychly, J., Groll, J. & Brenner, R.E. (2014). Guidance of mesenchymal stem cells on fibronectin structured hydrogel films, PLoS ONE, Vol. 9(10), .

Khetan, S. & Burdick, J. (2009). Cellular Encapsulation in 3D Hydrogels for Tissue Engineering, - Journal of Visualized Experiments : JoVE, (32), pp. 1590.

Khetan, S., Guvendiren, M., Legant, W.R., Cohen, D.M., Chen, C.S. & Burdick, J.A. (2013). Degradation-mediated cellular traction directs stem cell fate in covalently cross-linked three-dimensional hydrogels, Nature Materials, Vol. 12(5), pp. 458-465.

Kilian, K.A., Bugarija, B., Lahn, B.T. & Mrksich, M. (2010). Geometric cues for directing the differentiation of mesenchymal stem cells, Proceedings of the National Academy of Sciences of the United States of America, Vol. 107(11), pp. 4872-4877.

Kim, Y. & Kumar, S. (2014). CD44-mediated adhesion to hyaluronic acid contributes to mechanosensing and invasive motility, Molecular Cancer Research, Vol. 12(10), pp. 1416-1429.

Kisiel, M., Martino, M.M., Ventura, M., Hubbell, J.A., Hilborn, J. & Ossipov, D.A. (2013). Improving the osteogenic potential of BMP-2 with hyaluronic acid hydrogel modified with integrin-specific fibronectin fragment, Biomaterials, Vol. 34(3), pp. 704-712.

Kong, F., García, A.J., Mould, A.P., Humphries, M.J. & Zhu, C. (2009). Demonstration of catch bonds between an integrin and its ligand, Journal of Cell Biology, Vol. 185(7), pp. 1275-1284.

Kong, F., Li, Z., Parks, W.M., Dumbauld, D.W., García, A.J., Mould, A.P., Humphries, M.J. & Zhu, C. (2013). Cyclic mechanical reinforcement of integrin-ligand interactions, Molecular cell, Vol. 49(6), pp. 1060-1068.

Köster, N., Schmiermund, A., Grubelnig, S., Leber, J., Ehlicke, F., Czermak, P. & Salzig, D. (2016). Single-Step RNA Extraction from Different Hydrogel-Embedded Mesenchymal Stem Cells for Quantitative Reverse Transcription-Polymerase Chain Reaction Analysis, Tissue Engineering - Part C: Methods, Vol. 22(6), pp. 552-560.

Lammerding, J., Fong, L.G., Ji, J.Y., Reue, K., Stewart, C.L., Young, S.G. & Lee, R.T. (2006). Lamins a and C but not lamin B1 regulate nuclear mechanics, Journal of Biological Chemistry, Vol. 281(35), pp. 25768-25780.

Lane, S.W., Williams, D.A. & Watt, F.M. (2014). Modulating the stem cell niche for tissue regeneration, Nature biotechnology, Vol. 32(8), pp. 795-803.

Lian, J.B. & Stein, G.S. (1995). Development of the osteoblast phenotype: molecular mechanisms mediating osteoblast growth and differentiation. The Iowa orthopaedic journal, Vol. 15pp. 118-140.

Lombardi, M.L., Jaalouk, D.E., Shanahan, C.M., Burke, B., Roux, K.J. & Lammerding, J. (2011). The interaction between nesprins and sun proteins at the nuclear envelope is critical for force transmission between the nucleus and cytoskeleton, Journal of Biological Chemistry, Vol. 286(30), pp. 26743-26753.

Lv, H., Li, L., Sun, M., Zhang, Y., Chen, L., Rong, Y. & Li, Y. (2015). Mechanism of regulation of stem cell differentiation by matrix stiffness, Stem Cell Research and Therapy, .

Mason, C. & Dunnill, P. (2008). A brief definition of regenerative medicine, Regenerative Medicine, Vol. 3(1), pp. 1-5.

McBeath, R., Pirone, D.M., Nelson, C.M., Bhadriraju, K. & Chen, C.S. (2004). Cell Shape, Cytoskeletal Tension, and RhoA Regulate Stem Cell Lineage Commitment, Developmental Cell, Vol. 6(4), pp. 483-495.

Mhanna, R., Oeztuerk, E., Vallmajo-Martin, Q., Millan, C., Mueller, M. & Zenobi-Wong, M. (2014). GFOGER-Modified MMP-Sensitive Polyethylene Glycol Hydrogels Induce Chondrogenic Differentiation of Human Mesenchymal Stem Cells, Tissue Engineering Part a, Vol. 20(7-8), pp. 1165-1174.

Mitra, S.K., Hanson, D.A. & Schlaepfer, D.D. (2005). Focal adhesion kinase: In command and control of cell motility, Nature Reviews Molecular Cell Biology, Vol. 6(1), pp. 56-68.

Nakayama, K.H., Batchelder, C.A., Lee, C.I. & Tarantal, A.F. (2010). Decellularized rhesus monkey kidney as a three-dimensional scaffold for renal tissue engineering, Tissue Engineering - Part A, Vol. 16(7), pp. 2207-2216.

Nuttelman, C.R., Tripodi, M.C. & Anseth, K.S. (2005). Synthetic hydrogel niches that promote hMSC viability, Matrix Biology, Vol. 24(3), pp. 208-218.

Orford, K.W. & Scadden, D.T. (2008). Deconstructing stem cell self-renewal: genetic insights into cell-cycle regulation, Nature reviews. Genetics, Vol. 9(2), pp. 115-128.

Peng, R., Yao, X. & Ding, J. (2011). Effect of cell anisotropy on differentiation of stem cells on micropatterned surfaces through the controlled single cell adhesion, Biomaterials, Vol. 32(32), pp. 8048-8057.

Peppas, N.A. & Hoffman, A.S. (2013). I.2.5 Hydrogels, in: Ratner, B.D., Hoffman, A.S., Schoen, F.J. & Lemons, J.E. (ed.), Biomaterials Science - An Introduction to Materials in Medicine, 3rd ed., Elsevier, pp. 166-179.

Pittenger, M.F., Mackay, A.M., Beck, S.C., Jaiswal, R.K., Douglas, R., Mosca, J.D., Moorman, M.A., Simonetti, D.W., Craig, S. & Marshak, D.R. (1999). Multilineage potential of adult human mesenchymal stem cells, Science, Vol. 284(5411), pp. 143-147.

Raza, A. & Lin, C.-. (2013). The influence of matrix degradation and functionality on cell survival and morphogenesis in PEG-based hydrogels, Macromolecular Bioscience, Vol. 13(8), pp. 1048-1058.

Rowlands, A.S., George, P.A. & Cooper-White, J.J. (2008). Directing osteogenic and myogenic differentiation of MSCs: Interplay of stiffness and adhesive ligand presentation, American Journal of Physiology - Cell Physiology, Vol. 295(4), .

Salinas, C.N. & Anseth, K.S. (2008a). The enhancement of chondrogenic differentiation of human mesenchymal stem cells by enzymatically regulated RGD functionalities, Biomaterials, Vol. 29(15), pp. 2370-2377.

Salinas, C.N. & Anseth, K.S. (2008b). The influence of the RGD peptide motif and its contextual presentation in PEG gels on human mesenchymal stem cell viability, Journal of Tissue Engineering and Regenerative Medicine, Vol. 2(5), pp. 296-304.

Scadden, D.T. (2006). The stem-cell niche as an entity of action, Nature, Vol. 441(7097), pp. 1075-1079.

Schlessinger, K., Hall, A. & Tolwinski, N. (2009). Wnt signaling pathways meet Rho GTPases, Genes and Development, Vol. 23(3), pp. 265-277.

Schofield, R. (1978). The relationship between the spleen colony-forming cell and the haemopoietic stem cell, Blood cells, Vol. 4(1-2), pp. 7-25.

Schwartz, M.A. (2010). Integrins and extracellular matrix in mechanotransduction. Cold Spring Harbor perspectives in biology, Vol. 2(12), .

Scott, J.E. (1995). Extracellular matrix, supramolecular organisation and shape, Journal of anatomy, Vol. 187(2), pp. 259-269.

Singh, A., Zhan, J., Ye, Z. & Elisseeff, J.H. (2013). Modular Multifunctional Poly(ethylene glycol) Hydrogels for Stem Cell Differentiation, Advanced Functional Materials, Vol. 23(5), pp. 575-582.

Slaughter, B.V., Khurshid, S.S., Fisher, O.Z., Khademhosseini, A. & Peppas, N.A. (2009). Hydrogels in regenerative medicine, Advanced Materials, Vol. 21(32-33), pp. 3307-3329.

Smith, M.L., Gourdon, D., Little, W.C., Kubow, K.E., Eguiluz, R.A., Luna-Morris, S. & Vogel, V. (2007). Force-induced unfolding of fibronectin in the extracellular matrix of living cells, PLoS Biology, Vol. 5(10), pp. 2243-2254.

Soheilypour, M., Peyro, M., Jahed, Z. & Mofrad, M.R.K. (2016). On the Nuclear Pore Complex and Its Roles in Nucleo-Cytoskeletal Coupling and Mechanobiology, Cellular and Molecular Bioengineering, Vol. 9(2), pp. 217-226.

Solchaga, L.A., Penick, K.J. & Welter, J.F. (2011). Chondrogenic differentiation of bone marrow-derived mesenchymal stem cells: tips and tricks. Methods in molecular biology (Clifton, N.J.), Vol. 698pp. 253-278.

Swift, J., Ivanovska, I.L., Buxboim, A., Harada, T., Dingal, P.C.D.P., Pinter, J., Pajerowski, J.D., Spinler, K.R., Shin, J.-., Tewari, M., Rehfeldt, F., Speicher, D.W. & Discher, D.E. (2013). Nuclear lamin-A scales with tissue stiffness and enhances matrix-directed differentiation, Science, Vol. 341(6149), .

Takahashi, K. & Yamanaka, S. (2006). Induction of Pluripotent Stem Cells from Mouse Embryonic and Adult Fibroblast Cultures by Defined Factors, Cell, Vol. 126(4), pp. 663-676.

Thompson, W.R., Rubin, C.T. & Rubin, J. (2012). Mechanical regulation of signaling pathways in bone, Gene, Vol. 503(2), pp. 179-193.

Théry, M., Pépin, A., Dressaire, E., Chen, Y. & Bornens, M. (2006). Cell distribution of stress fibres in response to the geometry of the adhesive environment, Cell motility and the cytoskeleton, Vol. 63(6), pp. 341-355.

Tibbitt, M.W. & Anseth, K.S. (2009). Hydrogels as extracellular matrix mimics for 3D cell culture, Biotechnology and bioengineering, Vol. 103(4), pp. 655-663.

Turgay, Y., Champion, L., Balazs, C., Held, M., Toso, A., Gerlich, D.W., Meraldi, P. & Kutay, U. (2014). SUN proteins facilitate the removal of membranes from chromatin during nuclear envelope breakdown, Journal of Cell Biology, Vol. 204(7), pp. 1099-1109.

Uccelli, A., Moretta, L. & Pistoia, V. (2008). Mesenchymal stem cells in health and disease, Nature reviews.Immunology, Vol. 8(9), pp. 726-736.

Ullah, I., Subbarao, R.B. & Rho, G.J. (2015). Human mesenchymal stem cells - Current trends and future prospective, Bioscience reports, Vol. 35.

Votteler, M., Kluger, P.J., Walles, H. & Schenke-Layland, K. (2010). Stem Cell Microenvironments - Unveiling the Secret of How Stem Cell Fate is Defined, Macromolecular Bioscience, Vol. 10(11), pp. 1302-1315.

Wang, N., Tytell, J.D. & Ingber, D.E. (2009). Mechanotransduction at a distance: Mechanically coupling the extracellular matrix with the nucleus, Nature Reviews Molecular Cell Biology, Vol. 10(1), pp. 75-82.

Wang, X., Yan, C., Ye, K., He, Y., Li, Z. & Ding, J. (2013). Effect of RGD nanospacing on differentiation of stem cells, Biomaterials, Vol. 34(12), pp. 2865-2874.

Wu, X., Tu, X., Joeng, K.S., Hilton, M.J., Williams, D.A. & Long, F. (2008). Rac1 Activation Controls Nuclear Localization of ß-catenin during Canonical Wnt Signaling, Cell, Vol. 133(2), pp. 340-353.

Yang, C., Tibbitt, M.W., Basta, L. & Anseth, K.S. (2014). Mechanical memory and dosing influence stem cell fate, Nature materials, Vol. 13(6), pp. 645-652.

Zhang, W. & Liu, H.T. (2002). MAPK signal pathways in the regulation of cell proliferation in mammalian cells, Cell research, Vol. 12(1), pp. 9-18.

Zhang, Z.-. & VanEtten, R.L. (1991). Pre-steady-state and steady-state kinetic analysis of the low molecular weight phosphotyrosyl protein phosphatase from bovine heart, Journal of Biological Chemistry, Vol. 266(3), pp. 1516-1525.

Zhu, H., Mitsuhashi, N., Klein, A., Barsky, L.W., Weinberg, K., Barr, M.L., Demetriou, A. & Wu, G.D. (2006). The role of the hyaluronan receptor CD44 in mesenchymal stem cell migration in the extracellular matrix, Stem Cells, Vol. 24(4), pp. 928-935.

Zhu, J. & Marchant, R.E. (2011). Design properties of hydrogel tissue-engineering scaffolds, Expert Review of Medical Devices, Vol. 8(5), pp. 607-626.

Zhu, J. (2010). Bioactive modification of poly(ethylene glycol) hydrogels for tissue engineering, Biomaterials, Vol. 31(17), pp. 4639-4656.

Zustiak, S.P., Boukari, H. & Leach, J.B. (2010). Solute diffusion and interactions in crosslinked poly(ethylene glycol) hydrogels studied by Fluorescence Correlation Spectroscopy, Soft matter, Vol. 6(15), pp. 10.1039/C0SM00111B.

APPENDIX A: DIFFERENTIATION POTENTIAL OF HBMSCS

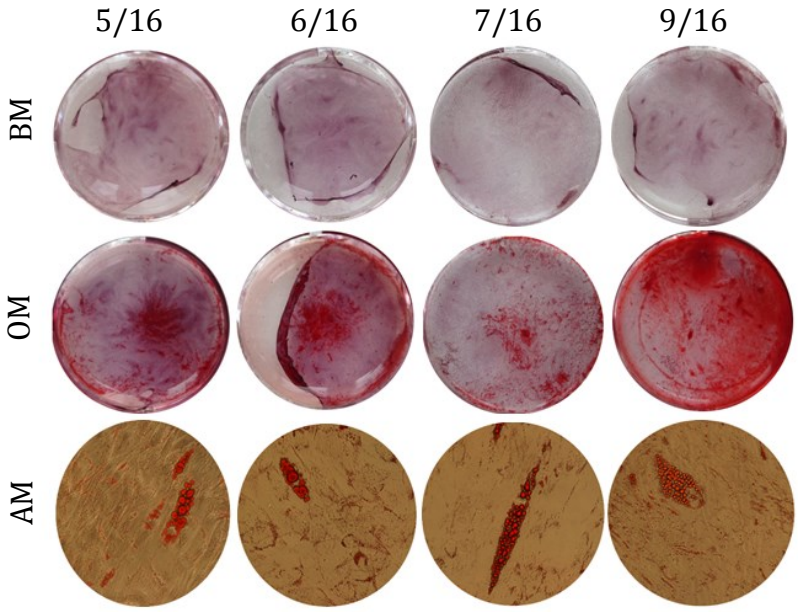

Figure 22. *Differentiation potential of hBMSCs from four different donors, labelled as 5/16, 6/16, 7/16 and 9/16. The cells were cultured in basic medium or in osteogenic medium for 20 days before Alizarin Red staining, or in adipogenic medium for 14 days before Oil Red O staining. The mineral content and lipid vacuoles are stained in red.*

APPENDIX B: NMR SPECTRA FOR PEG4NPC

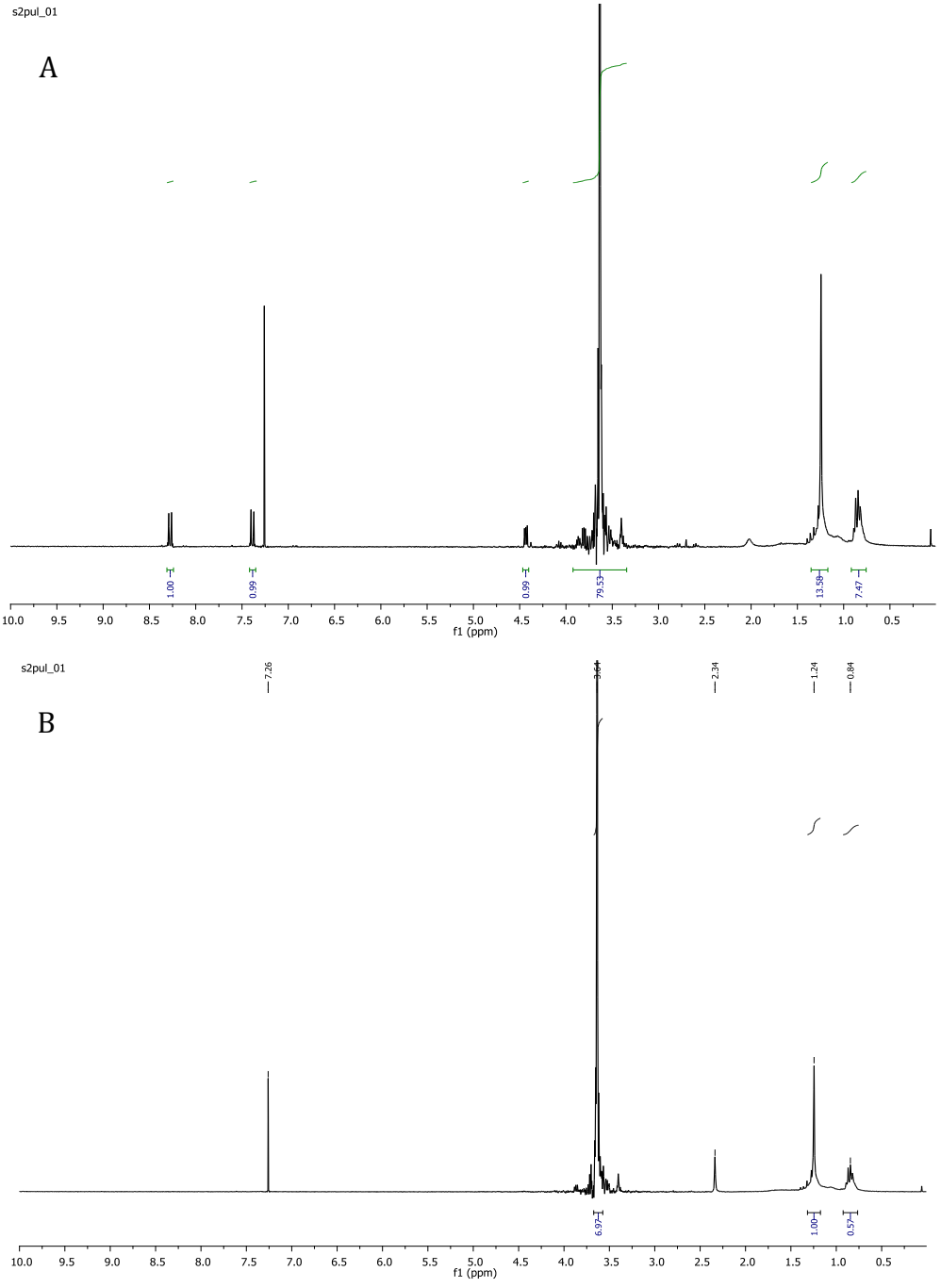

Figure 23. *^{1}H NMR spectrum for A) PEG4NPC and B) unmodified PEG4OH. The highest peak at 3.6 ppm indicates the presence on –CH_2 groups of the repeating unit of the polymer. The small peak shifted to 4.4 ppm in A) indicates the attachment of –CH2 to 4-NPC and peaks at 7.4 and 8.3 ppm indicate the presence of an aromatic ring. Solvent peak can be seen ~7.25 ppm and some impurities can be seen < 2.5 ppm.*